Supplementary Material for

Division of Labor by Dual Feedback Regulators Controls JAK2/STAT5 Signaling over Broad Ligand Range

Julie Bachmann[1,7], Andreas Raue[2,3,7], Marcel Schilling[1,7], Martin E. Böhm[4], Clemens Kreutz[2,3], Daniel Kaschek[2], Hauke Busch[3], Norbert Gretz[5], Wolf D. Lehmann[4], Jens Timmer[2,3,6], Ursula Klingmüller[1]

[1] Systems Biology of Signal Transduction, DKFZ-ZMBH Alliance, German Cancer Research Center, Heidelberg, Germany

[2] Physikalisches Institut, University of Freiburg, Center for Biological Signalling Studies (BIOSS), Freiburg, Germany

[3] Freiburg Institute for Advanced Studies (FRIAS), Zentrum für Biosystemanalyse (ZBSA), University of Freiburg, Freiburg, Germany

[4] Molecular Structure Analysis, German Cancer Research Center, Heidelberg, Germany

[5] Medical Research Center, Medical Faculty Mannheim, University of Heidelberg, Mannheim, Germany

[6] Department of Clinical and Experimental Medicine, Linköping University, Sweden

[7] equally contributed

Contents

1 Supplementary Data

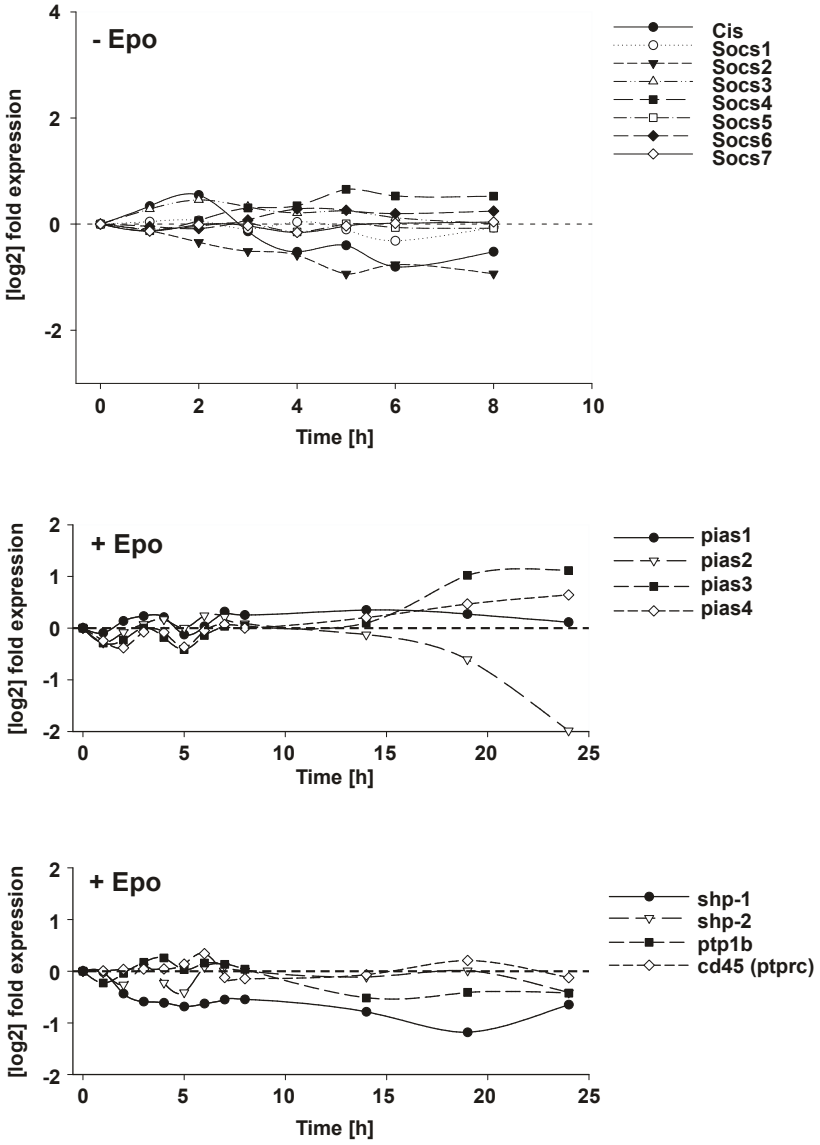

Figure S1: Additional time series of negative regulators of JAK-STAT signaling.
Top panel: Control time series in cells without Epo stimulation. Primary CFU-E cells were starved and left untreated over the period of 8 h. After 8 h the time course was stopped due to increase of CFU-E cell death without Epo stimulation. RNA was extracted at 8 different time-points and subjected to microarray analysis. Middle and bottom panel: Time course of expression profiling of other Epo-induced negative regulators of JAK-STAT signaling. Primary CFU-E cells were starved and stimulated with 0.5 U/ml Epo. RNA was extracted at 12 different time-points and subjected to microarray analysis. Log2-fold change of mRNA levels were calculated relative to the time-point $t = 0$.

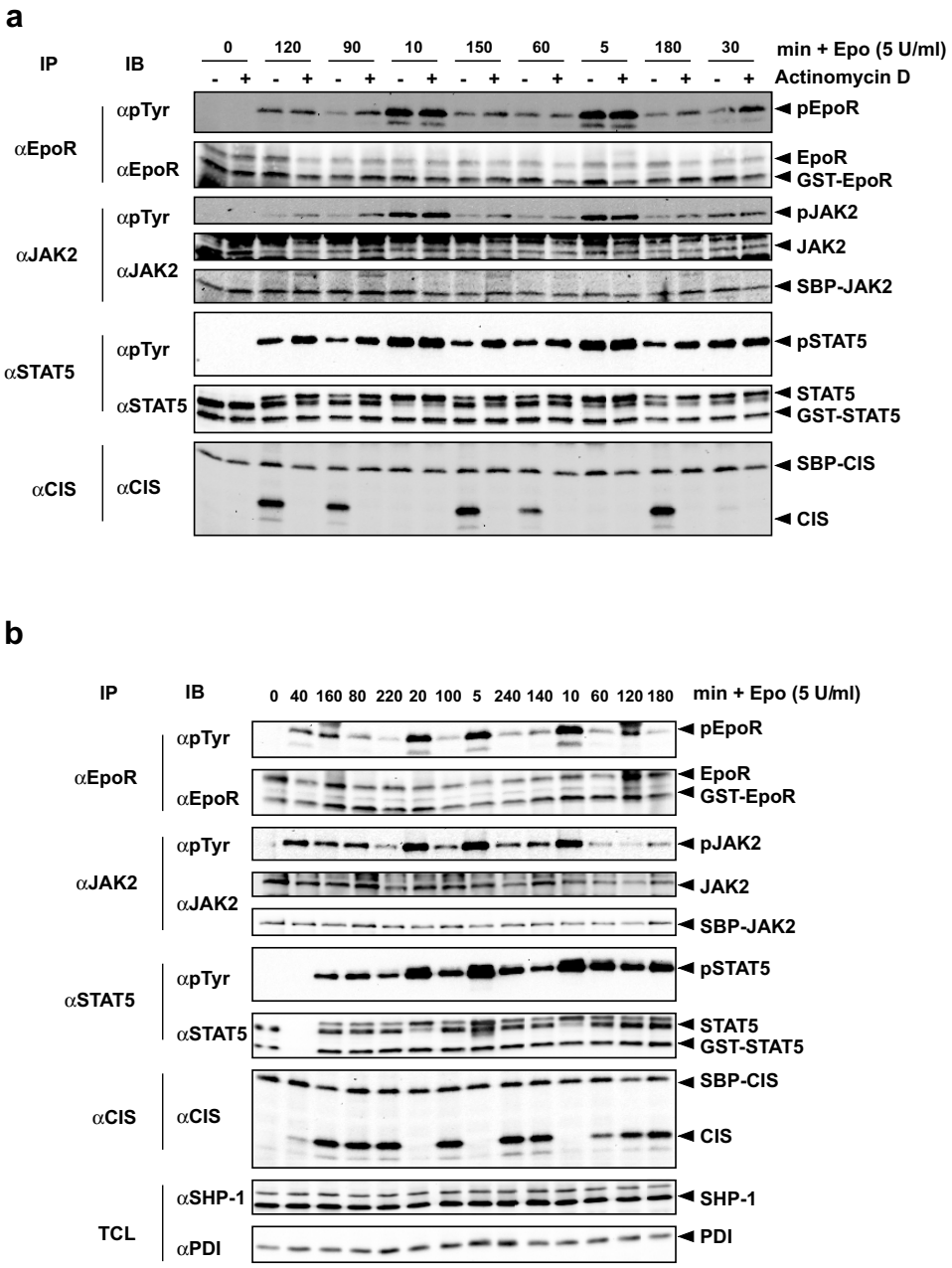

Figure S2: Quantitative immunoblotting data of time-course experiments in primary erythroid progenitor cells stimulated with erythropoietin

Freshly isolated primary erythroid progenitor cells of the colony-forming unit erythroid stage (CFU-E) were stimulated with 5 U/ml Epo and samples were taken up to 240 min. Representative examples are shown for (a) CFU-E cells treated with either 1 μg/ml actinomycin D or with vehicle (0.1 % dimethylsulfoxide) alone for 10 min prior to Epo stimulation and (b) CFU-E cells. At the indicated time points cellular lysates were subjected to immunoprecipitation (IP) and separated by SDS-PAGE order followed by quantitative immunoblotting (IB) based on chemiluminescence detection. SBP-JAK2, GST-EpoR, GST-STAT5, SBP-CIS were added prior to IP acting as calibrators to normalise the data. To prevent correlated errors in neighboring lanes due to inhomogenities in the polyacrylamide gel and the transfer to the membrane, samples were loaded in a randomized order on the gel (Schilling *et al.*, 2005).

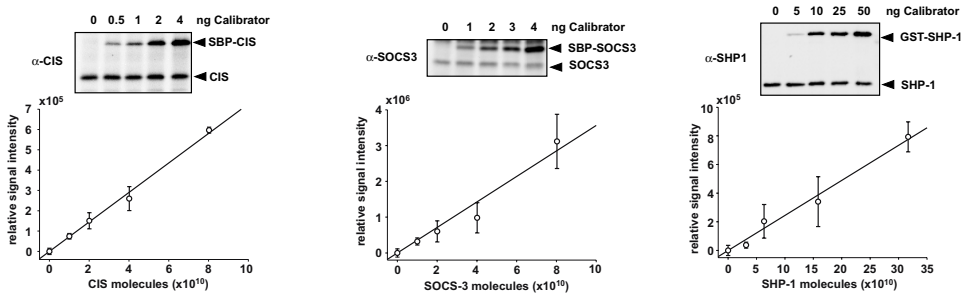

Figure S3: Quantification of molecules per cells of pathway components
Endogenous protein levels of JAK/STAT pathway components were estimated in cellular lysates of CFU-E cells by means of dilution series ($n = 3$) of added recombinant calibrator proteins. To determine CIS and SOCS3 levels, cells were stimulated with 5 U/ml Epo for 2 h. After lysis proteins were immunoprecipitated and analyzed by quantitative immunoblotting based on chemiluminescence detection. Dilution series of recombinant proteins were plotted with respective linear regression functions (solid lines) for SHP1 in $1 \cdot 10^7$ CFU-E cells, for CIS in $1 \cdot 10^7$ CFU-E cells and for SOCS3 in $5 \cdot 10^6$ CFU-E cells. Molecules per cell were calculated by means of the respective regression function.

species	molecules/cell		
JAK2	23700	±	13000
STAT5	20000	±	10000
SHP1	8500	±	1700
CIS	6500	±	700
SOCS3	2600	±	900
EpoR on surface	∼1000		

Table S1: Molecules per cell of JAK2/STAT5 pathway components estimated in CFU-E cells
The concentrations were calculated considering the volumes and surface areas for CFU-E cells (cytoplasm: 400 μm^3, nucleus; 275 μm^3, surface area: 372 μm^2). Cytoplasmic and nuclear volume was estimated from z-stack data by measuring the whole cell area or nuclear area of each slice in ImageJ and calculating the respective volume by summing up the voxels per slice (Pfeifer *et al.*, 2010). The number of molecules per cell for EpoR on the surface of CFU-E cells was reported previously (Landschulz *et al.*, 1989).

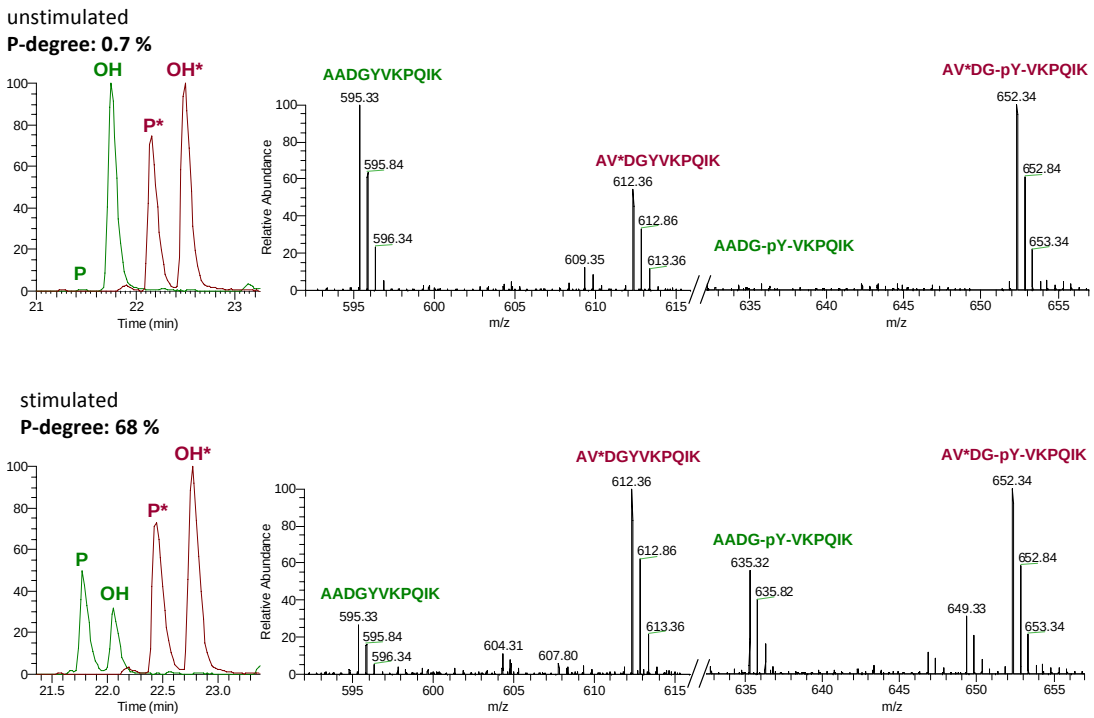

Figure S4: Determination of STAT5B phosphorylation degree by mass spectrometry
Phosphorylation degree determination of STAT5B at Tyr694. Primary CFU-E cells were starved and stimulated with 5 Units/ml Epo for 10 min. Lysates were subjected to immunoprecipitation and SDS-PAGE with STAT5 antibody. STAT5 corresponding bands were analyzed by UPLC-ESI-MS/MS using homologue and isotopically labelled standards, each for the phosphopeptide (-P*) and nonphosphorylated peptide (-OH*) added at a -P*:-OH* molar ratio of 1:1. The chromatograms (left hand panels) show elution of cell-derived peptides (-P and -OH) and their homologue isotopically labelled analogues and demonstrate the Epo-induced phosphorylation. The corresponding mass spectra (right hand panels) in addition show the mass shift of 34 Da between analytes and standards. Data represents one representative example of 4 independent replicates.

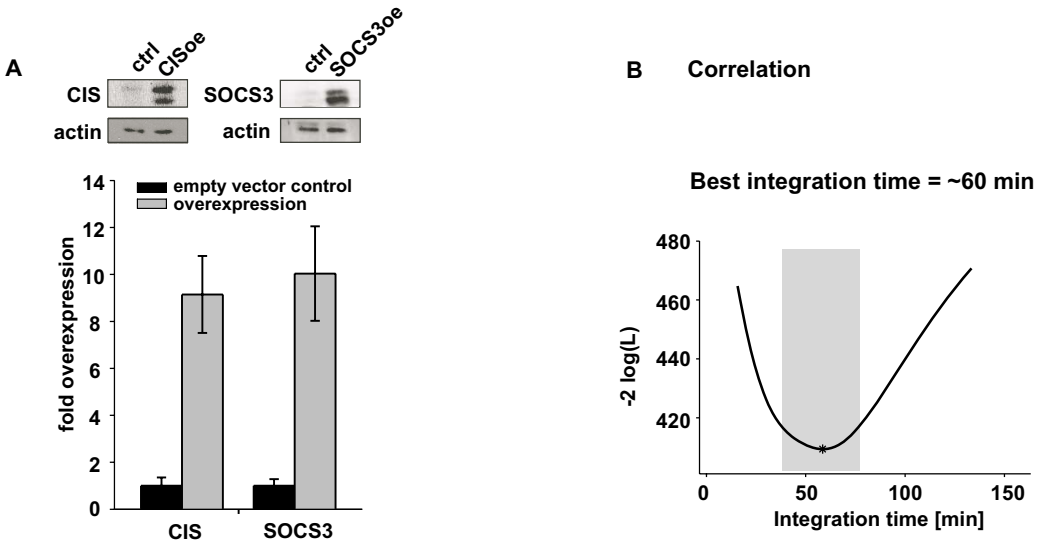

Figure S5: Quantification of CIS and SOCS3 overexpression and correlation analysis of npSTAT5 and survival data.
(A) Overexpression levels of CIS and SOCS3 determined by immunoblotting for TUNEL assay experiments. CFU-E cells were lysed and samples were subjected to immunoblotting with CIS and SOCS3 antibodies to determine overexpression levels. (B) Comparison of the agreement of experimental obtained survival data and the integral npSTAT5 response predicted by the model in terms of log-likelihood for varying integration times. As the duration of nuclear activated STAT5 presence that is necessary to induce a survival response is unknown, we tested which integration time showed the strongest relationship to the experimentally determined survival rates. The integral npSTAT5 response correlates best with the survival rate for an integration time of about 60 minutes. The grey shaded region displays the 95% confidence interval for the determined integration time.

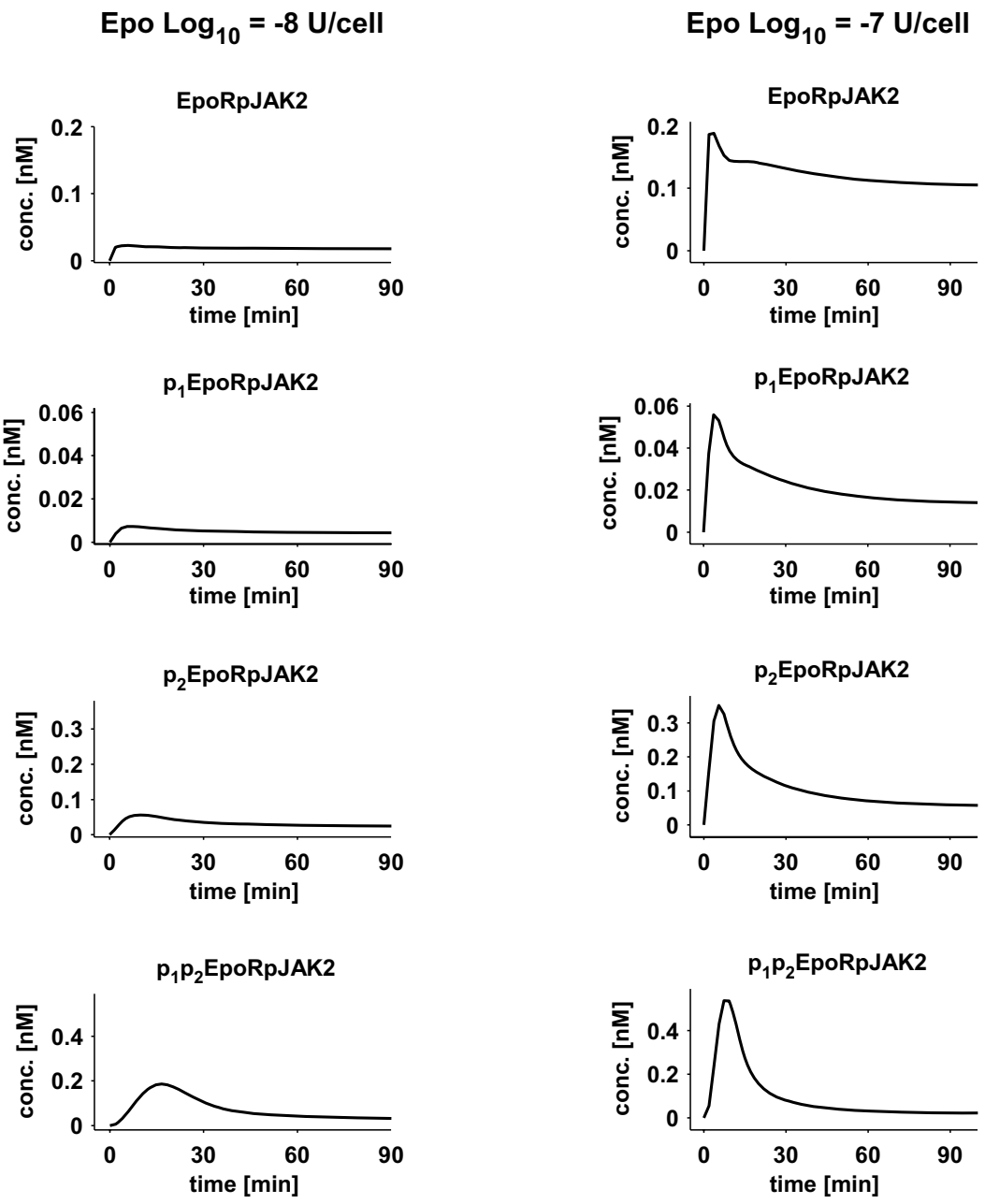

Figure S6: Calculation of increase of ratio pJAK2 relative to pEpoR
The four phosphorylated receptor complex variables were plotted for two different Epo concentrations: Epo $\log_{10} = -7$ and -8 Units/ml. At the higher Epo concentration the quantity EpoR_pJAK2 increases relative to the variables where the receptor is phosphorylated as well, see e.g. at t = 30 min. The observable pJAK2 is the sum of the four model variables p1EpoR_pJAK2, p2EpoR_pJAK2, p1p2_EpoRpJAK2 and EpoR_pJAK2. The observable pEpoR is represented by p1EpoR_pJAK2, p2EpoR_pJAK2 and p1p2_EpoRpJAK2.

variable	parameter	value	p-value	standardized coefficients	contribution [%]
pEpoRauc	p_1	$2.34 \cdot 10^{-14}$	0.5	$1.50 \cdot 10^{-14}$	$2.31 \cdot 10^{-24}$
pJAK2auc	p_2	$4.60 \cdot 10^{-10}$	0.5	$1.20 \cdot 10^{-9}$	$1.50 \cdot 10^{-16}$
npSTAT5auc	p_3	0.0621	$< 1 \cdot 10^{-6}$	0.9765	**99.32**
CISauc	p_4	$3.71 \cdot 10^{-5}$	0.38	0.0053	$2.99 \cdot 10^{-3}$
SOCS3auc	p_5	0.0011	$1 \cdot 10^{-5}$	0.0805	0.67

Table S2: Results of regression statistics for contribution to survival signal

1.1 Contributions to survival signal

In order to infer the contributions to the survival signal shown in Fig. 5 of the main text the following function was considered:

$$[\text{survival}] = p_0 + p_1 \cdot [\text{pEpoRauc}] + p_2 \cdot [\text{pJAK2auc}] + p_3 \cdot [\text{npSTAT5auc}] + p_4 \cdot [\text{CISauc}] + p_5 \cdot [\text{SOCS3auc}], \quad (1)$$

where p_0 is an offset parameter and 'auc' denotes the integrated signal of the respective species until 60 minutes, see in Fig. S5. We apply standard regression statistics for linear models, see in Table S2 and in Backhaus *et al.* (1996). The p-value of the one-sided t-test indicated that only the parameters p_3 and p_5 do have statistically significant non-zero contributions. Via the standardized regression coefficients we can translate the values of the parameters to percentage contributions of explained variance. p_3 and its corresponding variable, the integrated npSTAT5 response, contribute more than 99%.

1.2 Insufficient siRNA knockdown efficiency of SOCS members in primary murine CFU-E cells

We tested different techniques to generate siRNA knockdowns of the SOCS family members in primary erythroid progenitor cells. Retro-, lenti- and adenoviral vectors were used expressing different shRNA constructs targeting the mRNA of one of the SOCS family members in primary erythroid cells at the CFU-E stage. However, the knockdown efficiencies achieved with these experimental techniques were insufficient. A potential explanation for these results is the time period available for experiments of 12-20 h after transduction that may be too short to observe siRNA-mediated knockdown in these cells. The time frame of the experiments, however, can not be extended since erythroid progenitor cells start to terminally differentiate after 12 h. The study of Yu *et al.* (2003), reviewed in Alexander and Hilton (2004), generated stable Th2 cell lines overexpressing SOCS3 antisense constructs in the lymphoid lineage, a method that cannot be applied to primary cells.

Another possible explanation of the insufficient knockdown in the primary cells is the rapid turnover of SOCS mRNA that could limit siRNA efficacy. Larsson *et al.* (2010) have shown that high pre-existing mRNA turnover rate is associated with reduced susceptibility to silencing by siRNAs.

1.3 Expression of anti-apoptotic STAT5 target gene Pim-1

To further analyze the direct correlation between the integral response of phosphorylated STAT5 in the nucleus and the survival decision of erythroid progenitor cells (Fig. 6C of the main text), we investigated the induction of anti-apoptotic target genes. Global gene expression demonstrated that exclusively Pim-1 is rapidly induced compared to untreated control cells (Fig. S7A). Because it was also previously identified as STAT5-modulated anti-apoptotic effector (Menon *et al.*, 2006; Sathyanarayana *et al.*, 2008), we selected Pim-1 as representative candidate for further experiments. In contrast, Bcl-xL, which was discussed earlier to be important for survival in erythroid cell lines (Silva *et al.*, 1999; Socolovsky *et al.*, 1999), showed upregulation only very late after 15-20 h and Bcl-2 showed no significant modulation. BIM as pro-apoptotic factor was repressed upon Epo stimulation. These results are in line with the expression pattern of pro-survival factors observed by Sathyanarayana *et al.* (2008) who investigated Epo-dependent

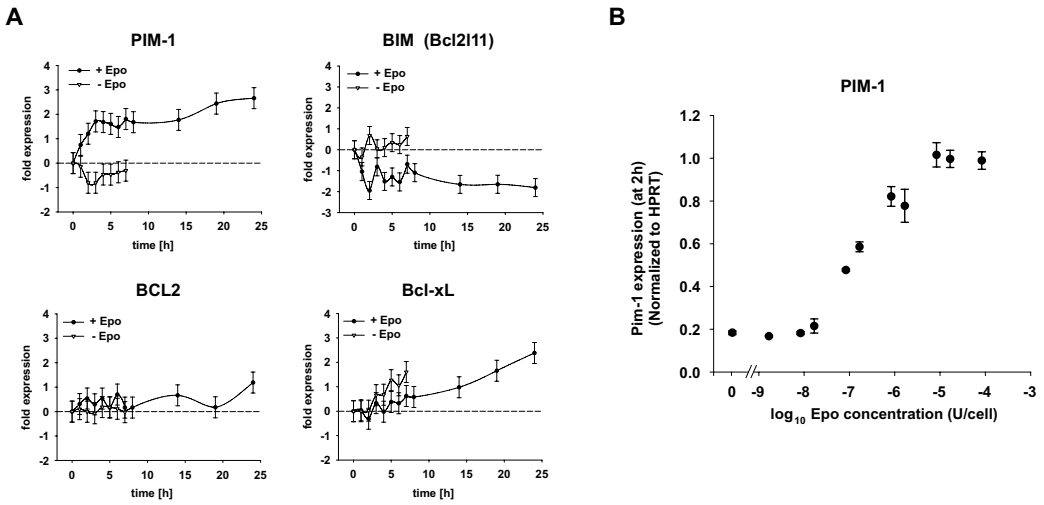

Figure S7: Epo-dependent expression of anti-apoptotic factors in primary erythroid progenitor cells at the CFU-E stage.
(A) Time series of Pim-1, BIM, BCL-2 and Bcl-xL with 0.5 Units/ml and without Epo stimulation as control. Freshly isolated and MACS sorted primary CFU-E cells from murine fetal livers were starved, stimulated or left untreated over a period of 8h or 24h. After 8h the untreated time course was stopped due to increase of CFU-E cell death without Epo stimulation. RNA was extracted at different time-points and subjected to microarray analysis. Log_2-fold change of mRNA levels were calculated relative to the time-point t = 0. (B) Quantitative RT-PCR analysis of Pim-1 expression stimulated with various Epo concentrations at 2h. Freshly isolated CFU-E cells were starved and stimulated with the indicated Epo concentrations, prepared RNA was reverse transcribed and used in qRT-PCR analysis. Values represent means with SD for n = 3 independent reverse transcription samples. Relative concentrations were normalized using HPRT as a reference gene.

regulation of pro-survival factors in primary murine $Kit^{(+)}CD71^{(high)}Ter119^{(-)}$ erythroblasts. To examine if Pim-1 follows the integrated nuclear STAT5 response over the entire range of Epo concentrations, the upregulation of Pim-1 was determined after 2h for various Epo concentrations (Fig. S7B). The dose-dependent expression of Pim-1 mirrors the behavior of the integral pSTAT5 response (Fig. 6C of the main text), implying that the integral STAT5 response is directly proportional to transcriptional responses of direct target genes.

1.4 Impact of stochasticity on nuclear phosphorylated STAT5

Intrinsic stochasticity was simulated using the Stochastic Simulation Algorithm (Gillespie, 1977), see Fig. S8. To mimic the effect of extrinsic stochasticity of a cell population, we simulated the ODE model for multiple protein initial concentrations drawn from a normal distributed centered around the estimated value with 10% variation, see Fig. S9 and also in (Spencer *et al.*, 2009). If the variability in the STAT5 response in single cells simulated by intrinsic or extrinsic stochasticity is the main source to explain the all-or-none survival decision, a bi-stable behavior would be expected. However, in both cases, the trajectory of npSTAT5 is rather negligibly affected by noise and does not show bi-stability. We therefore suggest that other individual cell-to-cell differences cause the all-or-none response of cell death or survival.

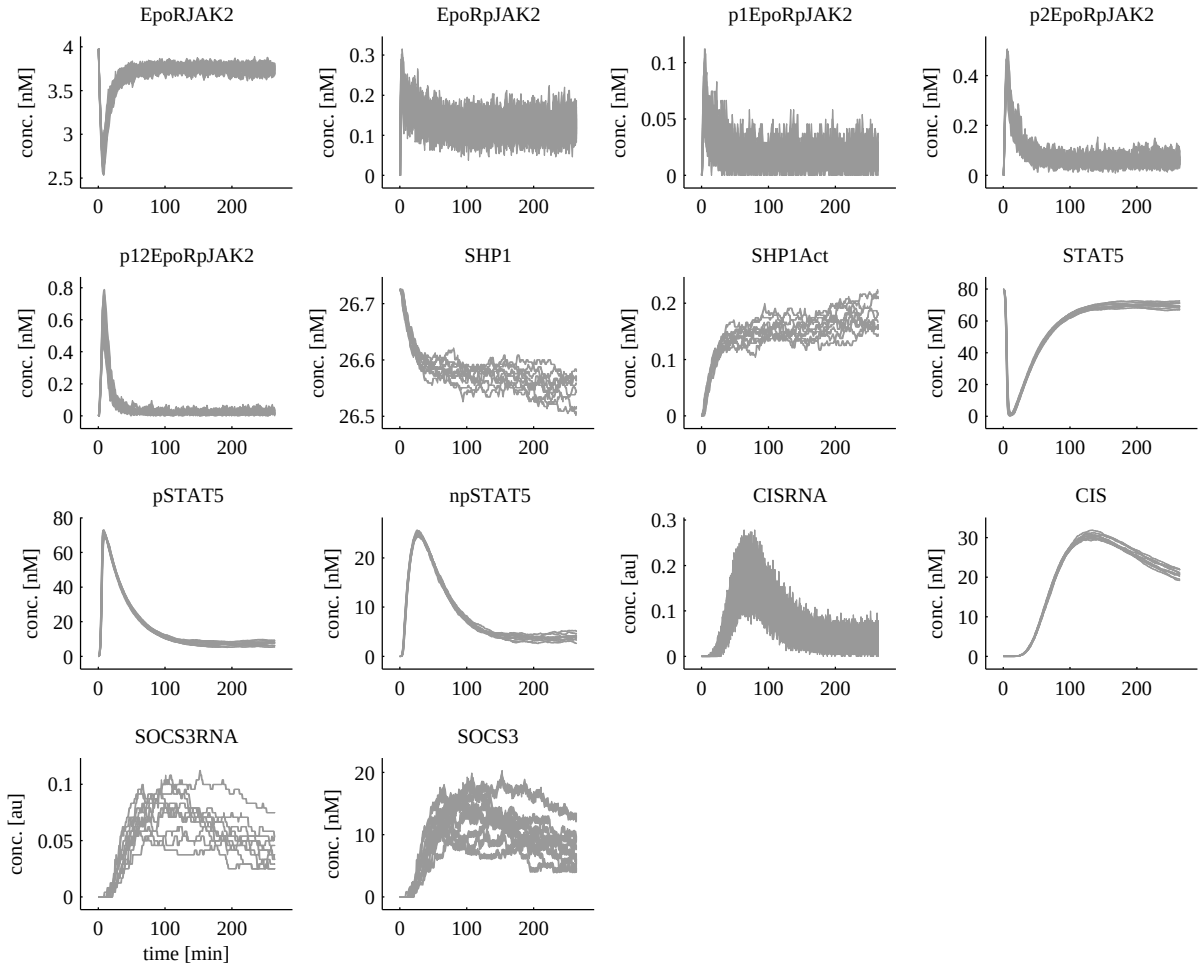

Figure S8: Simulation of the effect of intrinsic noise on the model dynamics.
The effect of intrinsic noise on the model dynamics were calculated by the Stochastic Simulation Algorithm (Gillespie, 1977). Ten realizations are displayed. As the profile likelihood analysis shows, see in Section 2.5, the upper bound for the parameters SOCS3Turn and CISRNATurn is not determined. To reduce the computation time for SSA these parameter were set to 10^1, which is in agreement with the experimental data. The dynamics of npSTAT5 is affected by intrinsic noise only negligibly.

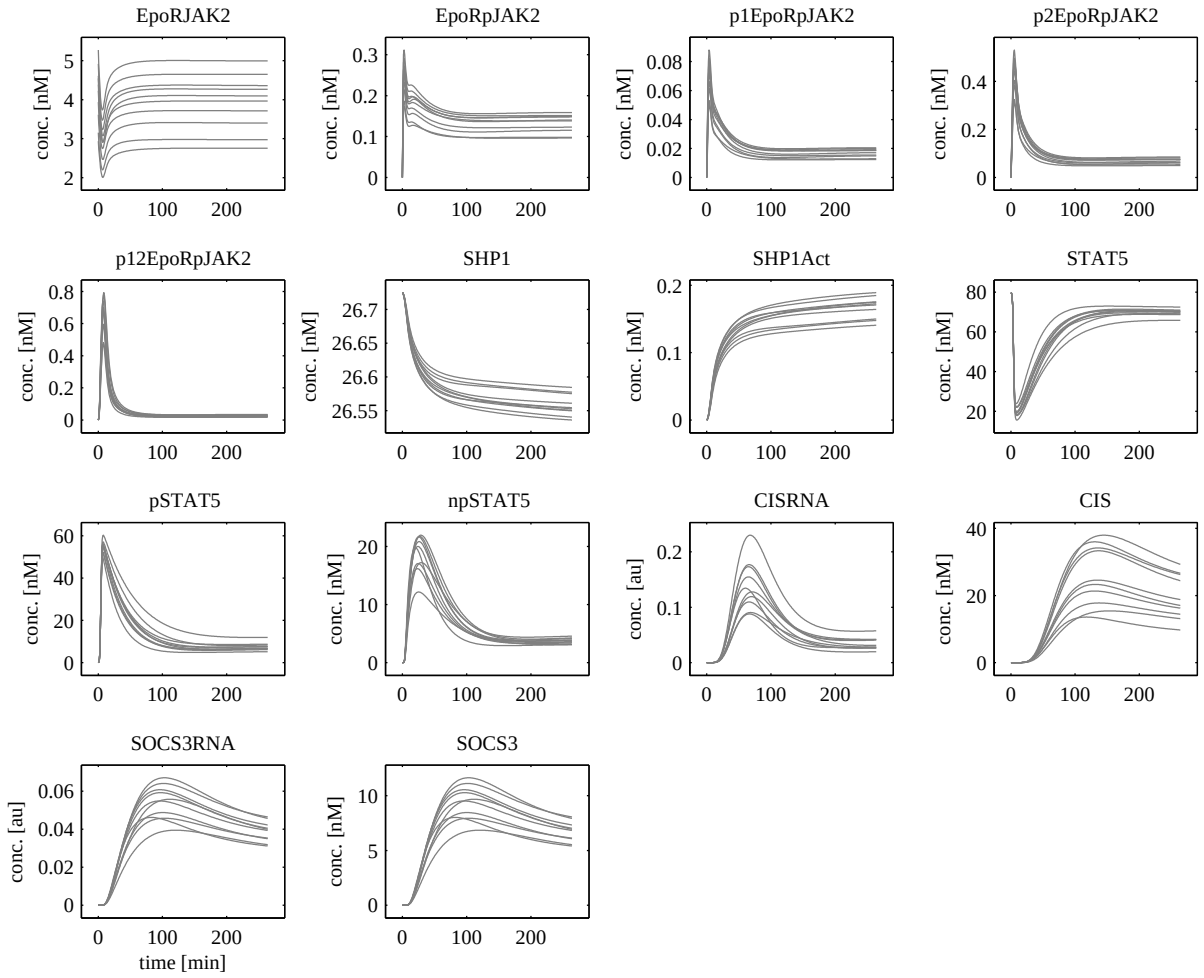

Figure S9: Simulation of the effect of extrinsic noise on the model dynamics.
The figure shows the effect of extrinsic noise on the model dynamics. For the computation, the parameters accounting for the concentration level of the modeled components, CISEqc, CISRNAEqc, SOCS3Eqc, SOCS3RNAEqc, init_EpoRJAK2, init_SHP1 and init_STAT5 where varied by 10% in logarithmic space around their estimated values. Ten realizations are displayed. The qualitative behaviour of the model dynamics, especially the STAT5 activation, is not affected by extrinsic noise, e.g. bi-stability does not occur in the parameter ranges that are determined by the experimental data.

2 Supplementary Model Results

In the following, the mathematical model describing the dynamics of the biological system by ordinary differential equations (ODEs), the mapping of the model outputs to the experimental data for each of the different experimental conditions, and the estimation of the unknown model parameters from the experimental data is described in detail. Furthermore, an analysis of the uncertainties in the estimated parameters due to the limited quality of the experimental data is presented in terms of identifiability and confidence intervals. Finally, the remaining parameter uncertainties are in turn translated to uncertainties in the model predictions in terms of confidence intervals of the model trajectories. This procedure allows for a realistic reasoning about the biological questions that should be addressed by the modeling approach.

On demand, we can supply MATLAB code that disburdens the re-implementation of the project by supplying the ODE model, the connection of model outputs to the data sets, the efficient ODE solver and the parameter estimation procedure itself.

2.1 Modeling concept

Cellular processes can be modeled using a system of ordinary differential equations (ODEs), see e.g. in Wolkenhauer (2008). To adequately describe the underlying biological process with this mathematical framework spatial effects have to be neglected by assuming that diffusion is fast compared to the reaction rates of the protein interactions and the spatial extend of a cell. Intrinsic stochasticity of the discrete dynamics of molecular reactions can be neglected, if the copy number of molecules is sufficiently large, i.e. for a protein copy number > 10 (Taniguchi *et al.*, 2010). In Fig. S8, intrinsic stochasticity was simulated ten times, using the Stochastic Simulation Algorithm (Gillespie, 1977) for the parameters values estimated by the ODE framework. The dynamics of npSTAT5, the quantity of interest for the biological question, are affected by intrinsic noise only negligibly. Extrinsic noise due to cell to cell variability, can be illustrated by simulating the ODE dynamics for varying parameter values, such as initial protein concentration. In Fig. S9, extrinsic stochasticity was simulated ten times, using parameters values estimated by the ODE framework with normally distributed variations in the initial protein concentrations of 10% in logarithmic space. The qualitative behaviour of the model dynamics, especially the STAT5 activation, is not affected by extrinsic noise, e.g. bi-stability does not occur for the parameter ranges that are determined by the experimental data. Moreover, stochastic effects are suppressed, if the dynamics of protein concentration is modeled as average over a cell population using experimental data obtained from averaging over many cells. This applies for many measurement techniques such as immunoblotting or quantitative RT-PCR. The experimental data used here contains an average over $\approx 4 \cdot 10^7$ cells. Consequently, the resulting ODE framework describes the average behaviour of a cell.

The dynamics of the concentrations of n biological compounds $\vec{x}$ such as proteins in different phosphorylation states that are involved in a biological system, described by an ODE framework, is given by

$$\dot{\vec{x}}(t,\theta) = \vec{f}(\vec{x}(t,\theta),\vec{u}(t),\theta) \quad (2)$$

$$\vec{x}(0,\theta) = \vec{w}(\theta). \quad (3)$$

The dynamical behavior may depend on an input function $\vec{u}(t)$ such as a treatment with ligands and model parameters $\theta = \{\theta_1 \dots \theta_l\}$ such as rate constants or initial concentrations that are usually unknown for *in vivo* systems and need to be estimated from experimental data. Each component of $\vec{f}$ in Eq. 2 is usually composed of a sum of several reaction fluxes v_j that correspond to the interactions present

$$\dot{\vec{x}}(t,\theta) = \mathbf{N} \cdot \vec{v}(\vec{x}(t,\theta),\vec{u}(t),\theta) \quad (4)$$

where $\mathbf{N}$ is the stoichiometry matrix, see e.g. in Heinrich and Schuster (1996). Eq. 3 indicates that the initial conditions $\vec{x}(0)$ for Eq. 2 might also be dependent on the model parameters θ that need to be estimated.

In order to compare the simulated model dynamics with experimental data, the dynamics given by Eq. 2 are mapped by a function $\vec{g}$ to m model outputs

$$\vec{y}(t_i, \theta) = \vec{g}(\vec{x}(t_i, \theta), \theta) + \vec{\epsilon}(t_i). \tag{5}$$

The model outputs are the quantities accessible by experiments measured at times t_i. They may depend on additional parameters such as scaling or offset parameters included in θ.

The distribution of the measurement noise $\vec{\epsilon}(t_i)$ is assumed to be known, e.g. being independently normally distributed with $\epsilon_k(t_i) \sim \mathrm{N}(0, \sigma_k^2(t_i))$. For concentration measurements in biological applications it is reasonable, and was explicitly shown in the case of immunoblotting experiments (Kreutz *et al.*, 2007), that the measurement noise is log-normally distributed. Therefore, before proceeding with parameter estimation both experimental data and model outputs were transformed logarithmically.

Parameter estimation For the description of *in vivo* systems, commonly many model parameters θ are unknown and have to be estimated from experimental data $y^\dagger$. The parameters are estimated by the Maximum Likelihood Estimation (MLE) approach. For normally distributed measurement noise in Eq. 5, it is more common and equivalent to MLE to minimize $-2\log(L)$, where

$$L(y^\dagger | \, \theta) = \prod_{k=1}^{m} \prod_{i=1}^{d_k} \frac{1}{\sigma_k(t_i)\sqrt{2\pi}} \exp\left(-\frac{1}{2} \left(\frac{y_k^\dagger(t_i) - y_k(t_i, \theta)}{\sigma_k(t_i)} \right)^2 \right) \tag{6}$$

is the likelihood function. d_k denotes the number of experimental data $y_k^\dagger$ for each model output $k = 1 \dots m$ measured at time points t_i with $i = 1 \dots d_k$ and $\sigma_k(t_i)$ is the corresponding magnitude of the measurement noise. The value of this *objective function* indicates the mismatch of experimental data $y_k^\dagger(t_i)$ and the model outputs $y_k(t_i, \theta)$ predicted by the model for parameters θ. For a detailed discussion of MLE in the context of non-linear regression models, see e.g. in Seber and Wild (2003).

Measurement noise The magnitude of the measurement noise $\sigma_k(t_i)$ for each experimental technique is estimated simultaneously with the remaining parameters. Therefore, a parameterized *error model* of the form

$$\vec{\sigma}(t_i, \theta) = \vec{s}(\vec{y}(t_i, \theta), \theta) \tag{7}$$

describing the measurement noise for each model output is assumed. The additional parameters accounting for the magnitude of the measurement noise are estimated simultaneously with the remaining model parameters.

Parameter transformations Each ODE model that is realized as dimensional equations describing dimensional quantities has an intrinsic scaling invariance. This invariance originates from the free choice of units and can be exploited to reduce the number of free parameters and to disentangle dynamical parameters θ^d from "static" parameters θ^x like initial concentrations or others reflecting the concentration scale. The basic idea is to express a dynamical variable x in units of its corresponding θ^x:

$$X := \frac{x}{\theta^x}. \tag{8}$$

The unique solution $x(t, \theta^d, \theta^x)$ can then be expressed as

$$x(t, \theta^d, \theta^x) = \theta^x X(t, \Theta^d), \tag{9}$$

i.e. as the unique solution to the transformed system with transformed parameters Θ^d that are disentangled from θ^x. For most of the applied measurement techniques, the model output y is connected to the dynamical variable x by a scaling factor θ^s by

$$y(t_i) = \theta^s x(t_i). \tag{10}$$

Eq. (9) indicates that the scaling parameter θ^s is directly correlated to θ^x. This correlation is immediately resolved by the parameter transformation

$$\theta^s \rightarrow \frac{\Theta^s}{\theta^x}. \tag{11}$$

The resolution of this correlation facilitates a faster and more efficient parameter estimation. In some cases, such as for mRNA measurements of CIS and SOCS3, no experimental information was available about the absolute concentration scale that determines θ^x. Consequently these θ^x are structurally non-identifiable. Due to the nature of the applied transformations these structurally non-identifiabilities can be resolved easily by setting the corresponding θ^x to a constant value, e.g. to 1. Please note, this only fixes the scales of the dynamical variables without posing any restrictions on the shape of the dynamics. However, no prediction of absolute concentrations for the affected species can be made as long as no measurement of absolute concentration is available.

Identifiability and confidence intervals of the estimated model parameters In order to evaluate the identifiability of the model parameters and to assess confidence intervals the profile likelihood was evaluated, see in Sec. 2.5. Detailed instructions how to interpret the result are given in Raue *et al.* (2009). Briefly, the profile likelihood is sampled for each parameter individually in a manner that detects potential directions in parameter space that are not well determined by the experimental data. A profile likelihood resulting in a flat line indicates a parameter that is structurally non-identifiable, meaning that the parameter can not be inferred. A profile likelihood that rises but does not cross the desired threshold for 95% confidence intervals is practically non-identifiable, given the experimental data. A finite lower or upper confidence bound can still be available. If the profile likelihood exceeds the threshold on both sides the parameter is identifiable and can be determined with a confidence of 95% within its confidence intervals.

Confidence intervals of the predicted model dynamics In order to realistically assess the precision of model predictions, the remaining uncertainties in the parameter estimates have to be translated to the model trajectories, see in Sec. 2.6. In general, 95% time point-wise confidence intervals for the predicted dynamical model trajectories requires sampling of the respective point-wise 95% confidence region in the parameter space. Due to the high dimensionality sampling of a high-dimensional parameter space is only feasible in an approximative manner. In this work, the region of the parameter space has been sampled by evaluating the model predictions along the parameter vectors determined during the calculations of the profile likelihood, see in Raue *et al.* (2010) for details. This guarantees that the extreme points of the parameter confidence region for each parameter are sampled.

2.2 Definition of dual negative feedback model of JAK2/STAT5 signaling

The general topology of the model was constructed based on prior biological knowledge and experimental data generated in this study. To achieve reliable model predictions, we tailored the model complexity to the requirements of our biological question and generated extensive time-resolved data, using different experimental approaches. After systematically eliminating short lived protein-protein complexes and fast reactions, the model comprised 25 dynamical variables representing the time course of species concentrations and 36 reactions involving 29 parameters that characterize the dynamical behavior. The model structure is depicted in Fig. S10.

To explain the events at the plasma membrane EpoR and JAK2 were modeled as a protein complex since JAK2 modulates the expression of EpoR on the cell surface (Huang *et al.*, 2001). Upon ligand binding to the EpoR, rearrangements of EpoR lead to the activation of JAK2 by transphosphorylation. Activated JAK2 then phosphorylates various tyrosine residues on the cytoplasmic domain of the receptor. This activation mechanism was reflected by considering different activation states of the receptor complex. It has been previously shown that CIS-GFP can bind unspecifically to the EpoR lacking the STAT5 recruitment site Y401 if expressed in high amounts (Ketteler *et al.*, 2003). To include this information in

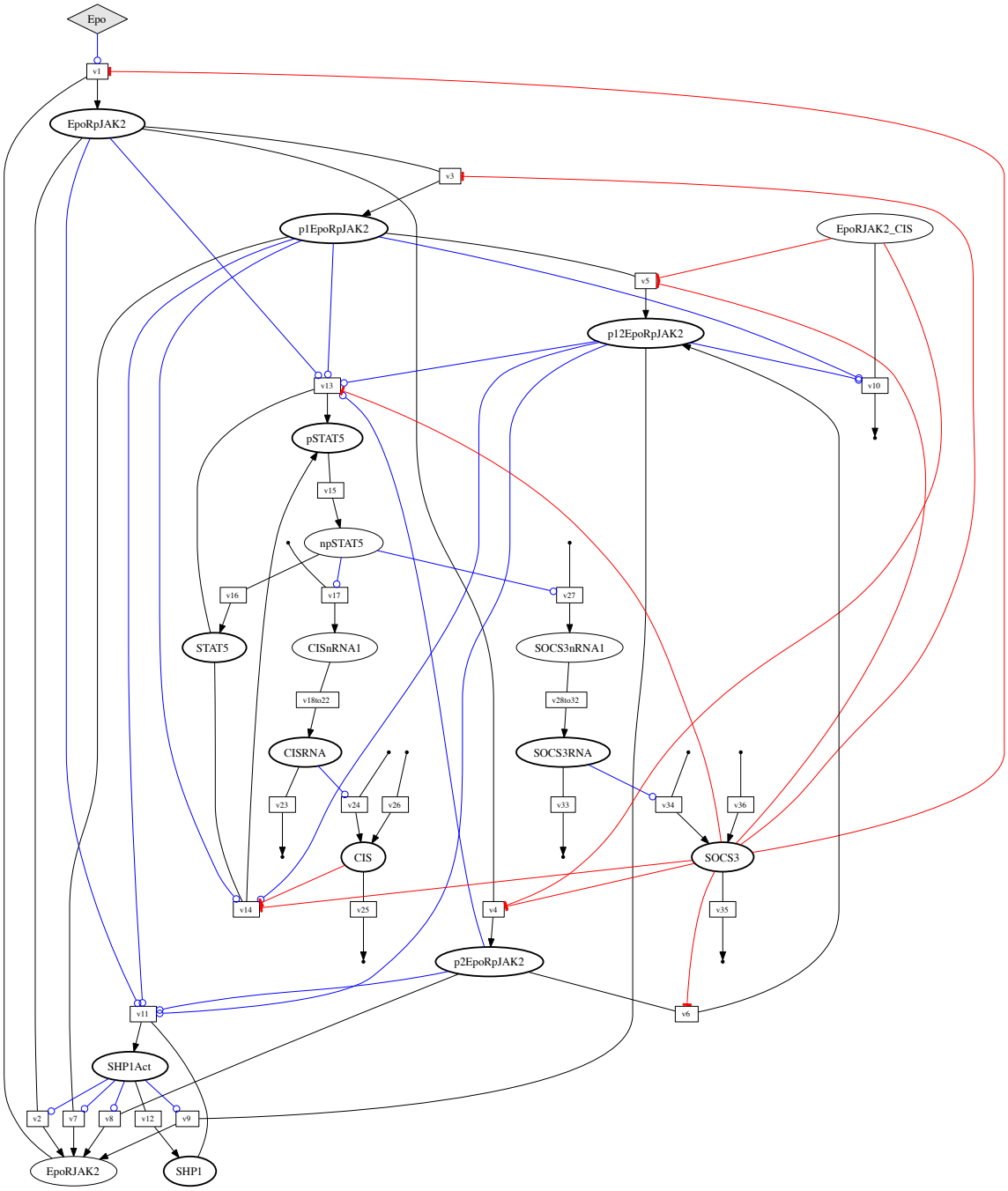

Figure S10: Network representation of dual negative feedback model of JAK2/STAT5 signaling
Diamond shaped nodes correspond to model inputs, see Eq. 12. Ellipsoid shaped nodes correspond to dynamical variables described by the ODE system, see Eq. 49 – 73. Species npSTAT5, CISnRNA1–5 and SOCS3nRNA1–5 are located in the nuclear compartment, the remaining species in the cytoplasmatic compartment. Black arrows and box shaped nodes indicate reactions with corresponding rate equations given in Eq. 13 – 48. Red T-shaped arrows indicated inhibitorial influence on a reaction and blue O-shaped arrows indicate catalyzing influence on a reaction. Reactions v_{18} to v_{22} and v_{28} to v_{32} account for a delay that reflects the processing steps of the mRNA.

the model, two subclasses of phosphorylated tyrosines at the receptor were incorporated into the model: (i) p1_EpoR_pJAK2 represents the phosphorylated tyrosine sites Y343 and Y401 that serve as recruitment sites for STAT5 and thereby facilitate STAT5 phosphorlyation. CIS inhibits phosphorylation of STAT5 induced by this variable. (ii) p2_EpoR_pJAK2 represents the remaining phosphorylated tyrosines sites of the EpoR that do not recruit STAT5. Phosphorylation of this variable can be inhibited by high levels of CIS due to unspecific binding of CIS to the unphosphorylated EpoR (EpoRJAK2_CIS). p12_EpoR_pJAK2 represents the completely phosphorylated complex. It is important to note that the EpoR_pJAK2 variable can also account for phosphorylated JAK2 that was dissociated from the EpoR.

In general, phosphatase activities were included in the model as dephosphorylation reactions that are proportional to the substrate with a time-independent kinetics. Ligand-dependent attenuation, for instance by receptor internalization and dephosphorylation was summarized by including SHP1-mediated deactivation of JAK2 and EpoR as described in a previous model of CFU-E cells (Schilling *et al.*, 2009). The tyrosine phosphatase SHP1 has previously been shown to require binding to the specific phosphorylated tyrosine residue Tyr429 on the EpoR to activate phosphatase activity (Pei *et al.*, 1996; Klingmüller *et al.*, 1995). Therefore, SHP1 was considered to exist in two states in the model: one active and one inactive form. The transition of inactive to catalytically active SHP1 is mediated by phosphorylated EpoR that reflects the recruitment to the specific phosphotyrosine residue. The activated form of SHP1 then catalyzes dephosphorylation of JAK2 and EpoR (pEpoR $\rightarrow$ EpoR, catalyzed by SHP1Act).

Phosphorylation of STAT5 by JAK2 is mediated by recruiting STAT5 to phosphotyrosine 343 and 401 of the EpoR cytoplasmic domain that functions as a scaffold (Gobert *et al.*, 1996; Barber *et al.*, 2001; Klingmüller *et al.*, 1996). Hence, phosphorylated JAK2 was considered in the model as the enzyme and the phosphorylated EpoR as an additional modifier. Both contribute as the p1(2)_EpoR_pJAK2 complexes to phosphorylation of STAT5 by a second order term reflecting the activation by a dimer. As STAT5 phosphorylation by JAK2 is impaired in the absence of docking sites (Gobert *et al.*, 1996), we included in the model that the activation of STAT5 by EpoR_pJAK2 must always occur slower than the activation by the complexes p1(2)_EpoR_pJAK2. Dimerization of STAT5 is known to occur very rapidly after phosphorylation and could be neglected on the time-scale of our measurements. The phosphorylated STAT5 shuttles into the nucleus and binds to consensus sequences on the DNA activating gene transcription. After a certain sojourn time in the nucleus, dephosphorylated STAT5 translocates back into the cytoplasm to enter a new cycle of activation, which is an important feature of the system to continuously monitor receptor activation (Swameye *et al.*, 2003). Hence, the different forms of STAT5 were integrated in the model by three distinct variables: unphosphorylated STAT5 in the cytosol (STAT5), phosphorylated STAT5 dimers in the cytosol (pSTAT5), and phosphorylated STAT5 dimers in the nucleus (npSTAT5). Three parameters describe the transitions between these variables: STAT5 activation, the import rate into the nucleus, and the export rate back into the cytosol that includes dissociation and dephosphorylation.

Phosphorylated STAT5 in the nucleus induces the expression of the negative feedback regulators CIS and SOCS3 based on our observations using gene expression profiling and immunoblotting analysis that revealed a rapid and strong upregulation of both SOCS members in Epo-induced CFU-E cells. Hence, CIS and SOCS3 were both included into the mathematical model as transcriptional feedbacks. Previously, SOCS3 has been proposed to bind via its SH2 domain to activated EpoR and JAK2 and to inhibit JAK2 activity by directly binding to the kinase activation loop via its KIR domain (Hörtner *et al.*, 2002; Sasaki *et al.*, 1999, 2000; Babon *et al.*, 2006). CIS was identified as negative regulator of JAK/STAT signaling by binding to phosphotyrosine 401 of the EpoR, thereby competing for receptor binding with STAT5 (Ketteler *et al.*, 2003; Yoshimura *et al.*, 1995). Hence, SOCS3 and CIS were included in the model at different levels of signal transmission: CIS was considered as inhibitor of STAT5 activation only mediated by the p1EpoR_pJAK2 complex. Additionally, CIS can inhibit phosphorylation of p2EpoRJAK2 due to unspecific binding (EpoR_JAK2_CIS). In contrast, SOCS3 can inhibit JAK2 activation and the downstream events of STAT5 activation, i.e. phosphorylation of EpoR and recruitment of STAT5 to the specific pTyr binding sites on the EpoR. Therefore, SOCS3 in the model inhibits STAT5 phosphorylation mediated by both EpoR_pJAK2 and p1(2)_EpoR_pJAK2.

The ODE model In the mathematical expressions that follow, the dynamical variables are indicated by square brackets and are given in nM. The model dynamics depends on an external treatment with erythropoietin, see in Eq. 2, given in units/cell:

$$[\text{Epo}](t) = \text{epo\_level} \tag{12}$$

The rate equations corresponding to the reactions included in the model are give by:

$$v_1 = \frac{[\text{Epo}] \cdot [\text{EpoRJAK2}] \cdot \text{JAK2ActEpo}}{[\text{SOCS3}] \cdot \text{SOCS3Inh} + 1} \tag{13}$$

$$v_2 = [\text{EpoRpJAK2}] \cdot \text{JAK2EpoRDeaSHP1} \cdot [\text{SHP1Act}] \tag{14}$$

$$v_3 = \frac{[\text{EpoRpJAK2}] \cdot \text{EpoRActJAK2}}{[\text{SOCS3}] \cdot \text{SOCS3Inh} + 1} \tag{15}$$

$$v_4 = \frac{3 \cdot [\text{EpoRpJAK2}] \cdot \text{EpoRActJAK2}}{(\text{EpoRCISInh} \cdot [\text{EpoRJAK2\_CIS}] + 1) \cdot ([\text{SOCS3}] \cdot \text{SOCS3Inh} + 1)} \tag{16}$$

$$v_5 = \frac{3 \cdot \text{EpoRActJAK2} \cdot [\text{p1EpoRpJAK2}]}{(\text{EpoRCISInh} \cdot [\text{EpoRJAK2\_CIS}] + 1) \cdot ([\text{SOCS3}] \cdot \text{SOCS3Inh} + 1)} \tag{17}$$

$$v_6 = \frac{\text{EpoRActJAK2} \cdot [\text{p2EpoRpJAK2}]}{[\text{SOCS3}] \cdot \text{SOCS3Inh} + 1} \tag{18}$$

$$v_7 = \text{JAK2EpoRDeaSHP1} \cdot [\text{SHP1Act}] \cdot [\text{p1EpoRpJAK2}] \tag{19}$$

$$v_8 = \text{JAK2EpoRDeaSHP1} \cdot [\text{SHP1Act}] \cdot [\text{p2EpoRpJAK2}] \tag{20}$$

$$v_9 = \text{JAK2EpoRDeaSHP1} \cdot [\text{SHP1Act}] \cdot [\text{p12EpoRpJAK2}] \tag{21}$$

$$v_{10} = [\text{EpoRJAK2\_CIS}] \cdot \text{EpoRCISRemove} \cdot ([\text{p12EpoRpJAK2}] + [\text{p1EpoRpJAK2}]) \tag{22}$$

$$v_{11} = [\text{SHP1}] \cdot \text{SHP1ActEpoR} \cdot ([\text{EpoRpJAK2}] + [\text{p12EpoRpJAK2}] + [\text{p1EpoRpJAK2}] + [\text{p2EpoRpJAK2}]) \tag{23}$$

$$v_{12} = \text{SHP1Dea} \cdot [\text{SHP1Act}] \tag{24}$$

$$v_{13} = \frac{[\text{STAT5}] \cdot \text{STAT5ActJAK2} \cdot ([\text{EpoRpJAK2}] + [\text{p12EpoRpJAK2}] + [\text{p1EpoRpJAK2}] + [\text{p2EpoRpJAK2}])}{[\text{SOCS3}] \cdot \text{SOCS3Inh} + 1} \tag{25}$$

$$v_{14} = \frac{[\text{STAT5}] \cdot \text{STAT5ActEpoR} \cdot ([\text{p12EpoRpJAK2}] + [\text{p1EpoRpJAK2}])^2}{([\text{CIS}] \cdot \text{CISInh} + 1) \cdot ([\text{SOCS3}] \cdot \text{SOCS3Inh} + 1)} \tag{26}$$

$$v_{15} = \text{STAT5Imp} \cdot [\text{pSTAT5}] \tag{27}$$

$$v_{16} = \text{STAT5Exp} \cdot [\text{npSTAT5}] \tag{28}$$

$$v_{17} = -\text{CISRNAEqc} \cdot \text{CISRNATurn} \cdot [\text{npSTAT5}] \cdot (\text{ActD} - 1) \tag{29}$$

$$v_{18} = [\text{CISnRNA1}] \cdot \text{CISRNADelay} \tag{30}$$

$$v_{19} = [\text{CISnRNA2}] \cdot \text{CISRNADelay} \tag{31}$$

$$v_{20} = [\text{CISnRNA3}] \cdot \text{CISRNADelay} \tag{32}$$

$$v_{21} = [\text{CISnRNA4}] \cdot \text{CISRNADelay} \tag{33}$$

$$v_{22} = [\text{CISnRNA5}] \cdot \text{CISRNADelay} \tag{34}$$

$$v_{23} = [\text{CISRNA}] \cdot \text{CISRNATurn} \tag{35}$$

$$v_{24} = [\text{CISRNA}] \cdot \text{CISEqc} \cdot \text{CISTurn} \tag{36}$$

$$v_{25} = [\text{CIS}] \cdot \text{CISTurn} \tag{37}$$

$$v_{26} = \text{CISoe} \cdot \text{CISTurn} \cdot \text{CISEqcOE} \tag{38}$$

$$v_{27} = -\text{SOCS3RNAEqc} \cdot \text{SOCS3RNATurn} \cdot [\text{npSTAT5}] \cdot (\text{ActD} - 1) \tag{39}$$

$$v_{28} = [\text{SOCS3nRNA1}] \cdot \text{SOCS3RNADelay} \tag{40}$$

$$v_{29} = [\text{SOCS3nRNA2}] \cdot \text{SOCS3RNADelay} \tag{41}$$

$$v_{30} = [\text{SOCS3nRNA3}] \cdot \text{SOCS3RNADelay} \tag{42}$$

$$v_{31} = [\text{SOCS3nRNA4}] \cdot \text{SOCS3RNADelay} \tag{43}$$

$$v_{32} = [\text{SOCS3nRNA5}] \cdot \text{SOCS3RNADelay} \tag{44}$$

$$v_{33} = [\text{SOCS3RNA}] \cdot \text{SOCS3RNATurn} \tag{45}$$

$$v_{34} = [\text{SOCS3RNA}] \cdot \text{SOCS3Eqc} \cdot \text{SOCS3Turn} \tag{46}$$

$$v_{35} = [\text{SOCS3}] \cdot \text{SOCS3Turn} \tag{47}$$

$$v_{36} = \text{SOCS3oe} \cdot \text{SOCS3Turn} \cdot \text{SOCS3EqcOE} \tag{48}$$

Reactions v_{18} to v_{22} and v_{28} to v_{32} account for a delay that summarize the processing steps of the mRNA by a linear chain of reactions (MacDonald, 1976) with common rate constant CISRNADelay

and SOCS3RNADelay, respectively. The ODE system, see Eq. 2, determining the time evolution of the dynamical variables is composed out of the rate equations, see Eq. 4, by:

$$\begin{aligned}
\mathrm{d[EpoRJAK2]}/\mathrm{d}t &= -v_1 + v_2 + v_7 + v_8 + v_9 && (49)\\
\mathrm{d[EpoRpJAK2]}/\mathrm{d}t &= +v_1 - v_2 - v_3 - v_4 && (50)\\
\mathrm{d[p1EpoRpJAK2]}/\mathrm{d}t &= +v_3 - v_5 - v_7 && (51)\\
\mathrm{d[p2EpoRpJAK2]}/\mathrm{d}t &= +v_4 - v_6 - v_8 && (52)\\
\mathrm{d[p12EpoRpJAK2]}/\mathrm{d}t &= +v_5 + v_6 - v_9 && (53)\\
\mathrm{d[EpoRJAK2_CIS]}/\mathrm{d}t &= -v_{10} && (54)\\
\mathrm{d[SHP1]}/\mathrm{d}t &= -v_{11} + v_{12} && (55)\\
\mathrm{d[SHP1Act]}/\mathrm{d}t &= +v_{11} - v_{12} && (56)\\
\mathrm{d[STAT5]}/\mathrm{d}t &= -v_{13} - v_{14} + v_{16} \cdot \frac{0.275}{0.4} && (57)\\
\mathrm{d[pSTAT5]}/\mathrm{d}t &= +v_{13} + v_{14} - v_{15} && (58)\\
\mathrm{d[npSTAT5]}/\mathrm{d}t &= +v_{15} \cdot \frac{0.4}{0.275} - v_{16} && (59)\\
\mathrm{d[CISnRNA1]}/\mathrm{d}t &= +v_{17} - v_{18} && (60)\\
\mathrm{d[CISnRNA2]}/\mathrm{d}t &= +v_{18} - v_{19} && (61)\\
\mathrm{d[CISnRNA3]}/\mathrm{d}t &= +v_{19} - v_{20} && (62)\\
\mathrm{d[CISnRNA4]}/\mathrm{d}t &= +v_{20} - v_{21} && (63)\\
\mathrm{d[CISnRNA5]}/\mathrm{d}t &= +v_{21} - v_{22} && (64)\\
\mathrm{d[CISRNA]}/\mathrm{d}t &= +v_{22} \cdot \frac{0.275}{0.4} - v_{23} && (65)\\
\mathrm{d[CIS]}/\mathrm{d}t &= +v_{24} - v_{25} + v_{26} && (66)\\
\mathrm{d[SOCS3nRNA1]}/\mathrm{d}t &= +v_{27} - v_{28} && (67)\\
\mathrm{d[SOCS3nRNA2]}/\mathrm{d}t &= +v_{28} - v_{29} && (68)\\
\mathrm{d[SOCS3nRNA3]}/\mathrm{d}t &= +v_{29} - v_{30} && (69)\\
\mathrm{d[SOCS3nRNA4]}/\mathrm{d}t &= +v_{30} - v_{31} && (70)\\
\mathrm{d[SOCS3nRNA5]}/\mathrm{d}t &= +v_{31} - v_{32} && (71)\\
\mathrm{d[SOCS3RNA]}/\mathrm{d}t &= +v_{32} \cdot \frac{0.275}{0.4} - v_{33} && (72)\\
\mathrm{d[SOCS3]}/\mathrm{d}t &= +v_{34} - v_{35} + v_{36} && (73)
\end{aligned}$$

The volume factors vol_cyt = 0.4 pl and vol_nuc = 0.275 pl account for transitions between different compartments and are determined experimentally. The species npSTAT5, CISnRNA1–5 and SOCS3nRNA1–5 are located in the nuclear compartment, the remaining species in the cytoplasmatic compartment. For the species initial concentrations, see Eq. 3,

$$\begin{aligned}
[\mathrm{EpoRJAK2}](0) &= \mathrm{init_EpoRJAK2} && (74)\\
[\mathrm{SHP1}](0) &= \mathrm{init_SHP1} && (75)\\
[\mathrm{STAT5}](0) &= \mathrm{init_STAT5} && (76)\\
& && (77)
\end{aligned}$$

was assumed. The initial concentrations of the remaining species was assumed to be zero.

Parameter transformations According to Eq. 8–11, the ODE system of Eq. 13 – 76 is modified by the following parameter transformations:

$$\text{CISEqc} \rightarrow \frac{\text{CISEqc}}{\text{CISRNAEqc}} \tag{78}$$

$$\text{CISEqcOE} \rightarrow \text{CISEqc} \cdot \text{CISEqcOE} \tag{79}$$

$$\text{CISInh} \rightarrow \frac{\text{CISInh}}{\text{CISEqc}} \tag{80}$$

$$\text{CISRNAEqc} \rightarrow \frac{\text{CISRNAEqc}}{\text{init\_STAT5}} \tag{81}$$

$$\text{EpoRCISRemove} \rightarrow \frac{\text{EpoRCISRemove}}{\text{init\_EpoRJAK2}} \tag{82}$$

$$\text{JAK2EpoRDeaSHP1} \rightarrow \frac{\text{JAK2EpoRDeaSHP1}}{\text{init\_SHP1}} \tag{83}$$

$$\text{SHP1ActEpoR} \rightarrow \frac{\text{SHP1ActEpoR}}{\text{init\_EpoRJAK2}} \tag{84}$$

$$\text{SOCS3Eqc} \rightarrow \frac{\text{SOCS3Eqc}}{\text{SOCS3RNAEqc}} \tag{85}$$

$$\text{SOCS3EqcOE} \rightarrow \text{SOCS3Eqc} \cdot \text{SOCS3EqcOE} \tag{86}$$

$$\text{SOCS3Inh} \rightarrow \frac{\text{SOCS3Inh}}{\text{SOCS3Eqc}} \tag{87}$$

$$\text{SOCS3RNAEqc} \rightarrow \frac{\text{SOCS3RNAEqc}}{\text{init\_STAT5}} \tag{88}$$

$$\text{STAT5ActEpoR} \rightarrow \frac{\text{STAT5ActEpoR}}{\text{init\_EpoRJAK2}^2} \tag{89}$$

$$\text{STAT5ActJAK2} \rightarrow \frac{\text{STAT5ActJAK2}}{\text{init\_EpoRJAK2}} \tag{90}$$

Model calibration To generate the complete model output the ODE system has to be evaluated for 24 different experimental conditions that will be explained in the next sections in detail. The model parameters consist of 29 kinetic parameter involved in the rate equations; 3 non-zero initial concentrations for the species EpoR_JAK2, SHP1 and STAT5; 86 offset and scaling parameters to account for measurement background and unknown scales of immunoblotting and qRT-PCR measurements respectively; 12 parameters representing the magnitude of the measurement noise for each measurement technique and, in case of immunoblotting, for each detection antibody utilized. The parameters were estimated by minimizing the objective function $-2\log(L)$, see Eq. 6, by applying the MATLAB implementation (lsqnonlin) of the trust-region method (Coleman and Li, 1996) with user supplied derivatives. For the calculation of the derivatives the sensitivity equations were simultaneously solved together with the original ODE system describing the dynamics by applying the CVODES solver (Hindmarsh *et al.*, 2005). To improve convergence of the estimation and due to the positive definite nature of the parameters such as rate constants, initial concentrations, concentration offsets and scales, and noise magnitudes, the parameters were estimated in logarithmic parameter space. In order to allow for normally distributed measurement noise the likelihood was evaluated in logarithmic concentration space (Kreutz *et al.*, 2007). The mainly multiplicative nature of the measurement noise transforms to an additive noise. To ensure for global parameter estimates, multiple optimization runs along the profile likelihood were performed. In total 115 free parameters are estimated from the experimental data, yielding a value of the objective function $-2\log(L) = -478.46$ for a total of 541 data points. The estimated parameter values are given in Section 2.4. For each parameter, with one exception, a flat prior distribution with hard bounds according to the values given in Sec. 2.4 was assumed. For the initial concentration of the EpoR_JAK2 complex, described by the parameter init_EpoRJAK2, a prior distribution of $\mathrm{N}(0.6, 0.2^2)$ was assumed (Landschulz *et al.*, 1989).

2.3 Mapping the model dynamics to the experimental data

In order to describe the quantities accessible by experiments, the dynamics of the species concentrations determined by the ODE system of Eq. 49 – 73 are mapped to model outputs. The model outputs can then be compared to the experimental data using the objective function of Eq. 6.

2.3.1 Experiment: Long time-course of JAK2-STAT5 phosphorylation dynamics in CFU-E cells (CFU-E_Long)

Treatment: Epo 5 units/ml (1.25e-7 units/cell)

The model outputs, see Eq. 5, available in this data set are given by:

$$\begin{aligned} \text{pJAK2\_au} &= \log_{10}(\text{offset\_pJAK2\_long} + \\ &+ \frac{2 \cdot \text{scale\_pJAK2\_long} \cdot (\text{[EpoRpJAK2]} + \text{[p12EpoRpJAK2]} + \text{[p1EpoRpJAK2]} + \text{[p2EpoRpJAK2]})}{\text{init\_EpoRJAK2}}) \end{aligned} \tag{91}$$

$$\begin{aligned} \text{pEpoR\_au} &= \log_{10}(\text{offset\_pEpoR\_long} + \\ &+ \frac{16 \cdot \text{scale\_pEpoR\_long} \cdot (\text{[p12EpoRpJAK2]} + \text{[p1EpoRpJAK2]} + \text{[p2EpoRpJAK2]})}{\text{init\_EpoRJAK2}}) \end{aligned} \tag{92}$$

$$\text{CIS\_au} = \log_{10}(\text{offset\_CIS\_long} + \frac{\text{[CIS]} \cdot \text{scale\_CIS\_long}}{\text{CISEqc} \cdot \text{CISRNAEqc} \cdot \text{init\_STAT5}}) \tag{93}$$

$$\text{SOCS3\_au} = \log_{10}(\text{offset\_SOCS3\_long} + \frac{\text{[SOCS3]} \cdot \text{scale\_SOCS3\_long}}{\text{SOCS3Eqc} \cdot \text{SOCS3RNAEqc} \cdot \text{init\_STAT5}}) \tag{94}$$

$$\text{tSTAT5\_au} = \log_{10}(\frac{\text{scale\_tSTAT5\_long} \cdot (\text{[STAT5]} + \text{[pSTAT5]})}{\text{init\_STAT5}}) \tag{95}$$

$$\text{pSTAT5\_au} = \log_{10}(\text{offset\_pSTAT5\_long} + \frac{\text{[pSTAT5]} \cdot \text{scale\_pSTAT5\_long}}{\text{init\_STAT5}}) \tag{96}$$

The error model that describes the measurement noise for each model output, see Eq. 7, is given by:

$$\sigma[\text{pJAK2\_au}] = \text{sd\_JAK2EpoR\_au} \tag{97}$$

$$\sigma[\text{pEpoR\_au}] = \text{sd\_JAK2EpoR\_au} \tag{98}$$

$$\sigma[\text{CIS\_au}] = \text{sd\_CIS\_au} \tag{99}$$

$$\sigma[\text{SOCS3\_au}] = \text{sd\_SOCS3\_au} \tag{100}$$

$$\sigma[\text{tSTAT5\_au}] = \text{sd\_STAT5\_au} \tag{101}$$

$$\sigma[\text{pSTAT5\_au}] = \text{sd\_STAT5\_au} \tag{102}$$

To evaluate the ODE system of Eq. 49 – 76 for the conditions in this experiment, the following parameters are set to:

$$\text{ActD} = 0 \tag{103}$$

$$\text{CISoe} = 0 \tag{104}$$

$$\text{SOCS3oe} = 0 \tag{105}$$

$$\text{SHP1oe} = 0 \tag{106}$$

$$\text{epo\_level} = 1.2 \cdot 10^{-07} \tag{107}$$

The agreement of the model outputs and the experimental data, given in Tab. S3, yields a value of the objective function $-2\log(L) = -54.19$ for 73 data points in this data set. The agreement of model outputs and experimental data is shown in Fig. S11.

The trajectories of the dynamical variables and external inputs that correspond to the experimental conditions in this experiment are shown, together with their prediction confidence intervals, later in Fig. S52.

time [min]	pJAK2_au conc. [au]	pEpoR_au conc. [au]	CIS_au conc. [au]	SOCS3_au conc. [au]	tSTAT5_au conc. [au]	pSTAT5_au conc. [au]
0.000000	0.011066	0.004412	0.017007	NaN	0.580253	0.001090
5.000000	1.000000	0.700809	0.038819	NaN	1.000000	1.000000
10.000000	0.745856	1.000000	0.021344	0.109721	0.685016	0.907589
20.000000	0.745856	0.606469	0.037086	0.281462	0.564744	0.560146
40.000000	0.262055	0.190846	0.128730	NaN	NaN	NaN
60.000000	0.043105	0.100787	0.282493	0.568877	0.859841	0.390882
80.000000	0.163199	0.110949	0.820831	NaN	0.680306	0.168972
100.000000	0.092608	0.069846	0.922259	NaN	0.747586	0.163322
120.000000	0.025276	0.283019	NaN	1.000000	0.874022	0.193886
140.000000	0.134138	0.134038	0.773095	NaN	0.640665	0.121703
160.000000	0.135856	0.239555	0.751558	NaN	0.702241	0.126579
180.000000	0.056232	0.050682	0.951127	1.000000	0.841180	0.291617
220.000000	0.059243	0.040019	0.911415	NaN	0.574873	0.085725
240.000000	0.102116	0.085332	1.000000	0.969746	0.722746	0.275913

Table S3: Experimental data for the experiment CFU-E_Long

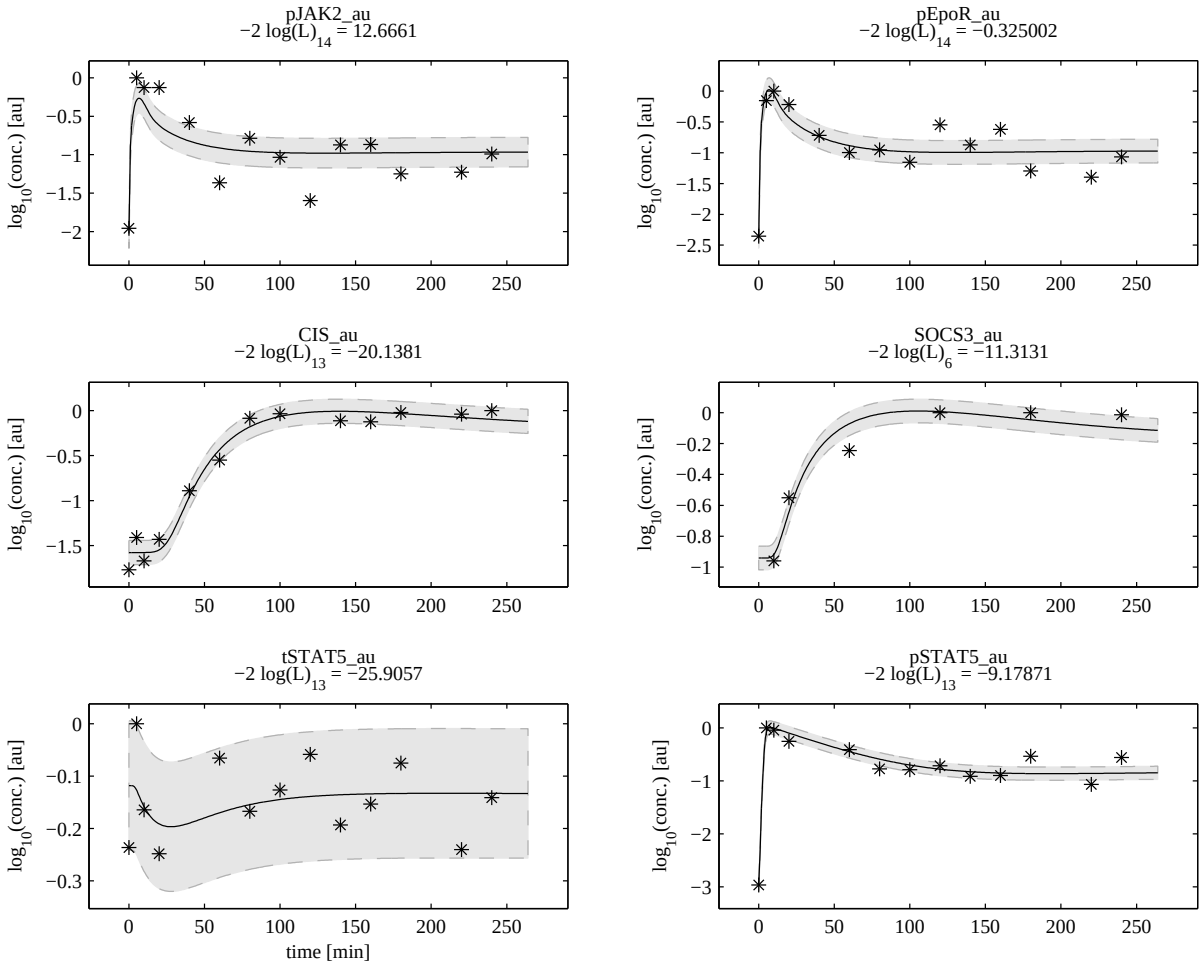

Figure S11: Agreement of model outputs and experimental data for the experiment CFU-E_Long
The displayed model outputs (solid lines) are defined by Eq. 92 – 96. The error model that describes the measurement noise for each model output is indicated by shades around the model outputs and is given by Eq. 97 – 102.

2.3.2 Experiment: Absolute concentrations of proteins in CFU-E cells (CFU-E_Concentrations)

Treatment: Epo 5 units/ml (1.25e-7 units/cell)

The model outputs, see Eq. 5, available in this data set are given by:

$$\text{STAT5\_abs} = \log_{10}([\text{STAT5}]) \tag{108}$$
$$\text{SHP1\_abs} = \log_{10}([\text{SHP1}] + [\text{SHP1Act}]) \tag{109}$$
$$\text{CIS\_abs} = \log_{10}([\text{CIS}]) \tag{110}$$
$$\text{SOCS3\_abs} = \log_{10}([\text{SOCS3}]) \tag{111}$$
$$\text{pSTAT5B\_rel} = \text{offset\_pSTAT5\_conc} + \frac{100 \cdot [\text{pSTAT5}]}{[\text{STAT5}] + [\text{pSTAT5}]} \tag{112}$$

The error model that describes the measurement noise for each model output, see Eq. 7, is given by:

$$\sigma[\text{STAT5\_abs}] = \text{sd\_STAT5\_abs} \tag{113}$$
$$\sigma[\text{SHP1\_abs}] = \text{sd\_SHP1\_abs} \tag{114}$$
$$\sigma[\text{CIS\_abs}] = \text{sd\_CIS\_abs} \tag{115}$$
$$\sigma[\text{SOCS3\_abs}] = \text{sd\_SOCS3\_abs} \tag{116}$$
$$\sigma[\text{pSTAT5B\_rel}] = \text{sd\_pSTAT5\_rel} \tag{117}$$

To evaluate the ODE system of Eq. 49 – 76 for the conditions in this experiment, the following parameters are set to:

$$\text{ActD} = 0 \tag{118}$$
$$\text{CISoe} = 0 \tag{119}$$
$$\text{SOCS3oe} = 0 \tag{120}$$
$$\text{SHP1oe} = 0 \tag{121}$$
$$\text{epo\_level} = 1.2 \cdot 10^{-07} \tag{122}$$

The agreement of the model outputs and the experimental data, given in Tab. S4, yields a value of the objective function $-2\log(L) = 13.22$ for 20 data points in this data set. The agreement of model outputs and experimental data is shown in Fig. S12.

time [min]	STAT5_abs conc. [nM]	SHP1_abs conc. [nM]	CIS_abs conc. [nM]	SOCS3_abs conc. [nM]	pSTAT5B_rel conc. [rel]
0.000000	62.683305	28.434776	NaN	NaN	0.508000
0.000000	117.228683	30.863729	NaN	NaN	0.684588
0.000000	69.034077	21.750069	NaN	NaN	1.147136
0.000000	NaN	NaN	NaN	NaN	1.160932
10.000000	NaN	NaN	NaN	NaN	78.020000
10.000000	NaN	NaN	NaN	NaN	68.447433
10.000000	NaN	NaN	NaN	NaN	74.054191
10.000000	NaN	NaN	NaN	NaN	71.551395
120.000000	NaN	NaN	29.061795	12.354824	NaN
120.000000	NaN	NaN	26.097567	7.255641	NaN
120.000000	NaN	NaN	19.652393	11.542239	NaN

Table S4: Experimental data for the experiment CFU-E_Concentrations

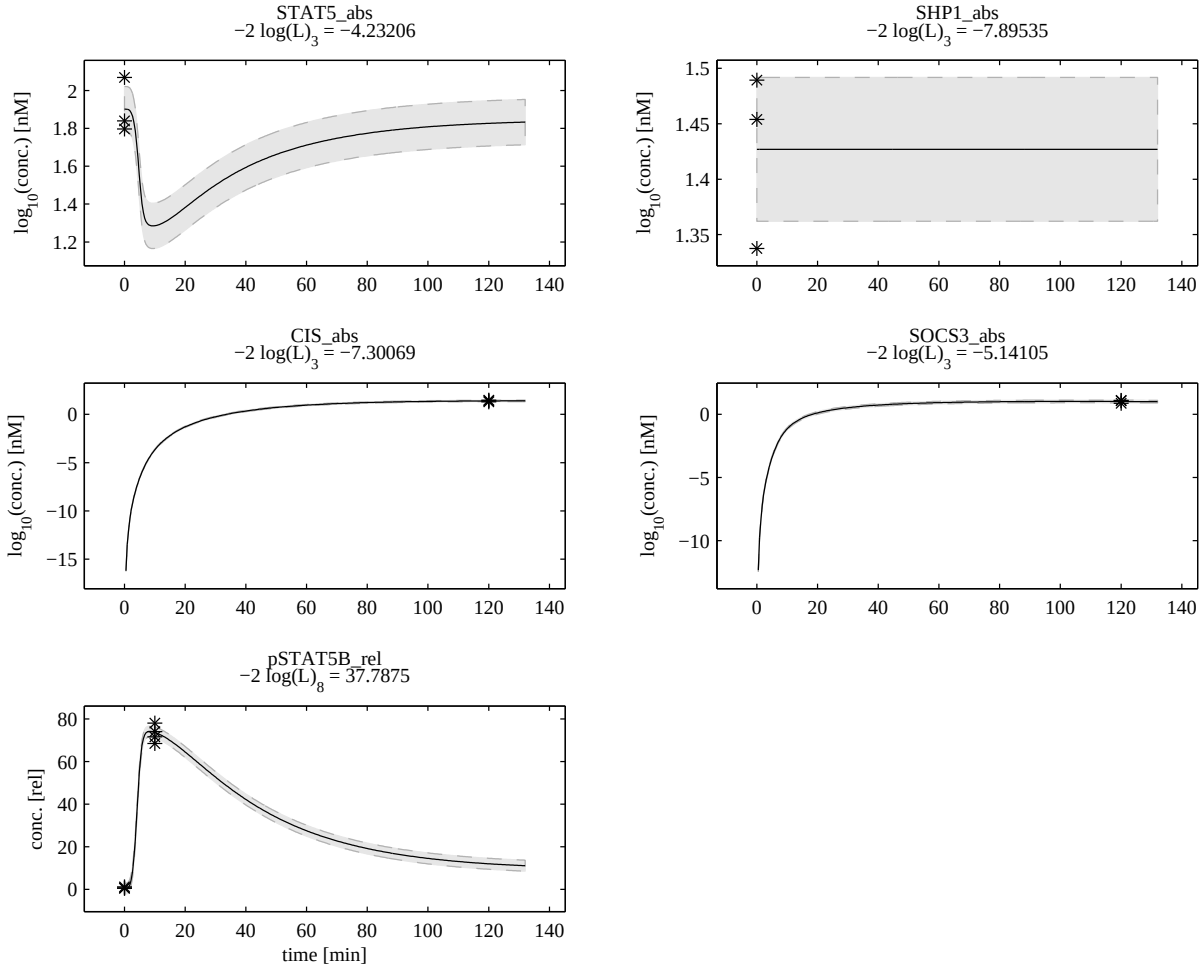

Figure S12: Agreement of model outputs and experimental data for the experiment CFU-E_Concentrations The displayed model outputs (solid lines) are defined by Eq. 108 – 112. The error model that describes the measurement noise for each model output is indicated by shades around the model outputs and is given by Eq. 113 – 117.

2.3.3 Experiment: Time-course of CIS and SOCS3 mRNA expression (CFU-E_RNA)

Treatment: Epo 5 units/ml (1.25e-7 units/cell)

The model outputs, see Eq. 5, available in this data set are given by:

$$\text{SOCS3RNA\_foldA} = \log_{10}\left(\frac{[\text{SOCS3RNA}] \cdot \text{scale\_SOCS3RNA\_foldA}}{\text{SOCS3RNAEqc} \cdot \text{init\_STAT5}} + 1\right) \tag{123}$$

$$\text{SOCS3RNA\_foldB} = \log_{10}\left(\frac{[\text{SOCS3RNA}] \cdot \text{scale\_SOCS3RNA\_foldB}}{\text{SOCS3RNAEqc} \cdot \text{init\_STAT5}} + 1\right) \tag{124}$$

$$\text{SOCS3RNA\_foldC} = \log_{10}\left(\frac{[\text{SOCS3RNA}] \cdot \text{scale\_SOCS3RNA\_foldC}}{\text{SOCS3RNAEqc} \cdot \text{init\_STAT5}} + 1\right) \tag{125}$$

$$\text{CISRNA\_foldA} = \log_{10}\left(\frac{[\text{CISRNA}] \cdot \text{scale\_CISRNA\_foldA}}{\text{CISRNAEqc} \cdot \text{init\_STAT5}} + 1\right) \tag{126}$$

$$\text{CISRNA\_foldB} = \log_{10}\left(\frac{[\text{CISRNA}] \cdot \text{scale\_CISRNA\_foldB}}{\text{CISRNAEqc} \cdot \text{init\_STAT5}} + 1\right) \tag{127}$$

$$\text{CISRNA\_foldC} = \log_{10}\left(\frac{[\text{CISRNA}] \cdot \text{scale\_CISRNA\_foldC}}{\text{CISRNAEqc} \cdot \text{init\_STAT5}} + 1\right) \tag{128}$$

The error model that describes the measurement noise for each model output, see Eq. 7, is given by:

$$\sigma[\text{SOCS3RNA\_foldA}] = \text{sd\_RNA\_fold} \tag{129}$$

$$\sigma[\text{SOCS3RNA\_foldB}] = \text{sd\_RNA\_fold} \tag{130}$$

$$\sigma[\text{SOCS3RNA\_foldC}] = \text{sd\_RNA\_fold} \tag{131}$$

$$\sigma[\text{CISRNA\_foldA}] = \text{sd\_RNA\_fold} \tag{132}$$

$$\sigma[\text{CISRNA\_foldB}] = \text{sd\_RNA\_fold} \tag{133}$$

$$\sigma[\text{CISRNA\_foldC}] = \text{sd\_RNA\_fold} \tag{134}$$

To evaluate the ODE system of Eq. 49 – 76 for the conditions in this experiment, the following parameters are set to:

$$\text{ActD} = 0 \tag{135}$$

$$\text{CISoe} = 0 \tag{136}$$

$$\text{SOCS3oe} = 0 \tag{137}$$

$$\text{SHP1oe} = 0 \tag{138}$$

$$\text{epo\_level} = 1.2 \cdot 10^{-07} \tag{139}$$

The agreement of the model outputs and the experimental data, given in Tab. S5, yields a value of the objective function $-2\log(L) = -58.03$ for 34 data points in this data set. The agreement of model outputs and experimental data is shown in Fig. S13.

The trajectories of the dynamical variables and external inputs that correspond to the experimental conditions in this experiment are shown, together with their prediction confidence intervals, later in Fig. S52.

time [min]	SOCS3RNA_fold1 fold change [au]	SOCS3RNA_fold2 fold change [au]	SOCS3RNA_fold3 fold change [au]
15.000000	1.337800	1.444570	1.164102
30.000000	1.251172	1.551426	1.663066
60.000000	5.272384	4.609046	9.505643
120.000000	3.621192	3.921473	4.310365
240.000000	3.952821	NaN	3.952821
360.000000	3.356143	2.243796	4.484969
time [min]	CISRNA_fold1 fold change [au]	CISRNA_fold2 fold change [au]	CISRNA_fold3 fold change [au]
15.000000	1.047766	1.056605	1.031556
30.000000	1.428928	1.454544	1.406978
60.000000	7.076947	5.468274	3.645027
120.000000	3.111870	3.616503	2.386977
240.000000	2.585902	NaN	2.210395
360.000000	1.890066	2.176100	1.473333

Table S5: Experimental data for the experiment CFU-E_RNA

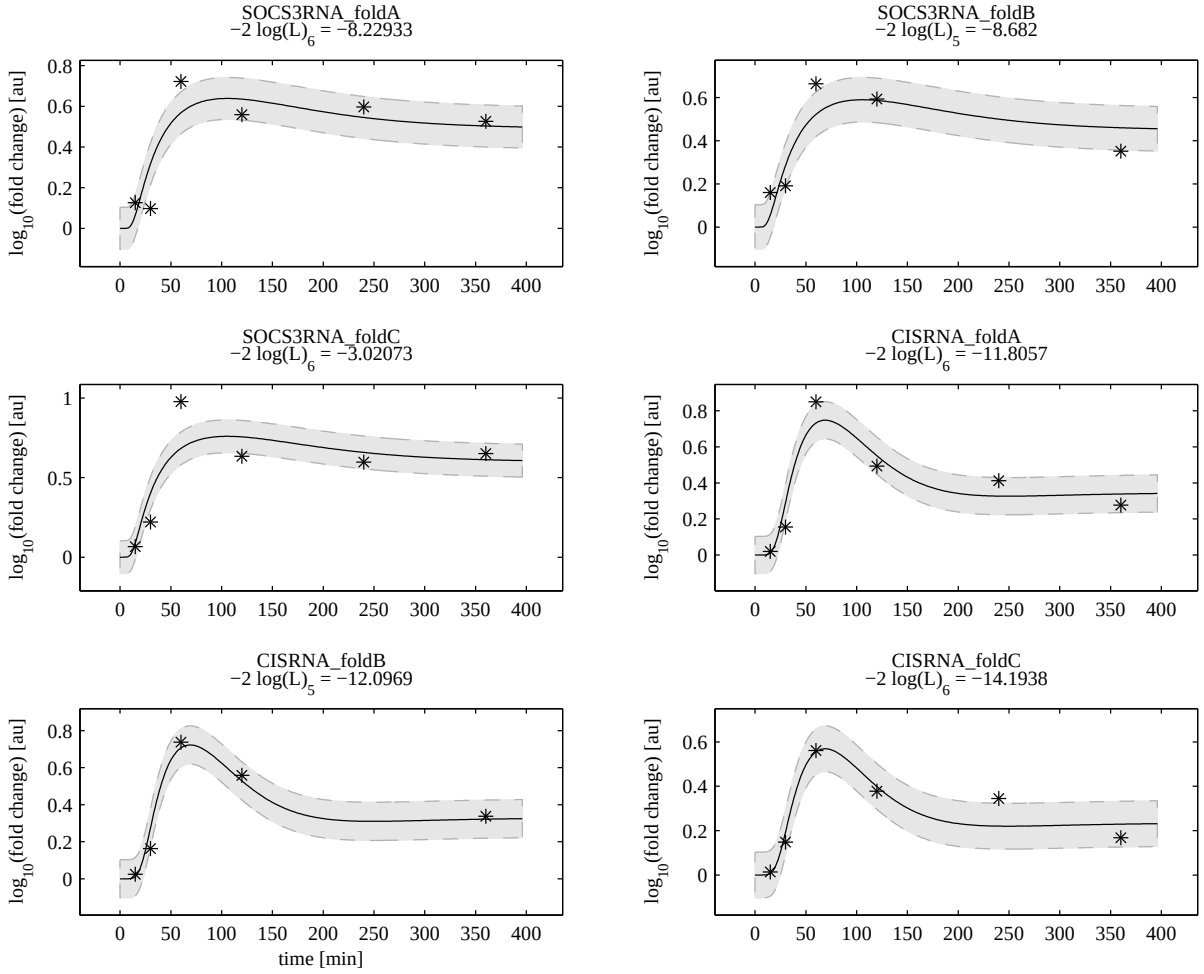

Figure S13: Agreement of model outputs and experimental data for the experiment CFU-E_RNA
The time course experiments of mature CIS and SOCS3 mRNA expression was performed independently three time and the different replicates are shown. The displayed model outputs (solid lines) are defined by Eq. 123 – 128. The error model that describes the measurement noise for each model output is indicated by shades around the model outputs and is given by Eq. 129 – 134.

2.3.4 Experiment: Time-course of JAK2-STAT5 phosphorylation dynamics in CFU-E cells with Actinomycin D treatment (CFU-E_ActD)

Treatment: Epo 5 units/ml (1.25e-7 units/cell) + ActD 1 mug/ml

The model outputs, see Eq. 5, available in this data set are given by:

$$\begin{aligned}
\text{pJAK2_au} &= \log_{10}(\text{offset_pJAK2_actd} + \\
&+ \frac{2 \cdot \text{scale_pJAK2_actd} \cdot (\text{[EpoRpJAK2]} + \text{[p12EpoRpJAK2]} + \text{[p1EpoRpJAK2]} + \text{[p2EpoRpJAK2]})}{\text{init_EpoRJAK2}}) \qquad (140)\\
\text{pEpoR_au} &= \log_{10}(\text{offset_pEpoR_actd} + \\
&+ \frac{16 \cdot \text{scale_pEpoR_actd} \cdot (\text{[p12EpoRpJAK2]} + \text{[p1EpoRpJAK2]} + \text{[p2EpoRpJAK2]})}{\text{init_EpoRJAK2}}) \qquad (141)\\
\text{tSTAT5_au} &= \log_{10}(\frac{\text{scale_tSTAT5_actd} \cdot (\text{[STAT5]} + \text{[pSTAT5]})}{\text{init_STAT5}}) \qquad (142)\\
\text{pSTAT5_au} &= \log_{10}(\text{offset_pSTAT5_actd} + \frac{\text{[pSTAT5]} \cdot \text{scale_pSTAT5_actd}}{\text{init_STAT5}}) \qquad (143)\\
\text{CIS_au} &= \log_{10}(\text{offset_CIS_actd} + \frac{\text{[CIS]} \cdot \text{scale_CIS_actd}}{\text{CISEqc} \cdot \text{CISRNAEqc} \cdot \text{init_STAT5}}) \qquad (144)
\end{aligned}$$

The error model that describes the measurement noise for each model output, see Eq. 7, is given by:

$$\begin{aligned}
\sigma[\text{pJAK2_au}] &= \text{sd_JAK2EpoR_au} \qquad (145)\\
\sigma[\text{pEpoR_au}] &= \text{sd_JAK2EpoR_au} \qquad (146)\\
\sigma[\text{tSTAT5_au}] &= \text{sd_STAT5_au} \qquad (147)\\
\sigma[\text{pSTAT5_au}] &= \text{sd_STAT5_au} \qquad (148)\\
\sigma[\text{CIS_au}] &= \text{sd_CIS_au} \qquad (149)
\end{aligned}$$

To evaluate the ODE system of Eq. 49 – 76 for the conditions in this experiment, the following parameters are set to:

$$\begin{aligned}
\text{ActD} &= 0, 1 \qquad (150)\\
\text{CISoe} &= 0 \qquad (151)\\
\text{SOCS3oe} &= 0 \qquad (152)\\
\text{SHP1oe} &= 0 \qquad (153)\\
\text{epo_level} &= 1.2 \cdot 10^{-07} \qquad (154)
\end{aligned}$$

The agreement of the model outputs and the experimental data, given in Tab. S6, yields a value of the objective function $-2\log(L) = -92.61$ for 90 data points in this data set. The agreement of model outputs and experimental data is shown in Fig. S14.

The trajectories of the dynamical variables and external inputs that correspond to the experimental conditions in this experiment are shown, together with their prediction confidence intervals, later in Fig. S53.

time [min]	ActD	pJAK2_au conc. [au]	pEpoR_au conc. [au]	tSTAT5_au conc. [au]	pSTAT5_au conc. [au]	CIS_au conc. [au]
0.000000	0	0.018583	0.033087	0.832432	0.001913	0.013228
5.000000	0	1.000000	0.864151	0.897297	0.860465	0.009361
10.000000	0	0.749594	0.841509	0.859459	0.944186	0.008917
30.000000	0	0.234697	0.126962	0.670270	0.479070	0.027977
60.000000	0	0.081389	0.125487	0.735135	0.170543	0.307400
90.000000	0	0.045459	0.053000	0.583784	0.081384	0.557875
120.000000	0	0.036175	0.158660	0.886486	0.184496	0.836812
150.000000	0	0.068541	0.099906	0.681081	0.131005	0.859583
180.000000	0	0.074649	0.079128	0.471351	0.115660	1.000000
0.000000	1	0.022248	0.011298	0.902703	0.001822	0.013949
5.000000	1	0.594490	1.000000	1.000000	0.959690	0.007951
10.000000	1	0.888415	0.788679	0.924324	1.000000	0.010046
30.000000	1	0.212550	0.328313	0.583784	0.438760	0.020216
60.000000	1	0.124319	0.123555	0.794595	0.322481	0.006040
90.000000	1	0.175585	0.177253	0.772973	0.331783	0.007545
120.000000	1	0.098708	0.192845	0.756757	0.421705	0.004163
150.000000	1	0.163742	0.170830	0.745946	0.462016	0.012579
180.000000	1	0.141824	0.135834	0.514595	0.336434	0.007964

Table S6: Experimental data for the experiment CFU-E_ActD

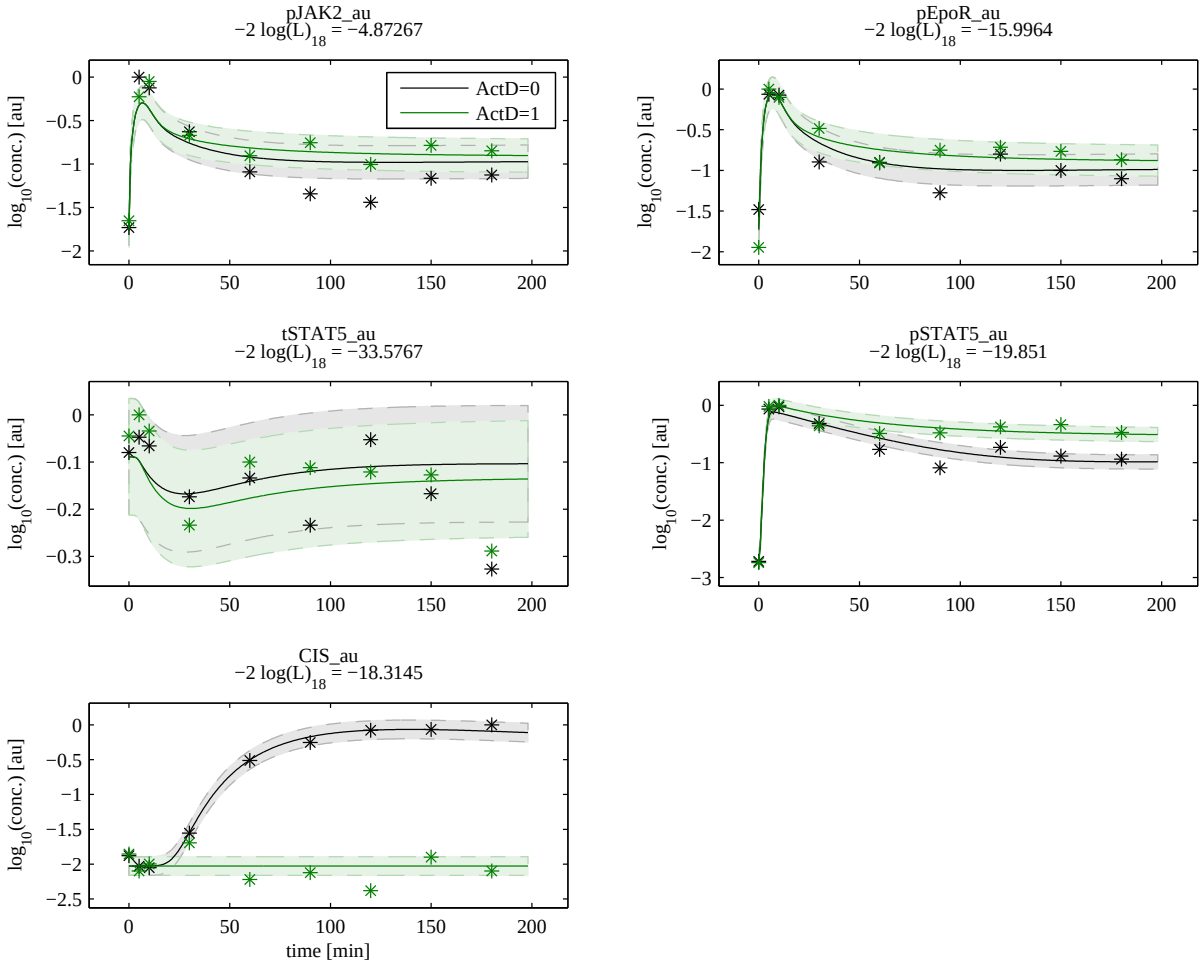

Figure S14: Agreement of model outputs and experimental data for the experiment CFU-E_ActD
The displayed model outputs (solid lines) are defined by Eq. 141 – 144. The error model that describes the measurement noise for each model output is indicated by shades around the model outputs and is given by Eq. 145 – 149.

2.3.5 Experiment: Time-course of JAK2-STAT5 phosphorylation dynamics in CFU-E cells densely sampled (CFU-E_Fine)

Treatment: Epo 50 units/ml (1.25e-6 units/cell)

The model outputs, see Eq. 5, available in this data set are given by:

$$\begin{aligned} \text{pJAK2\_au} &= \log_{10}(\text{offset\_pJAK2\_fine} + \qquad (155)\\ &+ \frac{2 \cdot \text{scale\_pJAK2\_fine} \cdot ([\text{EpoRpJAK2}] + [\text{p12EpoRpJAK2}] + [\text{p1EpoRpJAK2}] + [\text{p2EpoRpJAK2}])}{\text{init\_EpoRJAK2}}) \\ \text{pEpoR\_au} &= \log_{10}(\text{offset\_pEpoR\_fine} + \\ &+ \frac{16 \cdot \text{scale\_pEpoR\_fine} \cdot ([\text{p12EpoRpJAK2}] + [\text{p1EpoRpJAK2}] + [\text{p2EpoRpJAK2}])}{\text{init\_EpoRJAK2}}) \qquad (156) \end{aligned}$$

The error model that describes the measurement noise for each model output, see Eq. 7, is given by:

$$\sigma[\text{pJAK2\_au}] = \text{sd\_JAK2EpoR\_au} \qquad (157)$$

$$\sigma[\text{pEpoR\_au}] = \text{sd\_JAK2EpoR\_au} \qquad (158)$$

To evaluate the ODE system of Eq. 49 – 76 for the conditions in this experiment, the following parameters are set to:

$$\text{ActD} = 0 \qquad (159)$$

$$\text{CISoe} = 0 \qquad (160)$$

$$\text{SOCS3oe} = 0 \qquad (161)$$

$$\text{SHP1oe} = 0 \qquad (162)$$

$$\text{epo\_level} = 1.3 \cdot 10^{-06} \qquad (163)$$

The agreement of the model outputs and the experimental data, given in Tab. S7, yields a value of the objective function $-2\log(L) = -6.72$ for 60 data points in this data set. The agreement of model outputs and experimental data is shown in Fig. S15.

The trajectories of the dynamical variables and external inputs that correspond to the experimental conditions in this experiment are shown, together with their prediction confidence intervals, later in Fig. S54.

time [min]	pJAK2_au conc. [au]	pEpoR_au conc. [au]
0.000000	0.021170	0.309735
0.000000	0.026163	0.026991
0.500000	0.196809	0.210914
1.000000	0.379053	0.423965
1.500000	0.413121	0.911504
2.000000	0.368683	0.683624
3.000000	0.491135	0.998525
4.000000	0.906730	0.768711
5.000000	1.000000	1.000000
6.000000	0.799582	0.523721
7.500000	0.760638	0.417404
9.000000	0.653261	0.906609
10.500000	0.828014	0.199115
12.000000	0.603720	0.513451
13.500000	0.478723	0.339233
15.000000	0.240796	0.776046
16.500000	0.400709	0.951327
18.000000	0.752344	0.283131
20.000000	0.352837	0.166667
22.000000	0.228122	0.217117
25.000000	0.186170	0.120501
28.000000	0.388270	0.143482
31.000000	0.172816	0.084532
35.000000	0.077106	0.080112
40.000000	0.163934	0.097754
45.000000	0.237340	0.121588
50.000000	0.126846	0.069500
60.000000	0.063812	0.148168
65.000000	0.113429	0.157817
70.000000	0.222362	0.104460

Table S7: Experimental data for the experiment CFU-E_Fine

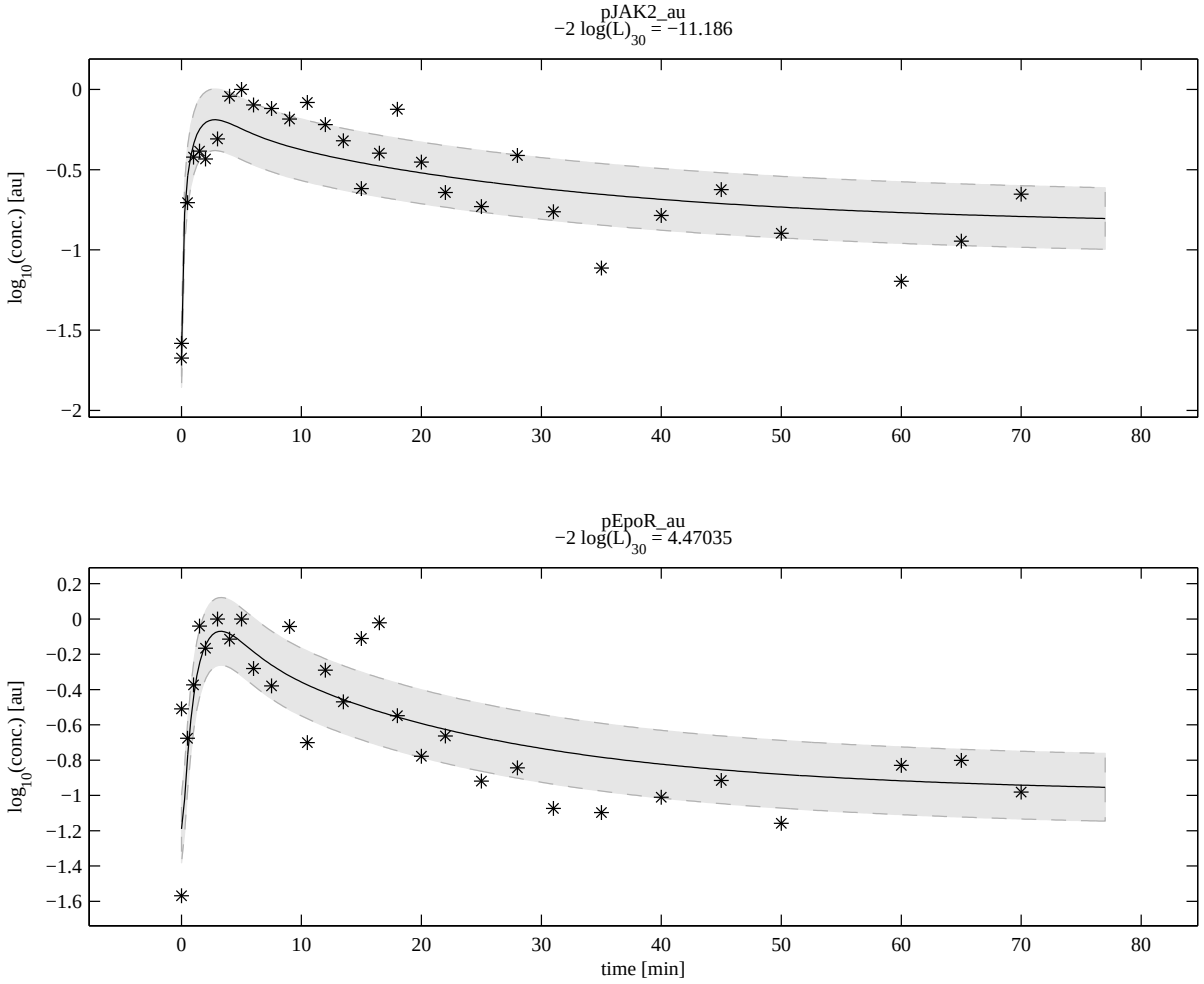

Figure S15: Agreement of model outputs and experimental data for the experiment CFU-E_Fine
The displayed model outputs (solid lines) are defined by Eq. 156 – 156. The error model that describes the measurement noise for each model output is indicated by shades around the model outputs and is given by Eq. 157 – 158.

2.3.6 Experiment: Time-course of JAK2-STAT5 phosphorylation dynamics in CFU-E cells over-expressing CIS (CFU-E_CISoe)

Treatment: Epo 5 units/ml (1.25e-7 units/cell) + CIS over-expression

The model outputs, see Eq. 5, available in this data set are given by:

$$\begin{aligned}
\text{pJAK2_au} &= \log_{10}(\text{offset_pJAK2_cisoe} + \qquad (164)\\
&+ \frac{2 \cdot \text{scale_pJAK2_cisoe} \cdot ([\text{EpoRpJAK2}] + [\text{p12EpoRpJAK2}] + [\text{p1EpoRpJAK2}] + [\text{p2EpoRpJAK2}])}{\text{init_EpoRJAK2}})\\
\text{pEpoR_au} &= \log_{10}(\text{offset_pEpoR_cisoe} +\\
&+ \frac{16 \cdot \text{scale_pEpoR_cisoe} \cdot ([\text{p12EpoRpJAK2}] + [\text{p1EpoRpJAK2}] + [\text{p2EpoRpJAK2}])}{\text{init_EpoRJAK2}}) \qquad (165)\\
\text{CIS_au} &= \log_{10}(\text{offset_CIS_cisoe} + \frac{[\text{CIS}] \cdot \text{scale_CIS_cisoe}}{\text{CISEqc} \cdot \text{CISRNAEqc} \cdot \text{init_STAT5}}) \qquad (166)\\
\text{SOCS3_au} &= \log_{10}(\text{offset_SOCS3_cisoe} + \frac{[\text{SOCS3}] \cdot \text{scale_SOCS3_cisoe}}{\text{SOCS3Eqc} \cdot \text{SOCS3RNAEqc} \cdot \text{init_STAT5}}) \qquad (167)\\
\text{pSTAT5_au} &= \log_{10}(\text{offset_pSTAT5_cisoe} + \frac{[\text{pSTAT5}] \cdot \text{scale_pSTAT5_cisoe}}{\text{init_STAT5}}) \qquad (168)
\end{aligned}$$

The error model that describes the measurement noise for each model output, see Eq. 7, is given by:

$$\begin{aligned}
\sigma[\text{pJAK2_au}] &= \text{sd_JAK2EpoR_au} \qquad (169)\\
\sigma[\text{pEpoR_au}] &= \text{sd_JAK2EpoR_au} \qquad (170)\\
\sigma[\text{CIS_au}] &= \text{sd_CIS_au} \qquad (171)\\
\sigma[\text{SOCS3_au}] &= \text{sd_SOCS3_au} \qquad (172)\\
\sigma[\text{pSTAT5_au}] &= \text{sd_STAT5_au} \qquad (173)
\end{aligned}$$

To evaluate the ODE system of Eq. 49 – 76 for the conditions in this experiment, the following parameters are set to:

$$\begin{aligned}
\text{ActD} &= 0 \qquad (174)\\
\text{CISoe} &= 0, 1 \qquad (175)\\
\text{SOCS3oe} &= 0 \qquad (176)\\
\text{SHP1oe} &= 0 \qquad (177)\\
\text{epo_level} &= 1.2 \cdot 10^{-07} \qquad (178)
\end{aligned}$$

The agreement of the model outputs and the experimental data, given in Tab. S8, yields a value of the objective function $-2\log(L) = -49.42$ for 40 data points in this data set. The agreement of model outputs and experimental data is shown in Fig. S16.

The trajectories of the dynamical variables and external inputs that correspond to the experimental conditions in this experiment are shown, together with their prediction confidence intervals, later in Fig. S55.

time [min]	CISoe	pJAK2_au conc. [au]	pEpoR_au conc. [au]	CIS_au conc. [au]	SOCS3_au conc. [au]	pSTAT5_au conc. [au]
0.000000	0	0.026772	0.023098	0.028805	0.275751	0.070604
10.000000	0	1.000000	1.000000	0.026064	0.351145	1.000000
60.000000	0	0.248910	0.226178	0.101835	0.921120	0.711207
120.000000	0	0.224042	0.240681	0.075319	1.000000	0.633621
0.000000	1	0.017810	0.032018	1.000000	0.325700	0.062931
10.000000	1	0.835979	0.227847	0.702752	0.192880	0.352586
60.000000	1	0.307672	0.186534	0.744954	0.554707	0.411207
120.000000	1	0.268365	0.205215	0.660550	0.516478	0.534483

Table S8: Experimental data for the experiment CFU-E_CISoe

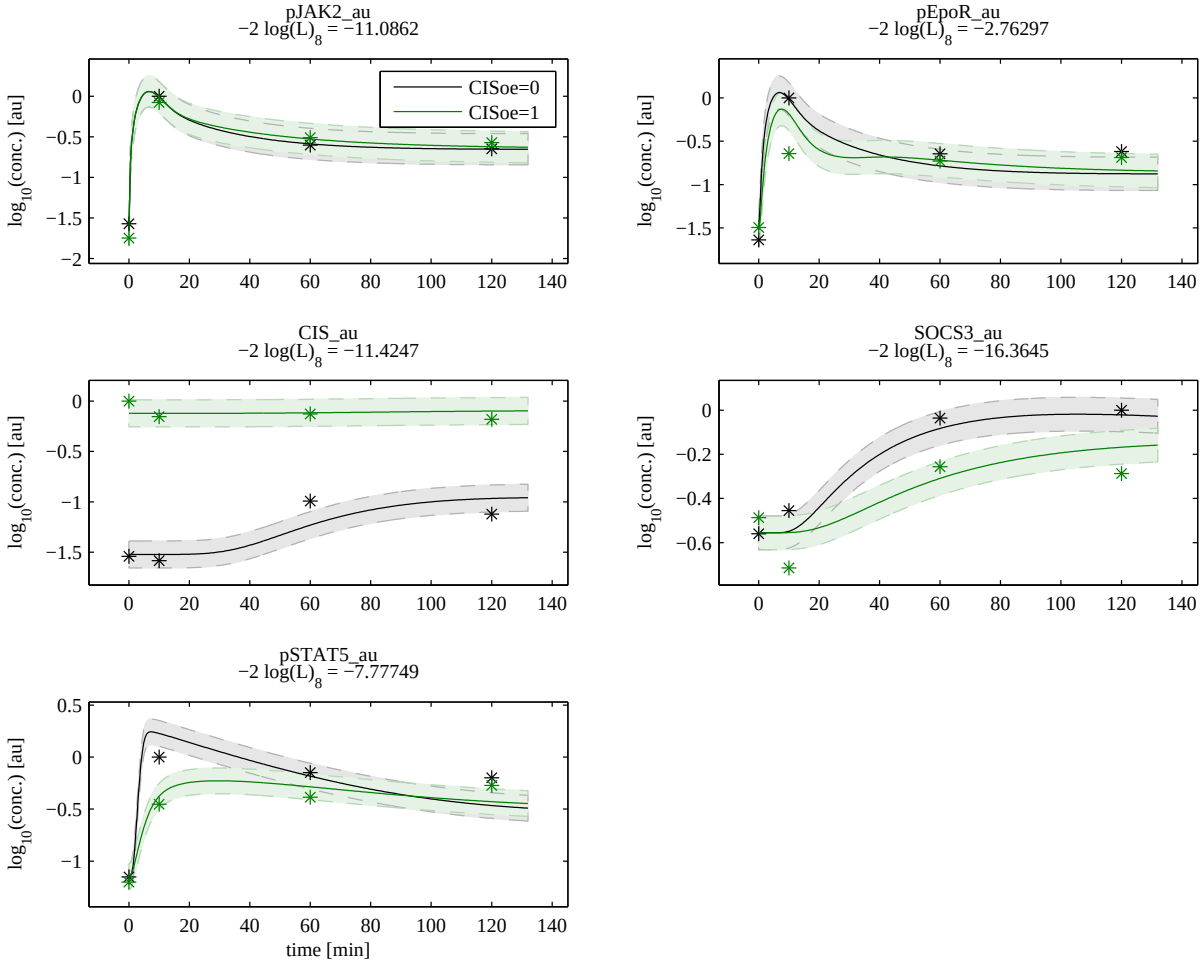

Figure S16: Agreement of model outputs and experimental data for the experiment CFU-E_CISoe
The displayed model outputs (solid lines) are defined by Eq. 165 – 168. The error model that describes the measurement noise for each model output is indicated by shades around the model outputs and is given by Eq. 169 – 173.

2.3.7 Experiment: Time-course of EpoR phosphorylation dynamics in CFU-E cells over-expressing CIS (CFU-E_CISoe)

Treatment: Epo 5 units/ml (1.25e-7 units/cell) + CIS over-expression

The model outputs, see Eq. 5, available in this data set are given by:

$$\begin{aligned} \text{pEpoR\_au} &= \log_{10}(\text{offset\_pEpoR\_cisoe\_pepor} + \\ &+ \frac{16 \cdot \text{scale\_pEpoR\_cisoe\_pepor} \cdot ([\text{p12EpoRpJAK2}] + [\text{p1EpoRpJAK2}] + [\text{p2EpoRpJAK2}])}{\text{init\_EpoRJAK2}}) \end{aligned} \tag{179}$$

The error model that describes the measurement noise for each model output, see Eq. 7, is given by:

$$\sigma[\text{pEpoR\_au}] = \text{sd\_JAK2EpoR\_}au \tag{180}$$

To evaluate the ODE system of Eq. 49 – 76 for the conditions in this experiment, the following parameters are set to:

$$\text{ActD} = 0 \tag{181}$$
$$\text{CISoe} = 0, 1 \tag{182}$$
$$\text{SOCS3oe} = 0 \tag{183}$$
$$\text{SHP1oe} = 0 \tag{184}$$
$$\text{epo\_level} = 1.2 \cdot 10^{-07} \tag{185}$$

The agreement of the model outputs and the experimental data, given in Tab. S9, yields a value of the objective function $-2\log(L) = -10.12$ for 10 data points in this data set. The agreement of model outputs and experimental data is shown in Fig. S17.

The trajectories of the dynamical variables and external inputs that correspond to the experimental conditions in this experiment are shown, together with their prediction confidence intervals, later in Fig. S55.

time [min]	CISoe	pEpoR_au conc. [au]
0.000000	0	0.128892
5.000000	0	1.000000
10.000000	0	0.884430
60.000000	0	0.314607
120.000000	0	0.211878
0.000000	1	0.115088
5.000000	1	0.329053
10.000000	1	0.266453
60.000000	1	0.231140
120.000000	1	0.176565

Table S9: Experimental data for the experiment CFUE_CISoe_pEpoR

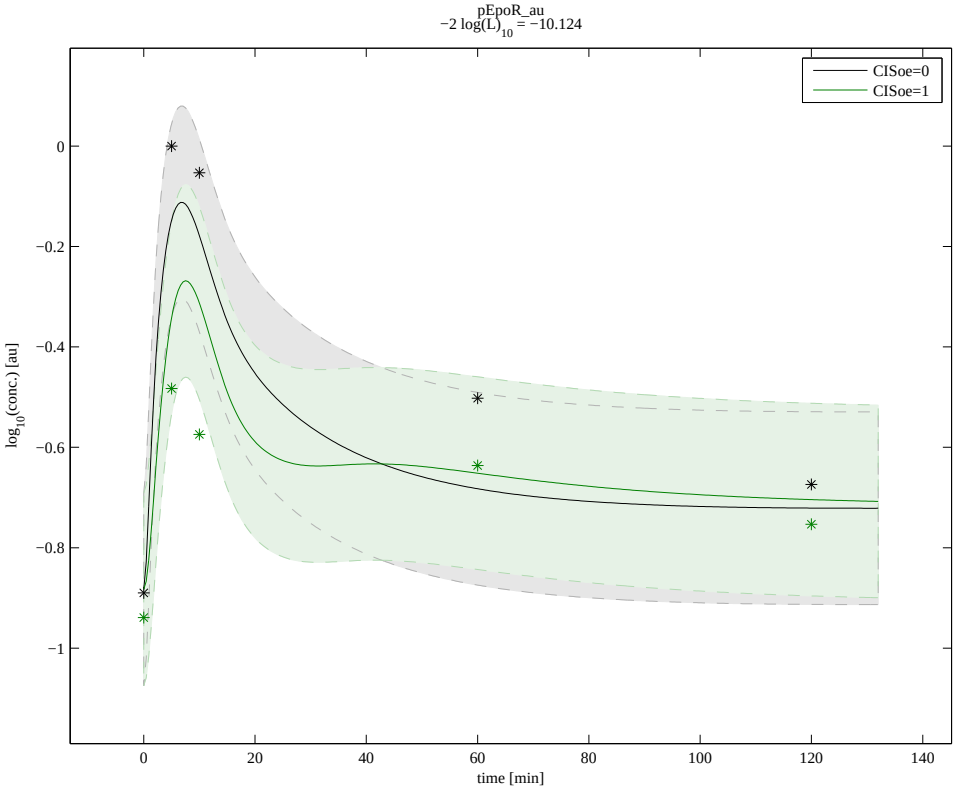

Figure S17: Agreement of model outputs and experimental data for the experiment CFU-E_pEpoR_CISoe The displayed model outputs (solid lines) are defined by Eq. 180. The error model that describes the measurement noise for each model output is indicated by shades around the model outputs and is given by Eq. 180.

2.3.8 Experiment: Time-course of JAK2-STAT5 phosphorylation dynamics in CFU-E cells over-expressing SOCS3 (CFU-E_SOCS3oe)

Treatment: Epo 5 units/ml (1.25e-7 units/cell) + SOCS3 over-expression

The model outputs, see Eq. 5, available in this data set are given by:

$$\begin{aligned} \text{pJAK2\_au} &= \log_{10}(\text{offset\_pJAK2\_socs3oe} + \\ &+ \frac{2 \cdot \text{scale\_pJAK2\_socs3oe} \cdot ([\text{EpoRpJAK2}] + [\text{p12EpoRpJAK2}] + [\text{p1EpoRpJAK2}] + [\text{p2EpoRpJAK2}])}{\text{init\_EpoRJAK2}}) \end{aligned} \tag{186}$$

$$\begin{aligned} \text{pEpoR\_au} &= \log_{10}(\text{offset\_pEpoR\_socs3oe} + \\ &+ \frac{16 \cdot \text{scale\_pEpoR\_socs3oe} \cdot ([\text{p12EpoRpJAK2}] + [\text{p1EpoRpJAK2}] + [\text{p2EpoRpJAK2}])}{\text{init\_EpoRJAK2}}) \end{aligned} \tag{187}$$

$$\text{CIS\_au} = \log_{10}(\text{offset\_CIS\_socs3oe} + \frac{[\text{CIS}] \cdot \text{scale\_CIS\_socs3oe}}{\text{CISEqc} \cdot \text{CISRNAEqc} \cdot \text{init\_STAT5}}) \tag{188}$$

$$\text{SOCS3\_au} = \log_{10}(\text{offset\_SOCS3\_socs3oe} + \frac{[\text{SOCS3}] \cdot \text{scale\_SOCS3\_socs3oe}}{\text{SOCS3Eqc} \cdot \text{SOCS3RNAEqc} \cdot \text{init\_STAT5}}) \tag{189}$$

$$\text{pSTAT5\_au} = \log_{10}(\text{offset\_pSTAT5\_socs3oe} + \frac{[\text{pSTAT5}] \cdot \text{scale\_pSTAT5\_socs3oe}}{\text{init\_STAT5}}) \tag{190}$$

The error model that describes the measurement noise for each model output, see Eq. 7, is given by:

$$\sigma[\text{pJAK2\_au}] = \text{sd\_JAK2EpoR\_au} \tag{191}$$

$$\sigma[\text{pEpoR\_au}] = \text{sd\_JAK2EpoR\_au} \tag{192}$$

$$\sigma[\text{CIS\_au}] = \text{sd\_CIS\_au} \tag{193}$$

$$\sigma[\text{SOCS3\_au}] = \text{sd\_SOCS3\_au} \tag{194}$$

$$\sigma[\text{pSTAT5\_au}] = \text{sd\_STAT5\_au} + \text{SOCS3oe} \cdot \text{sd\_pSTAT5\_socs3oe} \tag{195}$$

To evaluate the ODE system of Eq. 49 – 76 for the conditions in this experiment, the following parameters are set to:

$$\text{ActD} = 0 \tag{196}$$

$$\text{CISoe} = 0 \tag{197}$$

$$\text{SOCS3oe} = 0, 1 \tag{198}$$

$$\text{SHP1oe} = 0 \tag{199}$$

$$\text{epo\_level} = 1.2 \cdot 10^{-07} \tag{200}$$

The agreement of the model outputs and the experimental data, given in Tab. S10, yields a value of the objective function $-2\log(L) = -21.39$ for 40 data points in this data set. The agreement of model outputs and experimental data is shown in Fig. S18.

The trajectories of the dynamical variables and external inputs that correspond to the experimental conditions in this experiment are shown, together with their prediction confidence intervals, later in Fig. S56.

time [min]	SOCS3oe	pJAK2_au conc. [au]	pEpoR_au conc. [au]	CIS_au conc. [au]	SOCS3_au conc. [au]	pSTAT5_au conc. [au]
0.000000	0	0.074825	0.046290	0.179174	0.027811	0.005504
10.000000	0	1.000000	1.000000	0.136152	0.023494	1.000000
60.000000	0	0.237762	0.363958	1.000000	0.083936	0.342302
120.000000	0	0.265734	0.367491	0.969697	0.101606	0.333333
0.000000	1	0.086247	0.063251	0.069424	1.000000	0.014742
10.000000	1	0.447552	0.897527	0.078250	0.886546	0.028251
60.000000	1	0.060606	0.137809	0.078962	0.802209	0.007425
120.000000	1	0.044056	0.124382	0.056576	0.678715	0.001610

Table S10: Experimental data for the experiment CFU-E_SOCS3oe

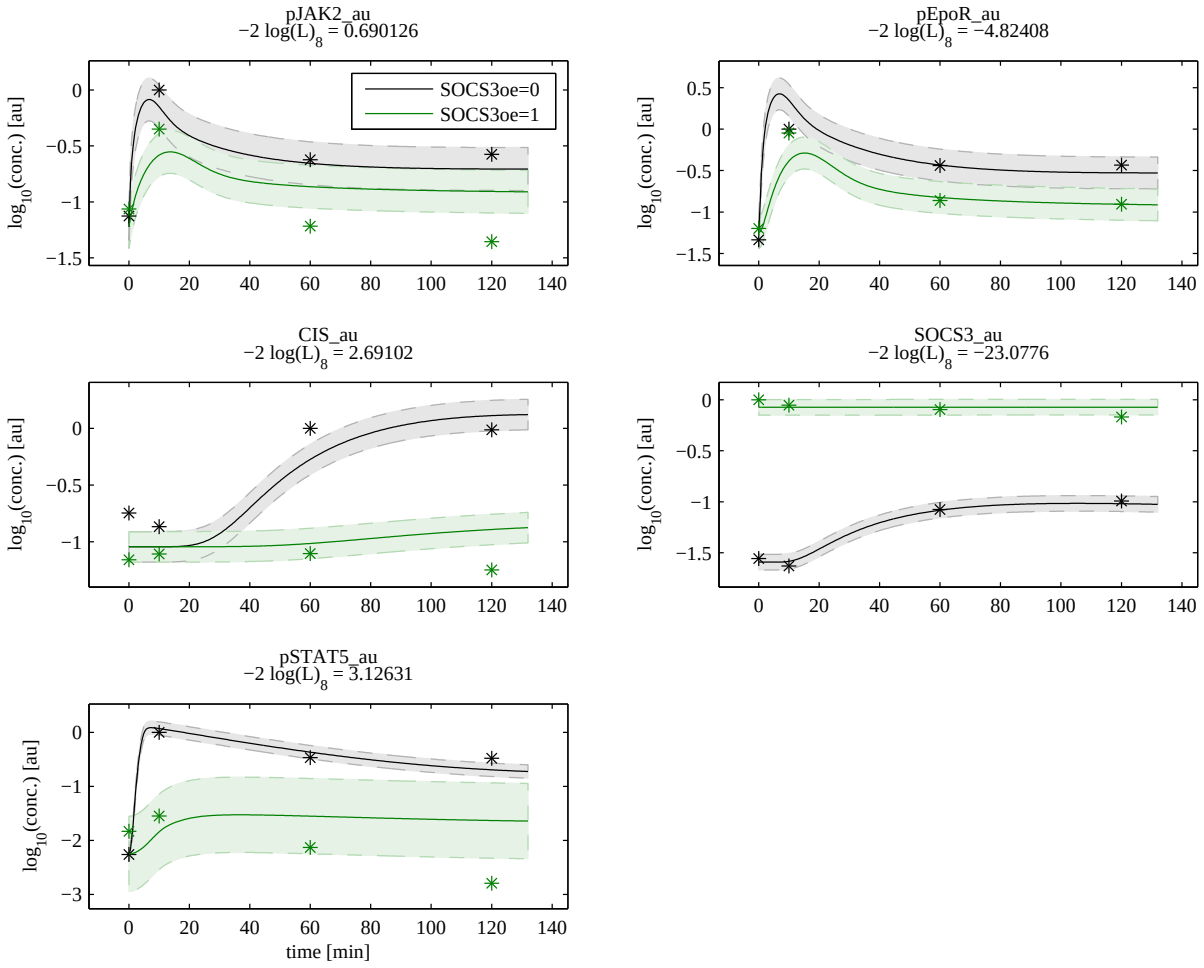

Figure S18: Agreement of model outputs and experimental data for the experiment CFU-E_SOCS3oe
The displayed model outputs (solid lines) are defined by Eq. 187 – 190. The error model that describes the measurement noise for each model output is indicated by shades around the model outputs and is given by Eq. 191 – 195.

2.3.9 Experiment: Time-course of JAK2-STAT5 phosphorylation dynamics in CFU-E cells over-expressing SHP1 (CFU-E_SHP1oe)

Treatment: Epo 5 units/ml (1.25e-7 units/cell) + SHP1 3.5-fold over-expression

The model outputs, see Eq. 5, available in this data set are given by:

$$\begin{aligned} \text{pJAK2\_au} &= \log_{10}(\text{offset\_pJAK2\_shp1oe} + \\ &+ \frac{2 \cdot \text{scale\_pJAK2\_shp1oe} \cdot ([\text{EpoRpJAK2}] + [\text{p12EpoRpJAK2}] + [\text{p1EpoRpJAK2}] + [\text{p2EpoRpJAK2}])}{\text{init\_EpoRJAK2}}) \end{aligned} \tag{201}$$

$$\begin{aligned} \text{pEpoR\_au} &= \log_{10}(\text{offset\_pEpoR\_shp1oe} + \\ &+ \frac{16 \cdot \text{scale\_pEpoR\_shp1oe} \cdot ([\text{p12EpoRpJAK2}] + [\text{p1EpoRpJAK2}] + [\text{p2EpoRpJAK2}])}{\text{init\_EpoRJAK2}}) \end{aligned} \tag{202}$$

$$\text{CIS\_au} = \text{offset\_CIS\_shp1oe} + \frac{[\text{CIS}] \cdot \text{scale\_CIS\_shp1oe}}{\text{CISEqc}} \tag{203}$$

$$\text{tSTAT5\_au} = \frac{\text{scale\_tSTAT5\_shp1oe} \cdot ([\text{STAT5}] + [\text{pSTAT5}])}{\text{init\_STAT5}} \tag{204}$$

$$\text{pSTAT5\_au} = \text{offset\_pSTAT5\_shp1oe} + \frac{[\text{pSTAT5}] \cdot \text{scale\_pSTAT5\_shp1oe}}{\text{init\_STAT5}} \tag{205}$$

$$\text{tSHP1\_au} = \frac{\text{scale\_SHP1\_shp1oe} \cdot ([\text{SHP1}] + [\text{SHP1Act}]) \cdot (\text{SHP1oe} \cdot \text{SHP1ProOE} + 1)}{\text{init\_SHP1}} \tag{206}$$

The error model that describes the measurement noise for each model output, see Eq. 7, is given by:

$$\sigma[\text{pJAK2\_au}] = \text{sd\_JAK2EpoR\_au} \tag{207}$$

$$\sigma[\text{pEpoR\_au}] = \text{sd\_JAK2EpoR\_au} \tag{208}$$

$$\sigma[\text{CIS\_au}] = \text{sd\_CIS\_au} \tag{209}$$

$$\sigma[\text{tSTAT5\_au}] = \text{sd\_STAT5\_au} \tag{210}$$

$$\sigma[\text{pSTAT5\_au}] = \text{sd\_STAT5\_au} \tag{211}$$

$$\sigma[\text{tSHP1\_au}] = \text{sd\_SHP1\_au} \tag{212}$$

To evaluate the ODE system of Eq. 49 – 76 for the conditions in this experiment, the following parameters are set to:

$$\text{ActD} = 0 \tag{213}$$

$$\text{CISoe} = 0 \tag{214}$$

$$\text{SOCS3oe} = 0 \tag{215}$$

$$\text{SHP1oe} = 0, 1 \tag{216}$$

$$\text{epo\_level} = 1.2 \cdot 10^{-07} \tag{217}$$

The agreement of the model outputs and the experimental data, given in Tab. S11, yields a value of the objective function $-2\log(L) = -99.69$ for 60 data points in this data set. The agreement of model outputs and experimental data is shown in Fig. S19.

The trajectories of the dynamical variables and external inputs that correspond to the experimental conditions in this experiment are shown, together with their prediction confidence intervals, later in Fig. S57.

time [min]	SHP1oe	pJAK2_au conc. [au]	pEpoR_au conc. [au]	CIS_au conc. [au]	tSTAT5_au conc. [au]	pSTAT5_au conc. [au]	tSHP1_au conc. [au]
0.000000	0	0.019283	0.035222	0.071794	0.495370	0.061201	0.166346
5.000000	0	1.000000	1.000000	0.062287	0.583333	0.760736	0.183654
10.000000	0	0.991870	0.517241	0.072862	0.595370	1.000000	0.285577
30.000000	0	0.513008	0.317734	0.134231	0.576852	0.474847	0.300962
60.000000	0	0.306504	0.144089	1.000000	0.425926	0.342331	0.201923
0.000000	1	0.037398	0.024631	0.051126	1.000000	0.050071	0.812500
5.000000	1	0.983740	0.423645	0.043077	0.688889	0.473006	0.870192
10.000000	1	0.926829	0.435961	0.046109	0.753704	0.580982	1.000000
30.000000	1	0.337398	0.160837	0.157737	0.781481	0.420245	0.913462
60.000000	1	0.121138	0.075369	0.748988	0.623148	0.236196	0.815385

Table S11: Experimental data for the experiment CFU-E_SHP1oe

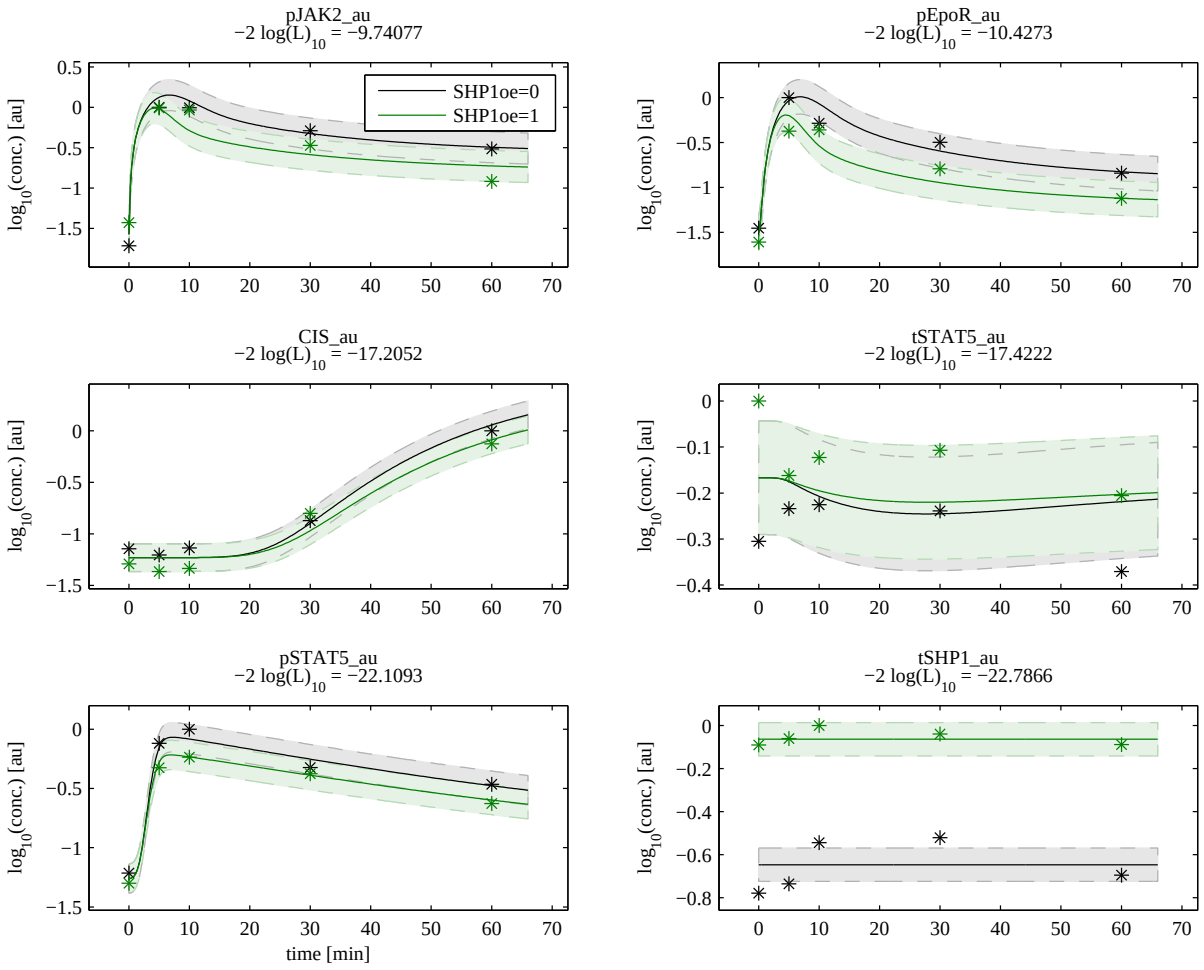

Figure S19: Agreement of model outputs and experimental data for the experiment CFU-E_SHP1oe
The displayed model outputs (solid lines) are defined by Eq. 202 – 206. The error model that describes the measurement noise for each model output is indicated by shades around the model outputs and is given by Eq. 207 – 212.

2.3.10 Experiment: Dose response of JAK2 and EpoR phosphorylation in CFU-E cells 7 minutes after Epo stimulation (CFU-E_DoseResp_7min)

Treatment: Epo dose response at 7 minutes

The model outputs, see Eq. 5, available in this data set are given by:

$$\begin{aligned} \text{pJAK2\_au} &= \log_{10}(\text{offset\_pJAK2\_dr7} + \\ &+ \frac{2 \cdot \text{scale\_pJAK2\_dr7} \cdot ([\text{EpoRpJAK2}] + [\text{p12EpoRpJAK2}] + [\text{p1EpoRpJAK2}] + [\text{p2EpoRpJAK2}])}{\text{init\_EpoRJAK2}}) \end{aligned} \tag{218}$$

$$\begin{aligned} \text{pEpoR\_au} &= \log_{10}(\text{offset\_pEpoR\_dr7} + \\ &+ \frac{16 \cdot \text{scale\_pEpoR\_dr7} \cdot ([\text{p12EpoRpJAK2}] + [\text{p1EpoRpJAK2}] + [\text{p2EpoRpJAK2}])}{\text{init\_EpoRJAK2}}) \end{aligned} \tag{219}$$

The error model that describes the measurement noise for each model output, see Eq. 7, is given by:

$$\sigma[\text{pJAK2\_au}] = \text{sd\_JAK2EpoR\_au} \tag{220}$$

$$\sigma[\text{pEpoR\_au}] = \text{sd\_JAK2EpoR\_au} \tag{221}$$

To evaluate the ODE system of Eq. 49 – 76 for the conditions in this experiment, the following parameters are set to:

$$\text{ActD} = 0 \tag{222}$$

$$\text{CISoe} = 0 \tag{223}$$

$$\text{SOCS3oe} = 0 \tag{224}$$

$$\text{SHP1oe} = 0 \tag{225}$$

$$\text{epo\_level} = 2.5 \cdot 10^{-09}, 2.5 \cdot 10^{-08}, 2.5 \cdot 10^{-07}, 2.5 \cdot 10^{-06}, 2.5 \cdot 10^{-05} \tag{226}$$

The agreement of the model outputs and the experimental data, given in Tab. S12, yields a value of the objective function $-2\log(L) = -31.22$ for 30 data points in this data set. The agreement of model outputs and experimental data is shown in Fig. S20.

The trajectories of the dynamical variables and external inputs that correspond to the experimental conditions in this experiment are shown, together with their prediction confidence intervals, later in Fig. S58.

time [min]	epo_level	pJAK2_au conc. [au]	pEpoR_au conc. [au]
7.000000	0.1	0.040590	0.052184
7.000000	0.1	0.045387	0.040024
7.000000	0.1	0.080443	0.036836
7.000000	1	0.154244	0.131051
7.000000	1	0.165314	0.270366
7.000000	1	0.225461	0.179457
7.000000	10	0.453875	0.599764
7.000000	10	0.590406	0.806375
7.000000	10	0.730627	0.335301
7.000000	100	0.564576	0.659976
7.000000	100	0.797048	0.785124
7.000000	100	1.000000	0.695396
7.000000	1000	0.501845	1.000000
7.000000	1000	0.760148	0.671783
7.000000	1000	0.826568	0.916175

Table S12: Experimental data for the experiment CFU-E_DoseResp_7min

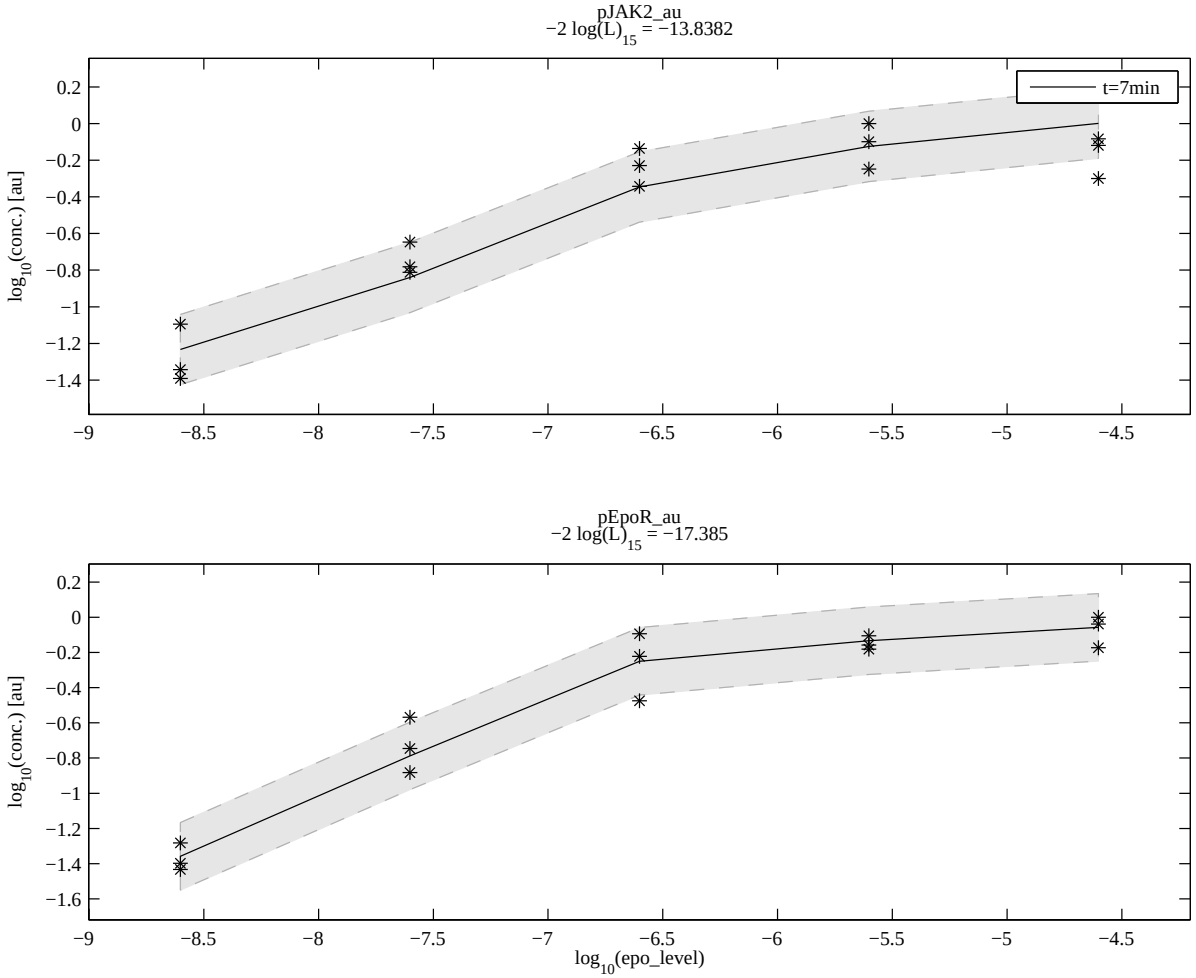

Figure S20: Agreement of model outputs and experimental data for the experiment CFU-E_DoseResp_7min The displayed model outputs (solid lines) are defined by Eq. 219 – 219. The error model that describes the measurement noise for each model output is indicated by shades around the model outputs and is given by Eq. 220 – 221.

2.3.11 Experiment: Dose response of JAK2 and EpoR phosphorylation in CFU-E cells 30 minutes after Epo stimulation (CFU-E_DoseResp_30min)

Treatment: Epo dose response at 30 minutes

The model outputs, see Eq. 5, available in this data set are given by:

$$\begin{aligned} \text{pJAK2\_au} &= \log_{10}(\text{offset\_pJAK2\_dr30} + \\ &+ \frac{2 \cdot \text{scale\_pJAK2\_dr30} \cdot ([\text{EpoRpJAK2}] + [\text{p12EpoRpJAK2}] + [\text{p1EpoRpJAK2}] + [\text{p2EpoRpJAK2}])}{\text{init\_EpoRJAK2}}) \end{aligned} \tag{227}$$

$$\begin{aligned} \text{pEpoR\_au} &= \log_{10}(\text{offset\_pEpoR\_dr30} + \\ &+ \frac{16 \cdot \text{scale\_pEpoR\_dr30} \cdot ([\text{p12EpoRpJAK2}] + [\text{p1EpoRpJAK2}] + [\text{p2EpoRpJAK2}])}{\text{init\_EpoRJAK2}}) \end{aligned} \tag{228}$$

The error model that describes the measurement noise for each model output, see Eq. 7, is given by:

$$\sigma[\text{pJAK2\_au}] = \text{sd\_JAK2EpoR\_au} \tag{229}$$

$$\sigma[\text{pEpoR\_au}] = \text{sd\_JAK2EpoR\_au} \tag{230}$$

To evaluate the ODE system of Eq. 49 – 76 for the conditions in this experiment, the following parameters are set to:

$$\text{ActD} = 0 \tag{231}$$

$$\text{CISoe} = 0 \tag{232}$$

$$\text{SOCS3oe} = 0 \tag{233}$$

$$\text{SHP1oe} = 0 \tag{234}$$

$$\text{epo\_level} = 2.5 \cdot 10^{-09}, 2.5 \cdot 10^{-08}, 1.2 \cdot 10^{-07}, 2.5 \cdot 10^{-07}, 1.3 \cdot 10^{-06}, 2.5 \cdot 10^{-06} \tag{235}$$

The agreement of the model outputs and the experimental data, given in Tab. S13, yields a value of the objective function $-2\log(L) = 22.26$ for 36 data points in this data set. The agreement of model outputs and experimental data is shown in Fig. S21.

The trajectories of the dynamical variables and external inputs that correspond to the experimental conditions in this experiment are shown, together with their prediction confidence intervals, later in Fig. S59.

time [min]	epo_level	pJAK2_au conc. [au]	pEpoR_au conc. [au]
30.000000	0.1	0.090671	0.121262
30.000000	0.1	0.069679	0.103322
30.000000	0.1	0.108746	0.246512
30.000000	1	0.381924	0.342193
30.000000	1	0.235277	0.481728
30.000000	1	0.228280	0.634551
30.000000	5	0.769679	0.657807
30.000000	5	0.667638	0.697674
30.000000	5	0.673469	0.740864
30.000000	10	0.725948	0.607973
30.000000	10	0.650146	0.657807
30.000000	10	0.626822	1.000000
30.000000	50	0.827988	0.744186
30.000000	50	0.758017	0.471761
30.000000	50	0.548105	0.787375
30.000000	100	1.000000	0.717608
30.000000	100	0.787172	0.687708
30.000000	100	0.755102	0.717608

Table S13: Experimental data for the experiment CFU-E_DoseResp_30min

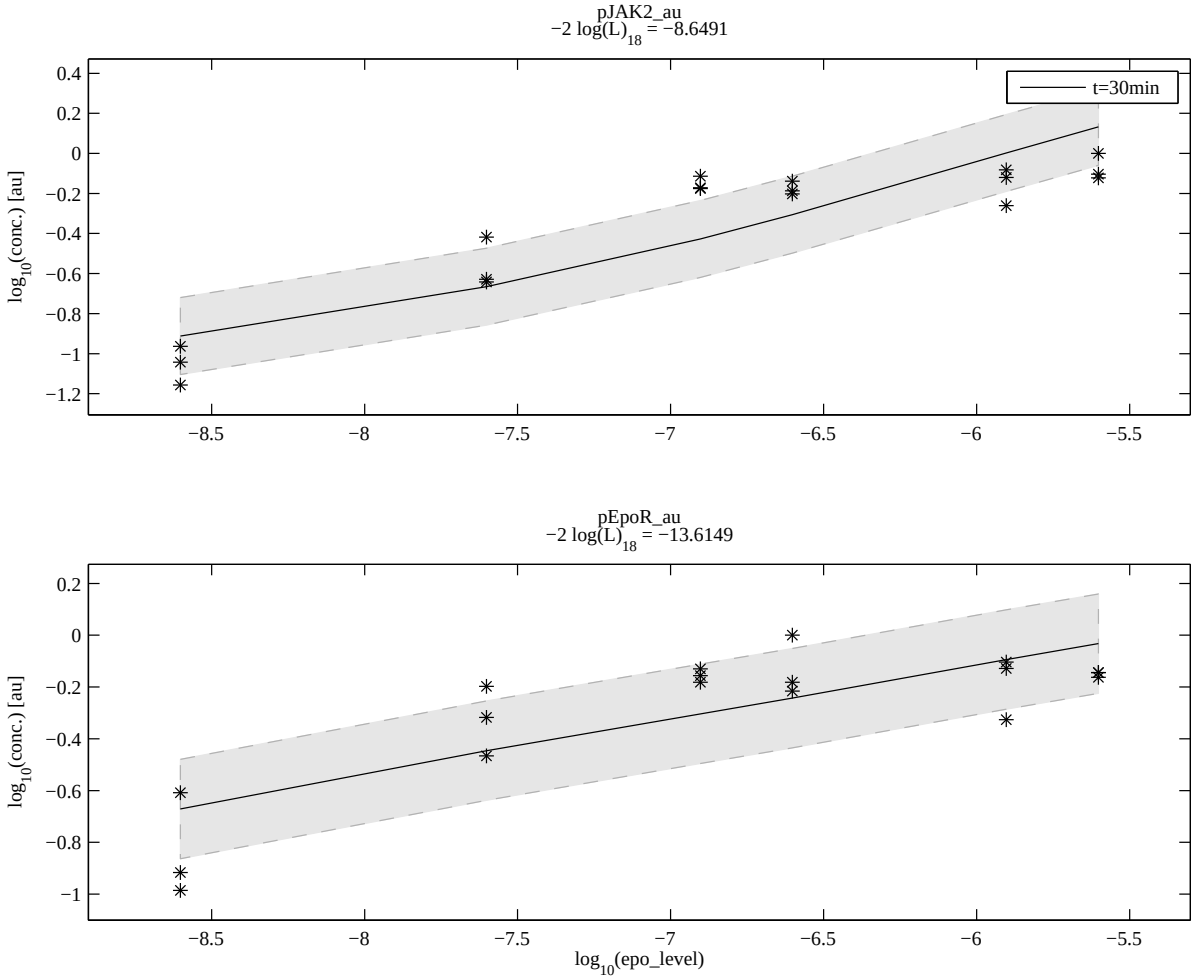

Figure S21: Agreement of model outputs and experimental data for the experiment CFU-E_DoseResp_30min
The displayed model outputs (solid lines) are defined by Eq. 228 – 228. The error model that describes the measurement noise for each model output is indicated by shades around the model outputs and is given by Eq. 229 – 230.

2.3.12 Experiment: Dose response of STAT5 phosphorylation in CFU-E cells 10 minutes after Epo stimulation (CFU-E_DoseResp_pSTAT5_10min)

Treatment: Epo dose response at 10 minutes

The model outputs, see Eq. 5, available in this data set are given by:

$$\text{pSTAT5\_au} = \frac{[\text{pSTAT5}] \cdot \text{scale\_pSTAT5\_dr10}}{\text{init\_STAT5}} \tag{236}$$

The error model that describes the measurement noise for each model output, see Eq. 7, is given by:

$$\sigma[\text{pSTAT5\_au}] = \text{sd\_STAT5\_au} \tag{237}$$

To evaluate the ODE system of Eq. 49 – 76 for the conditions in this experiment, the following parameters are set to:

$$\text{ActD} = 0 \tag{238}$$
$$\text{CISoe} = 0 \tag{239}$$
$$\text{SOCS3oe} = 0 \tag{240}$$
$$\text{SHP1oe} = 0 \tag{241}$$
$$\text{epo\_level} = 2.5 \cdot 10^{-09}, 1.2 \cdot 10^{-08}, 2.5 \cdot 10^{-08}, 1.2 \cdot 10^{-07}, 2.5 \cdot 10^{-07}, 2.5 \cdot 10^{-06} \tag{242}$$

The agreement of the model outputs and the experimental data, given in Tab. S14, yields a value of the objective function $-2\log(L) = -9.46$ for 18 data points in this data set. The agreement of model outputs and experimental data is shown in Fig. S22.

The trajectories of the dynamical variables and external inputs that correspond to the experimental conditions in this experiment are shown, together with their prediction confidence intervals, later in Fig. S60.

time [min]	epo_level	pSTAT5_au conc. [au]
10.000000	0.1	0.009338
10.000000	0.1	0.004178
10.000000	0.1	0.009596
10.000000	0.3162	NaN
10.000000	0.5	0.204456
10.000000	0.5	0.063670
10.000000	0.5	0.130130
10.000000	0.7	NaN
10.000000	1	0.393185
10.000000	1	0.193971
10.000000	1	0.275229
10.000000	1.58	NaN
10.000000	3.16	NaN
10.000000	5	0.647444
10.000000	5	0.596330
10.000000	5	0.711664
10.000000	7.07	NaN
10.000000	10	0.824377
10.000000	10	0.726081
10.000000	10	1.000000
10.000000	31.62	NaN
10.000000	100	0.845347
10.000000	100	0.699869
10.000000	100	0.968545

Table S14: Experimental data for the experiment CFU-E_DoseResp_pSTAT5_10min

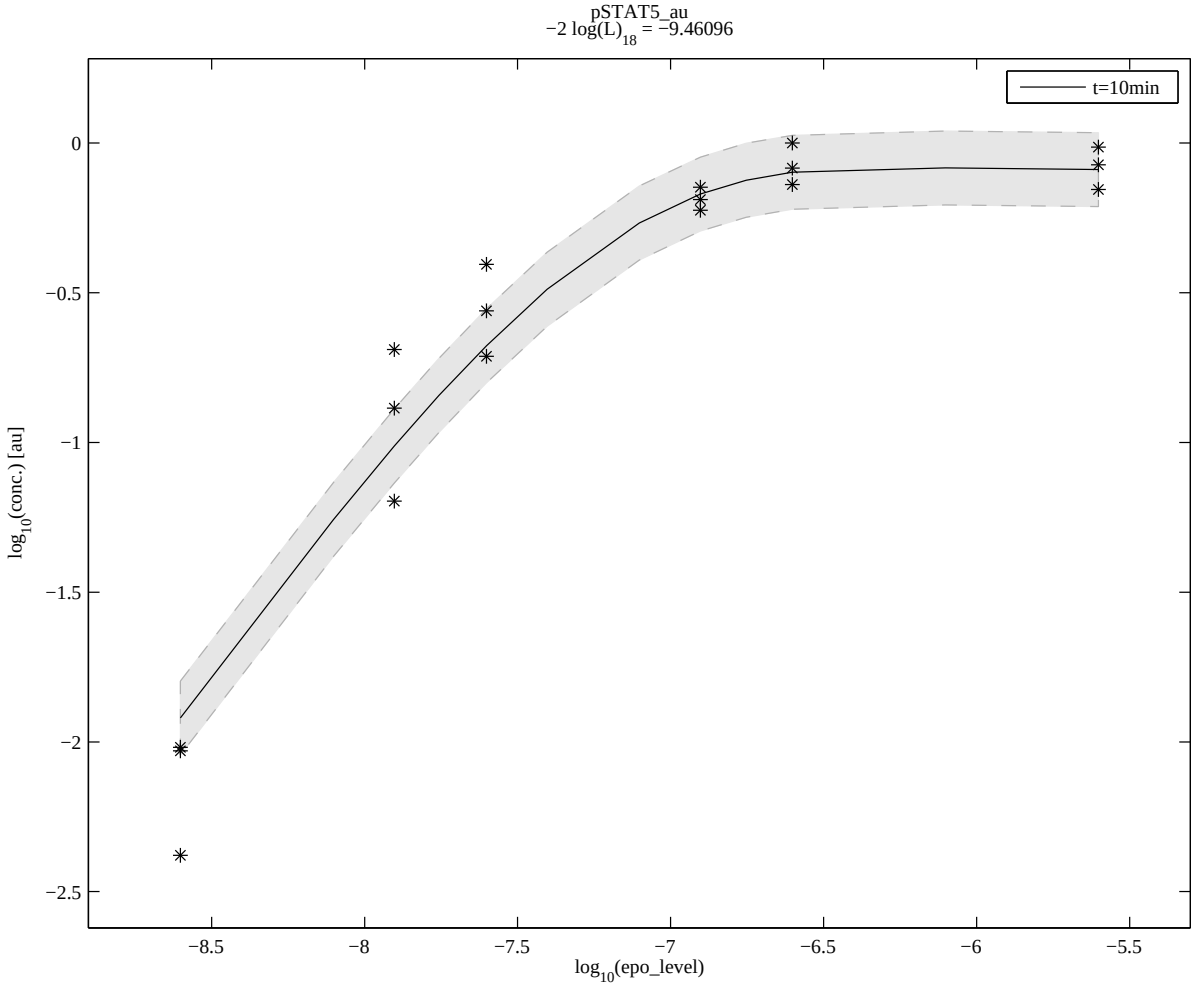

Figure S22: Agreement of model outputs and experimental data for the experiment CFU-E_DoseResp_pSTAT5_10min
The displayed model outputs (solid lines) are defined by Eq. 236 – 236. The error model that describes the measurement noise for each model output is indicated by shades around the model outputs and is given by Eq. 237 – 237.

2.3.13 Experiment: Dose response of CIS expression in CFU-E cells 90 minutes after Epo stimulation (CFU-E_DoseResp_CIS_90min)

Treatment: Epo dose response at 90 minutes

The model outputs, see Eq. 5, available in this data set are given by:

$$\text{CIS\_au1} = \frac{[\text{CIS}] \cdot \text{scale1\_CIS\_dr90}}{\text{CISEqc}} \tag{243}$$

$$\text{CIS\_au2} = \frac{[\text{CIS}] \cdot \text{scale2\_CIS\_dr90}}{\text{CISEqc}} \tag{244}$$

The error model that describes the measurement noise for each model output, see Eq. 7, is given by:

$$\sigma[\text{CIS\_au1}] = \text{sd\_CIS\_au} \tag{245}$$

$$\sigma[\text{CIS\_au2}] = \text{sd\_CIS\_au} \tag{246}$$

To evaluate the ODE system of Eq. 49 – 76 for the conditions in this experiment, the following parameters are set to:

$$\text{ActD} = 0 \tag{247}$$

$$\text{CISoe} = 0 \tag{248}$$

$$\text{SOCS3oe} = 0 \tag{249}$$

$$\text{SHP1oe} = 0 \tag{250}$$

$$\text{epo\_level} = 2.5 \cdot 10^{-09}, 2.5 \cdot 10^{-08}, 1.2 \cdot 10^{-07}, 2.5 \cdot 10^{-07}, 2.5 \cdot 10^{-06} \tag{251}$$

The agreement of the model outputs and the experimental data, given in Tab. S15, yields a value of the objective function $-2\log(L) = -38.39$ for 30 data points in this data set. The agreement of model outputs and experimental data is shown in Fig. S23.

The trajectories of the dynamical variables and external inputs that correspond to the experimental conditions in this experiment are shown, together with their prediction confidence intervals, later in Fig. S61.

time [min]	epo_level	CIS_au1 conc. [au]	CIS_au2 conc. [au]
90.000000	0.1	0.041597	0.036280
90.000000	0.1	0.037763	0.045195
90.000000	0.1	0.038971	0.041019
90.000000	1	0.513332	0.557756
90.000000	1	0.472805	0.403881
90.000000	1	0.452635	0.541982
90.000000	5	0.792155	0.713065
90.000000	5	0.970147	0.604428
90.000000	5	0.906889	0.519957
90.000000	10	0.970911	0.949133
90.000000	10	0.999971	0.586600
90.000000	10	0.853607	0.873716
90.000000	100	0.729914	1.000000
90.000000	100	0.886000	0.850285
90.000000	100	1.000000	0.912522

Table S15: Experimental data for the experiment CFU-E_DoseResp_CIS_90min

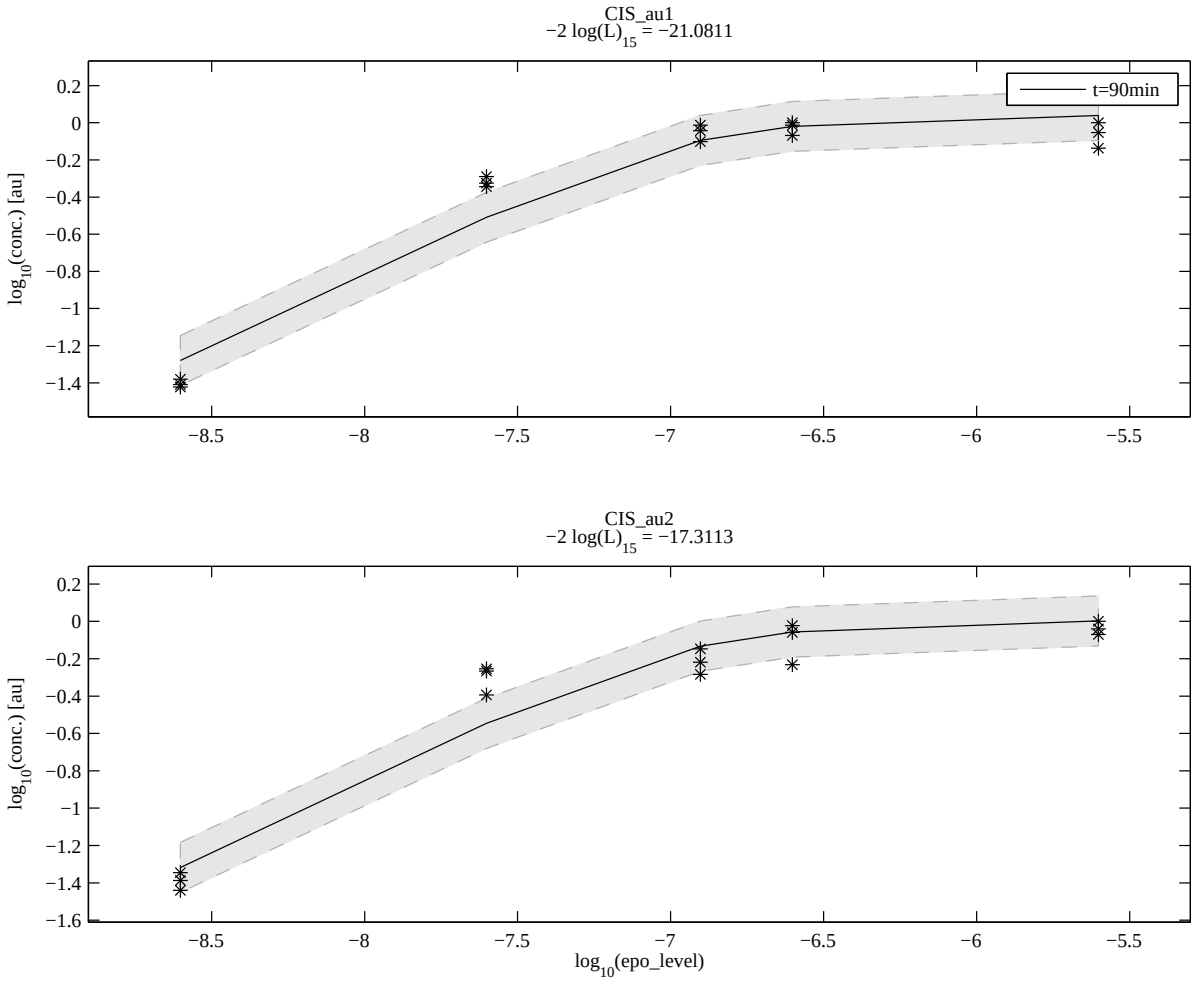

Figure S23: Agreement of model outputs and experimental data for the experiment CFU-E_DoseResp_CIS_90min
The displayed model outputs (solid lines) are defined by Eq. 243 – 244. The error model that describes the measurement noise for each model output is indicated by shades around the model outputs and is given by Eq. 245 – 246.

2.4 Estimated model parameters

The model parameters were estimated by maximum likelihood estimation applying the MATLAB lsqnonlin algorithm in logarithmic parameter space. In Tab. S16 – S19 the estimated parameter values are given. The parameter name prefix init_ indicates the initial value of a dynamic variable. The parameter name prefix offset_ indicates an offset of the experimental data. The parameter name prefix scale_ indicates a scaling factor of the experimental data. The parameter name prefix sd_ indicates the magnitude of the measurement noise for a specific measurement. Parameters highlighted in red color indicate that their estimated value is close to its bounds, see in Sec. 2.5 for reasons.

	name	θ_{min}	$\hat{\theta}$	θ_{max}	$10^{\hat{\theta}}$		unit
1	CISEqc	-3	+2.6364	+4	$+4.33 \cdot 10^{+02}$		nM
2	CISEqcOE	-3	-0.2755	+3	$+5.30 \cdot 10^{-01}$		-
3	CISInh	-3	+8.8947	+1e+01	$+7.85 \cdot 10^{+08}$		-
4	CISRNADelay	-3	-0.8393	+3	$+1.45 \cdot 10^{-01}$		1/min
5	CISRNAEqc		+0.0000		$+1.00 \cdot 10^{+00}$	fixed	nM
6	CISRNATurn	-3	+3.0000	+3	$+1.00 \cdot 10^{+03}$		1/min
7	CISTurn	-3	-2.0758	+3	$+8.40 \cdot 10^{-03}$		1/min
8	EpoRActJAK2	-3	-0.5730	+4	$+2.67 \cdot 10^{-01}$		1/min
9	EpoRCISInh	-3	+6.0000	+6	$+1.00 \cdot 10^{+06}$		-
10	EpoRCISRemove	-3	+0.7347	+3	$+5.43 \cdot 10^{+00}$		1/min
11	JAK2ActEpo	-3	+5.8016	+9	$+6.33 \cdot 10^{+05}$		1/(min · (units epo)/cell)
12	JAK2EpoRDeaSHP1	-3	+2.1545	+1e+01	$+1.43 \cdot 10^{+02}$		1/min
13	SHP1ActEpoR	-3	-3.0000	+3	$+1.00 \cdot 10^{-03}$		1/min
14	SHP1Dea	-3	-2.0881	+3	$+8.16 \cdot 10^{-03}$		1/min
15	SHP1ProOE	-3	+0.4511	+3	$+2.83 \cdot 10^{+00}$		-
16	SOCS3Eqc	-3	+2.2397	+3	$+1.74 \cdot 10^{+02}$		nM
17	SOCS3EqcOE	-3	-0.1680	+3	$+6.79 \cdot 10^{-01}$		-
18	SOCS3Inh	-3	+1.0174	+3	$+1.04 \cdot 10^{+01}$		-
19	SOCS3RNADelay	-3	+0.0272	+3	$+1.06 \cdot 10^{+00}$		1/min
20	SOCS3RNAEqc		+0.0000		$+1.00 \cdot 10^{+00}$	fixed	nM
21	SOCS3RNATurn	-3	-2.0805	+3	$+8.31 \cdot 10^{-03}$		1/min
22	SOCS3Turn	-3	+4.0000	+4	$+1.00 \cdot 10^{+04}$		1/min
23	STAT5ActEpoR	-3	+1.5908	+3	$+3.90 \cdot 10^{+01}$		1/min
24	STAT5ActJAK2	-3	-1.1074	+3	$+7.81 \cdot 10^{-02}$		1/min
25	STAT5Exp	-3	-1.1278	+3	$+7.45 \cdot 10^{-02}$		1/min
26	STAT5Imp	-3	-1.5704	+3	$+2.69 \cdot 10^{-02}$		1/min
27	init_EpoRJAK2	-3	+0.5995	+3	$+3.98 \cdot 10^{+00}$		nM
28	init_SHP1	-3	+1.4269	+3	$+2.67 \cdot 10^{+01}$		nM
29	init_STAT5	-3	+1.9017	+3	$+7.98 \cdot 10^{+01}$		nM

Table S16: Estimated values of the dynamic parameters
$\hat{\theta}$ indicates the estimated value of the parameter. θ_{min} and θ_{max} indicated the allowed upper and lower bounds for the parameter. $10^{\hat{\theta}}$ indicates the value of the parameter in normal space.

	name	θ_{min}	$\hat{\theta}$	θ_{max}	$10^{\hat{\theta}}$	unit
30	offset_CIS_actd	-3	-2.0274	+3	$+9.39 \cdot 10^{-03}$	a.u.
31	offset_CIS_cisoe	-3	-1.5227	+3	$+3.00 \cdot 10^{-02}$	a.u.
32	offset_CIS_long	-3	-1.5774	+3	$+2.65 \cdot 10^{-02}$	a.u.
33	offset_CIS_shp1oe	-3	-1.2307	+3	$+5.88 \cdot 10^{-02}$	a.u.
34	offset_CIS_socs3oe	-3	-1.0434	+3	$+9.05 \cdot 10^{-02}$	a.u.
35	offset_SOCS3_cisoe	-3	-0.5555	+3	$+2.78 \cdot 10^{-01}$	a.u.
36	offset_SOCS3_long	-3	-0.9413	+3	$+1.14 \cdot 10^{-01}$	a.u.
37	offset_SOCS3_socs3oe	-3	-1.5920	+3	$+2.56 \cdot 10^{-02}$	a.u.
38	offset_pEpoR_actd	-3	-1.7249	+3	$+1.88 \cdot 10^{-02}$	a.u.
39	offset_pEpoR_cisoe	-3	-1.5199	+3	$+3.02 \cdot 10^{-02}$	a.u.
40	offset_pEpoR_cisoe_pepor	-3	-0.8826	+3	$+1.31 \cdot 10^{-01}$	a.u.
41	offset_pEpoR_dr30	-3	-3.0000	+3	$+1.00 \cdot 10^{-03}$	a.u.
42	offset_pEpoR_dr7	-3	-1.5466	+3	$+2.84 \cdot 10^{-02}$	a.u.
43	offset_pEpoR_fine	-3	-1.1901	+3	$+6.46 \cdot 10^{-02}$	a.u.
44	offset_pEpoR_long	-3	-2.3574	+3	$+4.39 \cdot 10^{-03}$	a.u.
45	offset_pEpoR_shp1oe	-3	-1.5041	+3	$+3.13 \cdot 10^{-02}$	a.u.
46	offset_pEpoR_socs3oe	-3	-1.2463	+3	$+5.67 \cdot 10^{-02}$	a.u.
47	offset_pJAK2_actd	-3	-1.7680	+3	$+1.71 \cdot 10^{-02}$	a.u.
48	offset_pJAK2_cisoe	-3	-1.6590	+3	$+2.19 \cdot 10^{-02}$	a.u.
49	offset_pJAK2_dr30	-3	-1.5245	+3	$+2.99 \cdot 10^{-02}$	a.u.
50	offset_pJAK2_dr7	-3	-1.3248	+3	$+4.73 \cdot 10^{-02}$	a.u.
51	offset_pJAK2_fine	-3	-1.6644	+3	$+2.17 \cdot 10^{-02}$	a.u.
52	offset_pJAK2_long	-3	-2.0235	+3	$+9.47 \cdot 10^{-03}$	a.u.
53	offset_pJAK2_shp1oe	-3	-1.5740	+3	$+2.67 \cdot 10^{-02}$	a.u.
54	offset_pJAK2_socs3oe	-3	-1.2236	+3	$+5.98 \cdot 10^{-02}$	a.u.
55	offset_pSTAT5_actd	-3	-2.7284	+3	$+1.87 \cdot 10^{-03}$	a.u.
56	offset_pSTAT5_cisoe	-3	-1.1500	+3	$+7.08 \cdot 10^{-02}$	a.u.
57	offset_pSTAT5_conc	-3	-0.6255	+3	$+2.37 \cdot 10^{-01}$	a.u.
58	offset_pSTAT5_long	-3	-2.9614	+3	$+1.09 \cdot 10^{-03}$	a.u.
59	offset_pSTAT5_shp1oe	-3	-1.2601	+3	$+5.49 \cdot 10^{-02}$	a.u.
60	offset_pSTAT5_socs3oe	-3	-2.2508	+3	$+5.61 \cdot 10^{-03}$	a.u.

Table S17: Estimated values of the offset parameters
$\hat{\theta}$ indicates the estimated value of the parameter. θ_{min} and θ_{max} indicated the allowed upper and lower bounds for the parameter. $10^{\hat{\theta}}$ indicates the value of the parameter in normal space.

	name	θ_{min}	$\hat{\theta}$	θ_{max}	$10^{\hat{\theta}}$	unit
61	scale1_CIS_dr90	-3	+1.2446	+3	$+1.76 \cdot 10^{+01}$	a.u./nM
62	scale2_CIS_dr90	-3	+1.2074	+3	$+1.61 \cdot 10^{+01}$	a.u./nM
63	scale_CISRNA_foldA	-3	+1.5222	+3	$+3.33 \cdot 10^{+01}$	1/nM
64	scale_CISRNA_foldB	-3	+1.4916	+3	$+3.10 \cdot 10^{+01}$	1/nM
65	scale_CISRNA_foldC	-3	+1.2927	+3	$+1.96 \cdot 10^{+01}$	1/nM
66	scale_CIS_actd	-3	+1.1629	+3	$+1.45 \cdot 10^{+01}$	a.u./nM
67	scale_CIS_cisoe	-3	+0.1370	+3	$+1.37 \cdot 10^{+00}$	a.u./nM
68	scale_CIS_long	-3	+1.2150	+3	$+1.64 \cdot 10^{+01}$	a.u./nM
69	scale_CIS_shp1oe	-3	+1.7136	+3	$+5.17 \cdot 10^{+01}$	a.u./nM
70	scale_CIS_socs3oe	-3	+1.3253	+3	$+2.12 \cdot 10^{+01}$	a.u./nM
71	scale_SHP1_shp1oe	-3	-0.6468	+3	$+2.26 \cdot 10^{-01}$	a.u./nM
72	scale_SOCS3RNA_foldA	-3	+1.7556	+3	$+5.70 \cdot 10^{+01}$	1/nM
73	scale_SOCS3RNA_foldB	-3	+1.6909	+3	$+4.91 \cdot 10^{+01}$	1/nM
74	scale_SOCS3RNA_foldC	-3	+1.9071	+3	$+8.07 \cdot 10^{+01}$	1/nM
75	scale_SOCS3_cisoe	-3	+1.0633	+3	$+1.16 \cdot 10^{+01}$	a.u./nM
76	scale_SOCS3_long	-3	+1.1900	+3	$+1.55 \cdot 10^{+01}$	a.u./nM
77	scale_SOCS3_socs3oe	-3	+0.0809	+3	$+1.20 \cdot 10^{+00}$	a.u./nM
78	scale_pEpoR_actd	-3	-0.6663	+3	$+2.16 \cdot 10^{-01}$	a.u./nM
79	scale_pEpoR_cisoe	-3	-0.5629	+3	$+2.74 \cdot 10^{-01}$	a.u./nM
80	scale_pEpoR_cisoe_pepor	-3	-0.8052	+3	$+1.57 \cdot 10^{-01}$	a.u./nM
81	scale_pEpoR_dr30	-3	-0.2697	+3	$+5.37 \cdot 10^{-01}$	a.u./nM
82	scale_pEpoR_dr7	-3	-0.9939	+3	$+1.01 \cdot 10^{-01}$	a.u./nM
83	scale_pEpoR_fine	-3	-1.0955	+3	$+8.03 \cdot 10^{-02}$	a.u./nM
84	scale_pEpoR_long	-3	-0.5909	+3	$+2.56 \cdot 10^{-01}$	a.u./nM
85	scale_pEpoR_shp1oe	-3	-0.6175	+3	$+2.41 \cdot 10^{-01}$	a.u./nM
86	scale_pEpoR_socs3oe	-3	-0.1957	+3	$+6.37 \cdot 10^{-01}$	a.u./nM
87	scale_pJAK2_actd	-3	-0.0918	+3	$+8.09 \cdot 10^{-01}$	a.u./nM
88	scale_pJAK2_cisoe	-3	+0.2681	+3	$+1.85 \cdot 10^{+00}$	a.u./nM
89	scale_pJAK2_dr30	-3	+0.2494	+3	$+1.78 \cdot 10^{+00}$	a.u./nM
90	scale_pJAK2_dr7	-3	-0.2956	+3	$+5.06 \cdot 10^{-01}$	a.u./nM
91	scale_pJAK2_fine	-3	-0.3971	+3	$+4.01 \cdot 10^{-01}$	a.u./nM
92	scale_pJAK2_long	-3	-0.0542	+3	$+8.83 \cdot 10^{-01}$	a.u./nM
93	scale_pJAK2_shp1oe	-3	+0.3636	+3	$+2.31 \cdot 10^{+00}$	a.u./nM
94	scale_pJAK2_socs3oe	-3	+0.1026	+3	$+1.27 \cdot 10^{+00}$	a.u./nM
95	scale_pSTAT5_actd	-3	+0.0404	+3	$+1.10 \cdot 10^{+00}$	a.u./nM
96	scale_pSTAT5_cisoe	-3	+0.3837	+3	$+2.42 \cdot 10^{+00}$	a.u./nM
97	scale_pSTAT5_dr10	-3	+0.0041	+3	$+1.01 \cdot 10^{+00}$	a.u./nM
98	scale_pSTAT5_long	-3	+0.1684	+3	$+1.47 \cdot 10^{+00}$	a.u./nM
99	scale_pSTAT5_shp1oe	-3	+0.0613	+3	$+1.15 \cdot 10^{+00}$	a.u./nM
100	scale_pSTAT5_socs3oe	-3	+0.2456	+3	$+1.76 \cdot 10^{+00}$	a.u./nM
101	scale_tSTAT5_actd	-3	-0.0887	+3	$+8.15 \cdot 10^{-01}$	a.u./nM
102	scale_tSTAT5_long	-3	-0.1180	+3	$+7.62 \cdot 10^{-01}$	a.u./nM
103	scale_tSTAT5_shp1oe	-3	-0.1668	+3	$+6.81 \cdot 10^{-01}$	a.u./nM

Table S18: Estimated values of the scaling parameters
$\hat{\theta}$ indicates the estimated value of the parameter. θ_{min} and θ_{max} indicated the allowed upper and lower bounds for the parameter. $10^{\hat{\theta}}$ indicates the value of the parameter in normal space.

	name	θ_{min}	$\hat{\theta}$	θ_{max}	$10^{\hat{\theta}}$	unit
104	sd_CIS_abs	-3	-1.1447	+3	$+7.17 \cdot 10^{-02}$	nM
105	sd_CIS_au	-3	-0.8728	+3	$+1.34 \cdot 10^{-01}$	a.u.
106	sd_JAK2EpoR_au	-3	-0.7171	+3	$+1.92 \cdot 10^{-01}$	a.u.
107	sd_RNA_fold	-3	-0.9868	+3	$+1.03 \cdot 10^{-01}$	-
108	sd_SHP1_abs	-3	-1.1877	+3	$+6.49 \cdot 10^{-02}$	nM
109	sd_SHP1_au	-3	-1.1110	+3	$+7.74 \cdot 10^{-02}$	a.u.
110	sd_SOCS3_abs	-3	-0.9884	+3	$+1.03 \cdot 10^{-01}$	nM
111	sd_SOCS3_au	-3	-1.1172	+3	$+7.63 \cdot 10^{-02}$	a.u.
112	sd_STAT5_abs	-3	-0.9226	+3	$+1.20 \cdot 10^{-01}$	nM
113	sd_STAT5_au	-3	-0.9083	+3	$+1.24 \cdot 10^{-01}$	a.u.
114	sd_pSTAT5_rel	-3	+0.4094	+3	$+2.57 \cdot 10^{+00}$	-
115	sd_pSTAT5_socs3oe	-3	-0.2412	+3	$+5.74 \cdot 10^{-01}$	a.u.

Table S19: Estimated values of the measurement noise parameters
$\hat{\theta}$ indicates the estimated value of the parameter. θ_{min} and θ_{max} indicated the allowed upper and lower bounds for the parameter. $10^{\hat{\theta}}$ indicates the value of the parameter in normal space.

2.5 Identifiability and confidence intervals of the estimated model parameters

In order to evaluate the identifiability of the model parameters and to assess confidence intervals the profile likelihood was evaluated. Instructions how to interpret the result are given in Raue *et al.* (2009). We restrict the further analysis to the parameters that influence the model dynamics and hence are relevant for the biological questions that are addressed. The remaining parameters such as offset and scaling parameters necessary to describe the experimental setup do not influence the dynamics directly and can be treated as nuisance parameters. Please note that using the profile likelihood the indirect influence of the nuisance parameters on the estimation uncertainty of the dynamical parameters is still considered.

The mean calculation time of the profile likelihood per parameter was 9.1 ± 6.6 minutes on a standard desktop computer (2.66 GHz Intel Core i5 with 8 GB RAM). An overview of the profile likelihood is displayed in Fig. S24. In Fig. S25 – S51 the profile likelihood of each parameter is shown in more detail. Also the functional relations to the other parameters are displayed. Finally, in Tab. S20, 95% point-wise confidence intervals for the estimated parameter values derived by the profile likelihood are given.

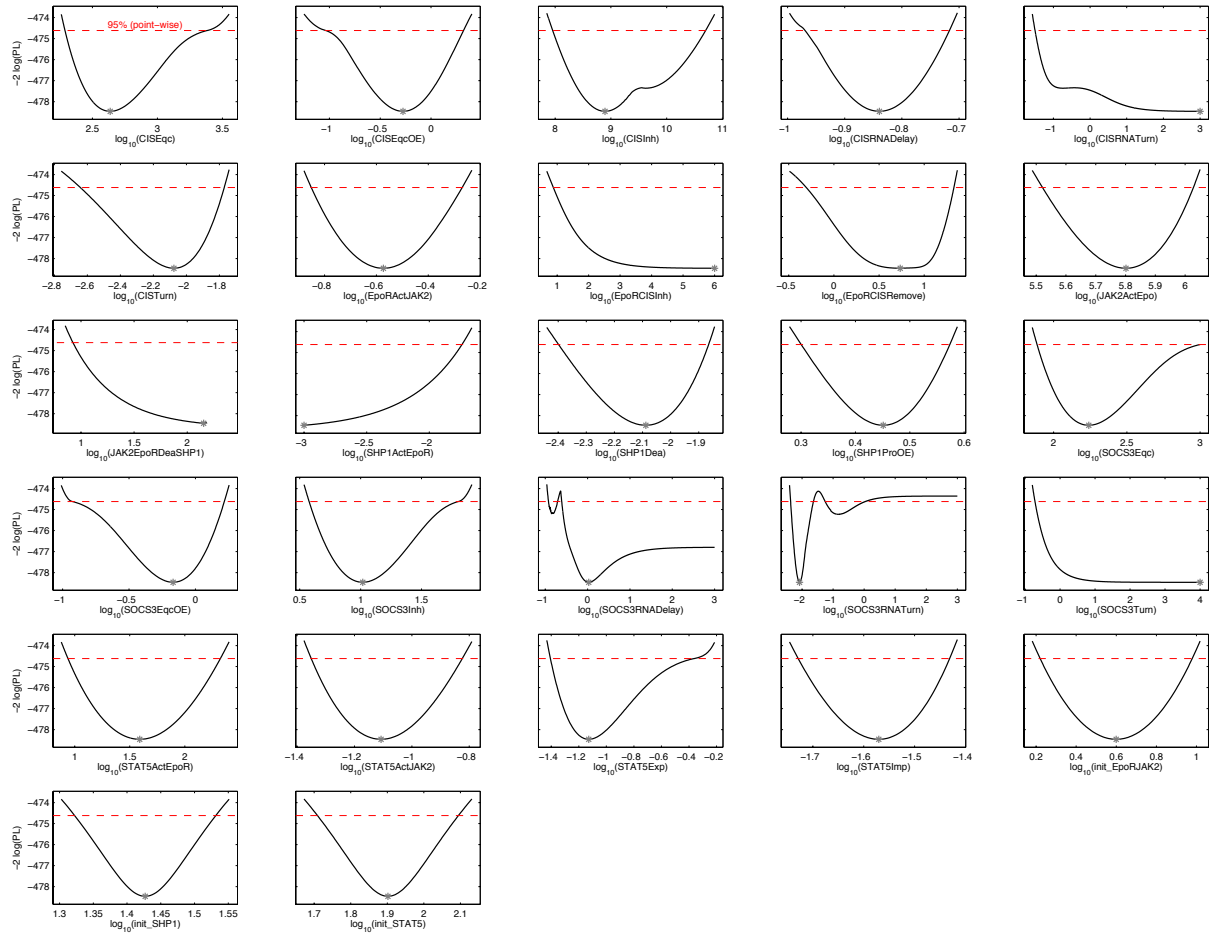

Figure S24: Overview of the profile likelihood of the model parameters
The solide lines indicate the profile likelihood. The broken line indicates the threshold to assess point-wise 95% confidence intervals. The asterisk indicate the optimal parameter values.

The profile likelihood for parameters CISInh, CISRNATurn, SOCS3RNADelay and SOCS3RNATurn reveal two local optima in the likelihood landscape with larger value of the objective function. With respect to the 95% confidence level these local optima are compliant with the experimental data as well and are considered for the calculation of the uncertainty of the model predictions.

Given the experimental data available the parameters CISRNATurn, EpoCISInh, JAK2EpoRDeaSHP1, SHP1ActEpoR, SOCS3RNADelay and SOCS3Turn are practically non-identifiable. For each of these parameters only a lower respectively upper confidence bound is finite. This means that the model is undetermined in the sense that:

- The turnover of CIS RNA described by the parameter CISRNATurn can be arbitrarily fast, see more detailed in Fig. S29. This is a consequence of the limited experimental resolution of the processes at the RNA level.
- The inhibition strength of receptor phosphorylation by the EpoRJAK2_CIS complex described by the parameter EpoCISInh can be arbitrarily large, see more detailed in Fig. S32. Please note that this parameter only effects the CIS overexpression setting.
- Increased deactivation of JAK2EpoR by SHP1 can be compensated by decreased activation of SHP1 by JAK2EpoR. Parameters JAK2EpoRDeaSHP1 and SHP1ActEpoR are anti-correlated, see the functional relations both in Fig. S35 and Fig. S36 and remember the logarithmic parameter scale. This is a consequence of missing information about the relative level of SHP1 activation.
- The delay utilized in SOCS3 RNA transcription described by the parameter SOCS3RNADelay can be arbitrarily small, see more detailed in Fig. S42. This is a consequence of the limited experimental resolution of the processes at the RNA level.
- The turnover of SOCS3 protein described by the parameter SOCS3Turn can be arbitrarily fast, see more detailed in Fig. S44. This is a consequence of the limited experimental resolution of the processes at the RNA level.

These observations are all consequences of uncertainties in the estimation of the parameters and are due to incomplete experimental data. They are not to be confused with biological robustness against perturbations. The remaining uncertainties in the parameter estimates were translated to the predicted model dynamics, see in Sec. 2.6. This allows to assess the precision of the model predictions realistically.

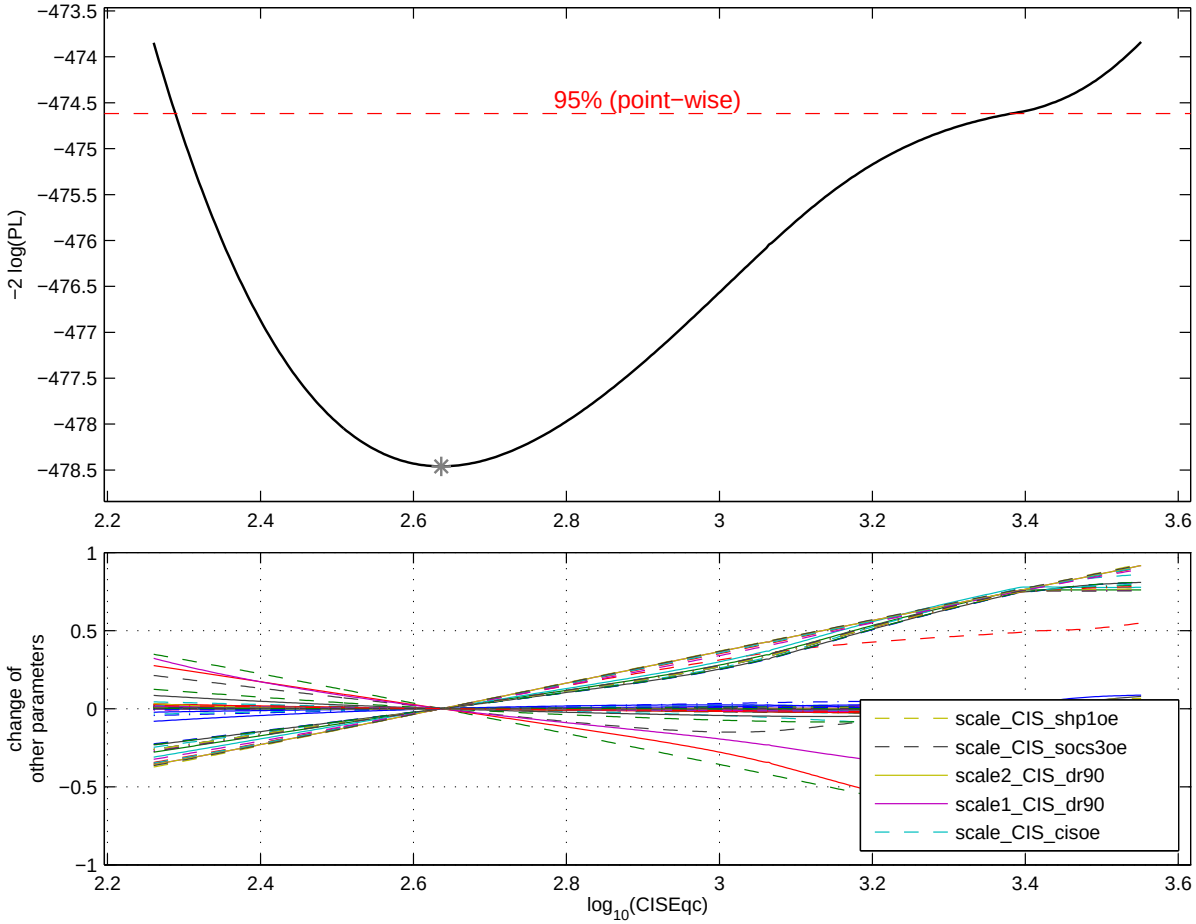

Figure S25: Profile likelihood of parameter CISEqc
Upper panel: The solide line indicates the profile likelihood. The broken line indicates the threshold to assess confidence intervals. The asterisk indicate the optimal parameter values. Lower panel: The functional relations to the other parameters along the profile likelihood of CISEqc are displayed. In the legend the top five parameters showing the strongest variations are given. The calculation time was 00:06:47.39.

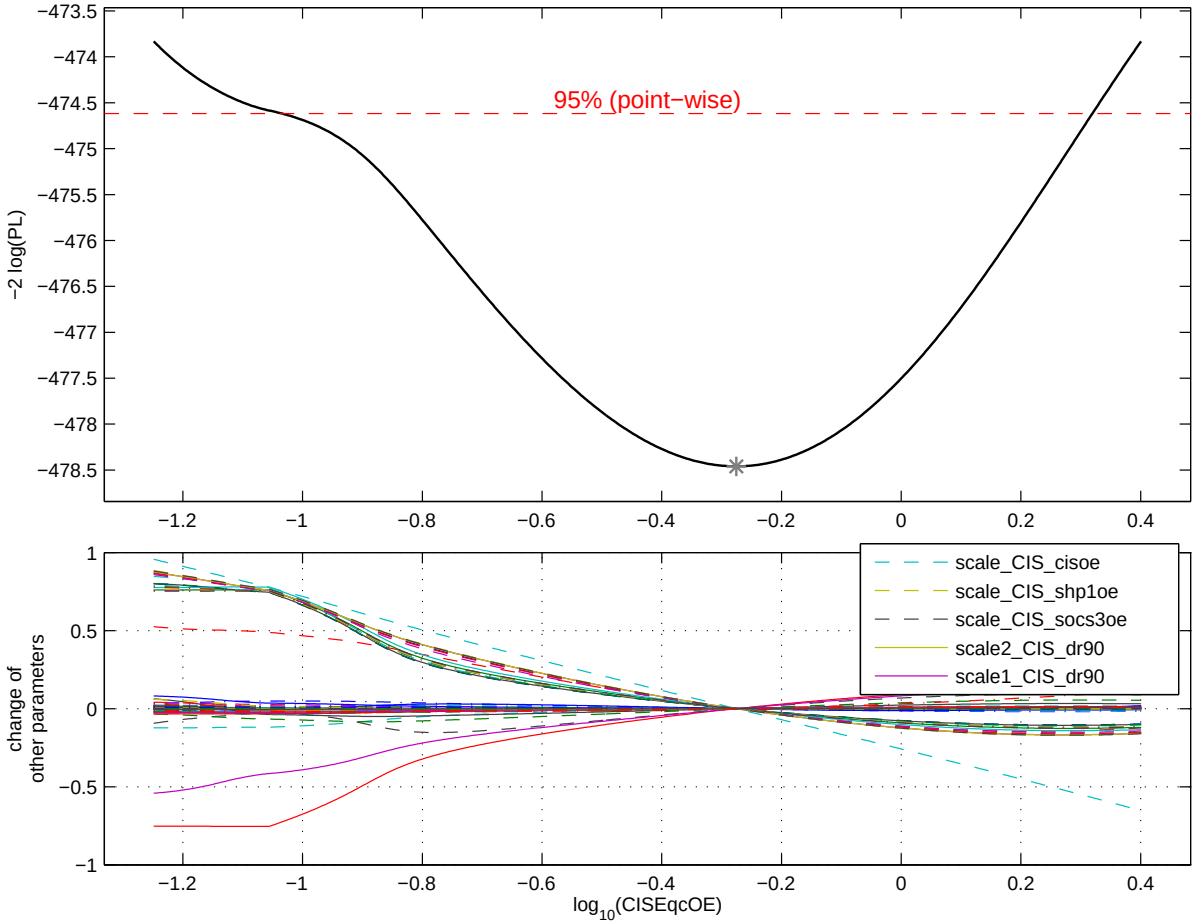

Figure S26: Profile likelihood of parameter CISEqcOE
Upper panel: The solide line indicates the profile likelihood. The broken line indicates the threshold to assess confidence intervals. The asterisk indicate the optimal parameter values. Lower panel: The functional relations to the other parameters along the profile likelihood of CISEqcOE are displayed. In the legend the top five parameters showing the strongest variations are given. The calculation time was 00:07:36.31.

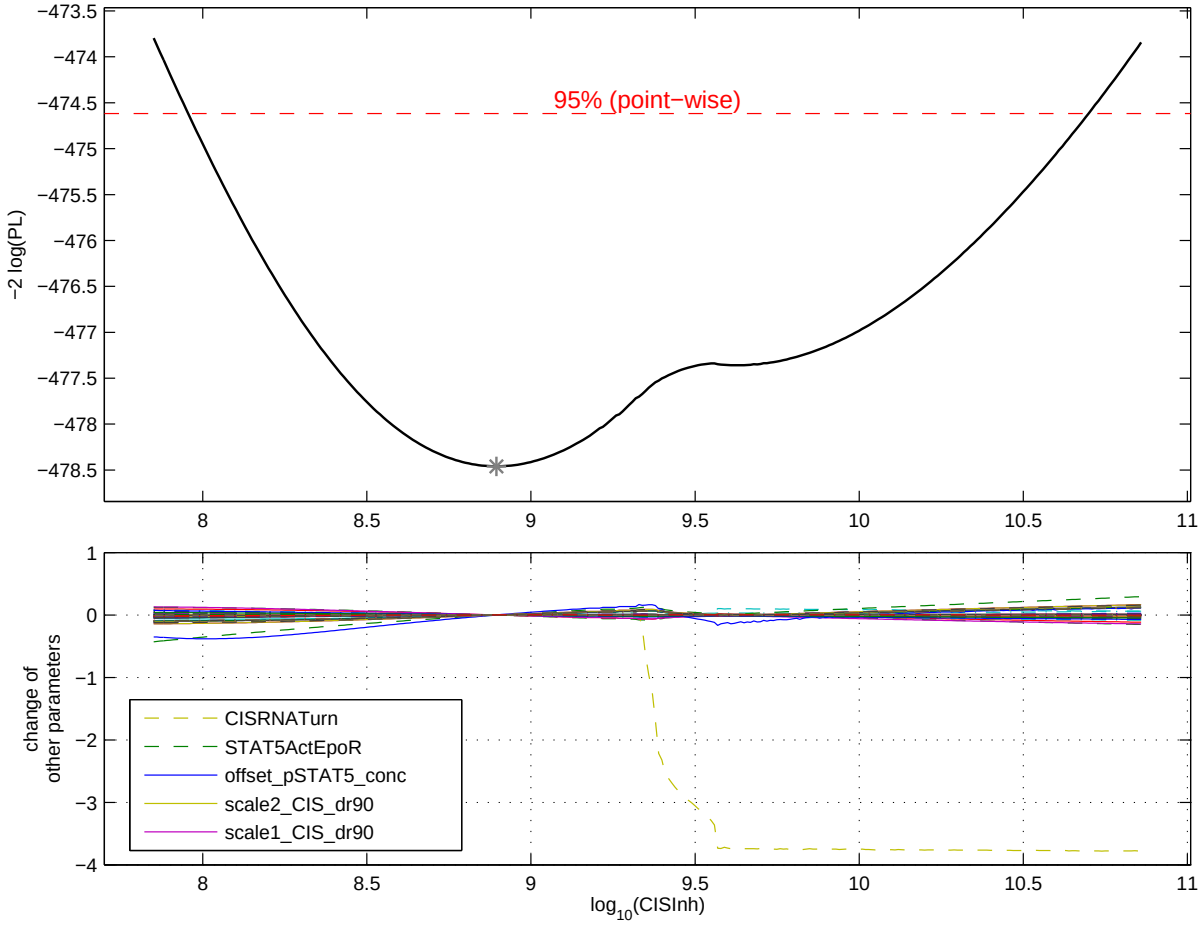

Figure S27: Profile likelihood of parameter CISInh
Upper panel: The solide line indicates the profile likelihood. The broken line indicates the threshold to assess confidence intervals. The asterisk indicate the optimal parameter values. Lower panel: The functional relations to the other parameters along the profile likelihood of CISInh are displayed. In the legend the top five parameters showing the strongest variations are given. The calculation time was 00:09:38.83.

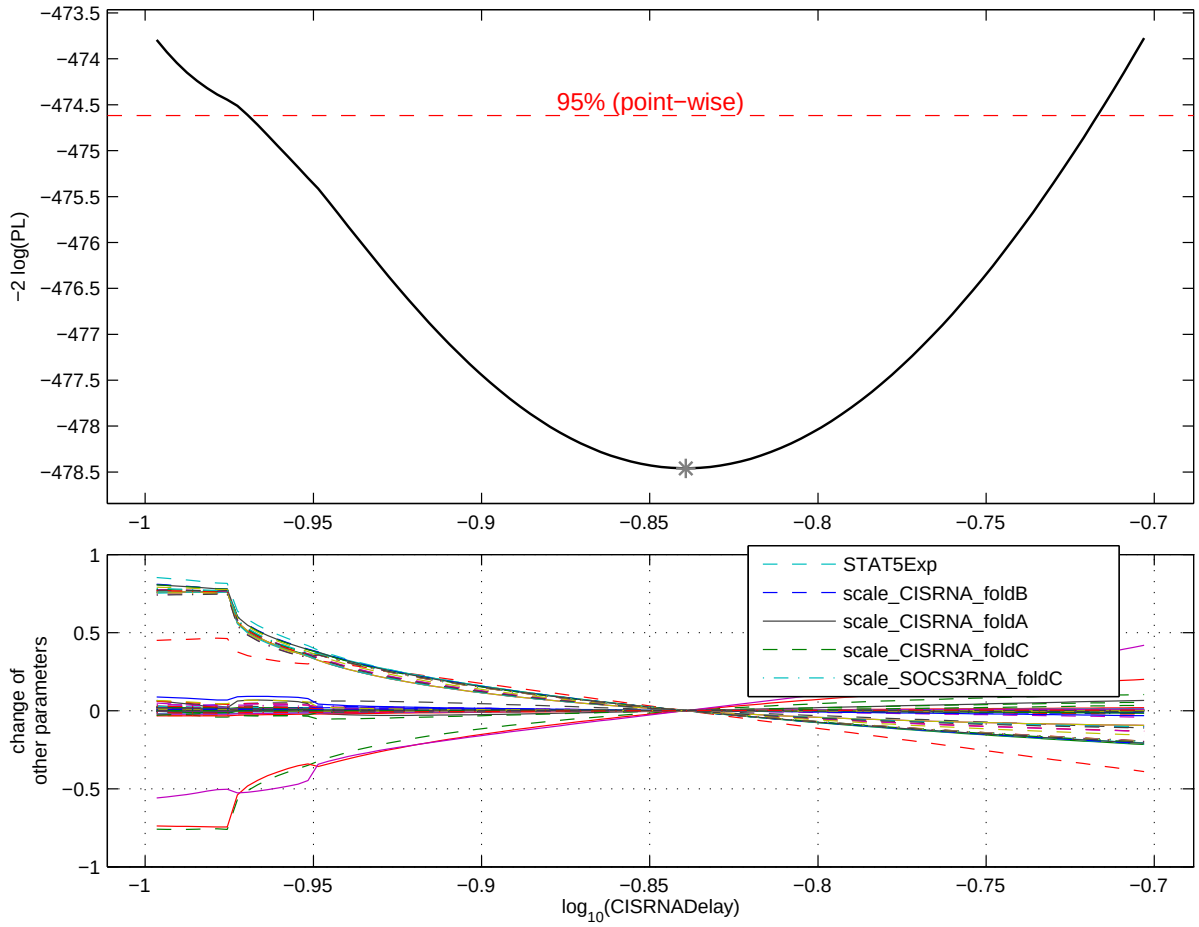

Figure S28: Profile likelihood of parameter CISRNADelay
Upper panel: The solide line indicates the profile likelihood. The broken line indicates the threshold to assess confidence intervals. The asterisk indicate the optimal parameter values. Lower panel: The functional relations to the other parameters along the profile likelihood of CISRNADelay are displayed. In the legend the top five parameters showing the strongest variations are given. The calculation time was 00:03:54.13.

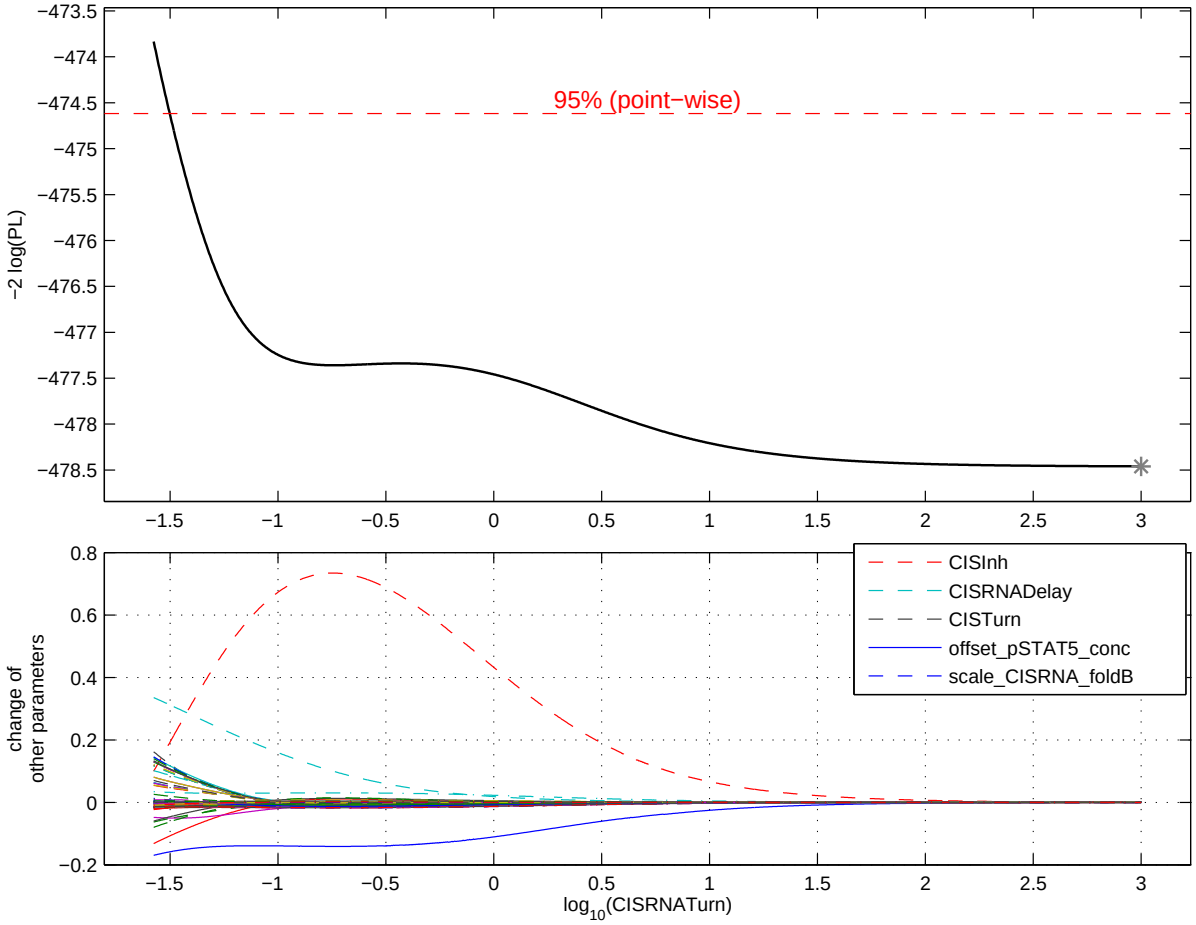

Figure S29: Profile likelihood of parameter CISRNATurn
Upper panel: The solide line indicates the profile likelihood. The broken line indicates the threshold to assess confidence intervals. The asterisk indicate the optimal parameter values. Lower panel: The functional relations to the other parameters along the profile likelihood of CISRNATurn are displayed. In the legend the top five parameters showing the strongest variations are given. The calculation time was 00:19:11.32.

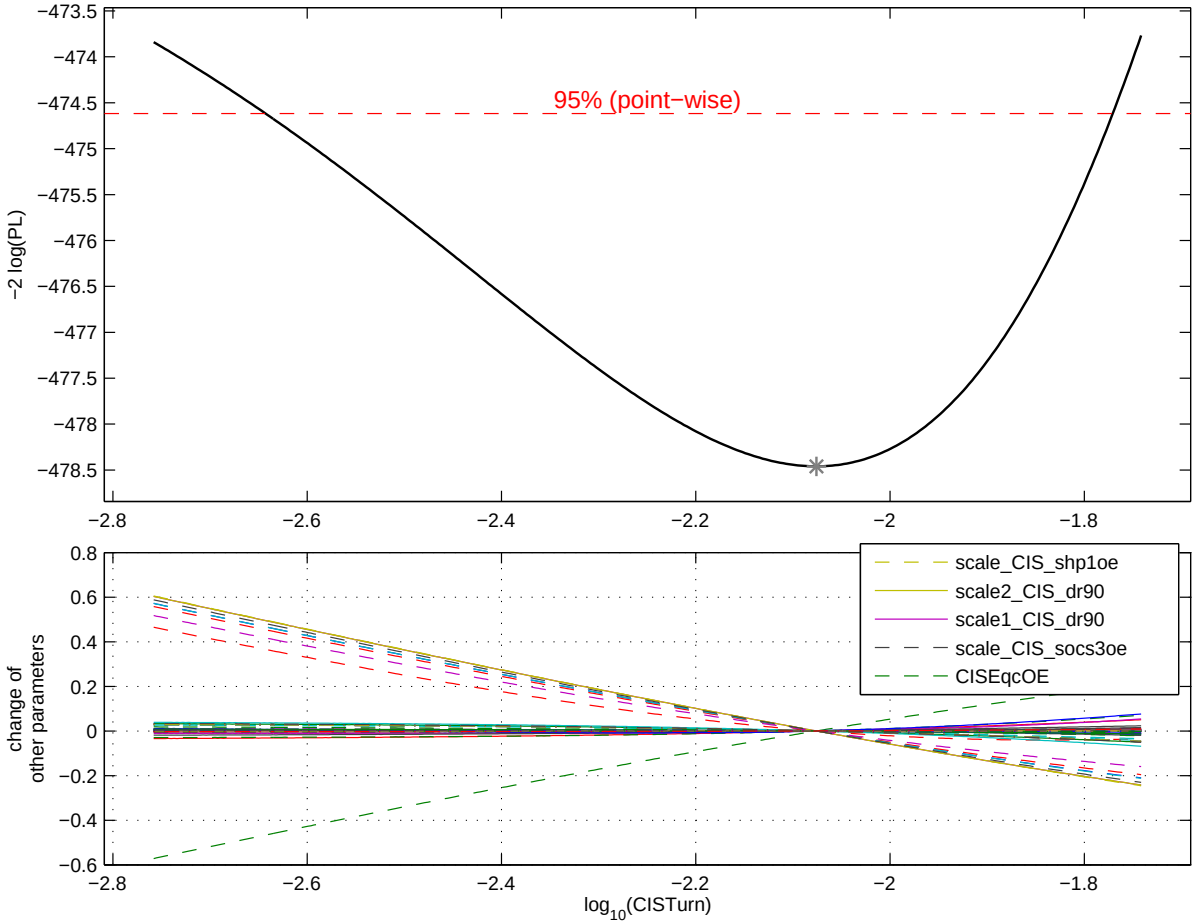

Figure S30: Profile likelihood of parameter CISTurn
Upper panel: The solide line indicates the profile likelihood. The broken line indicates the threshold to assess confidence intervals. The asterisk indicate the optimal parameter values. Lower panel: The functional relations to the other parameters along the profile likelihood of CISTurn are displayed. In the legend the top five parameters showing the strongest variations are given. The calculation time was 00:06:05.84.

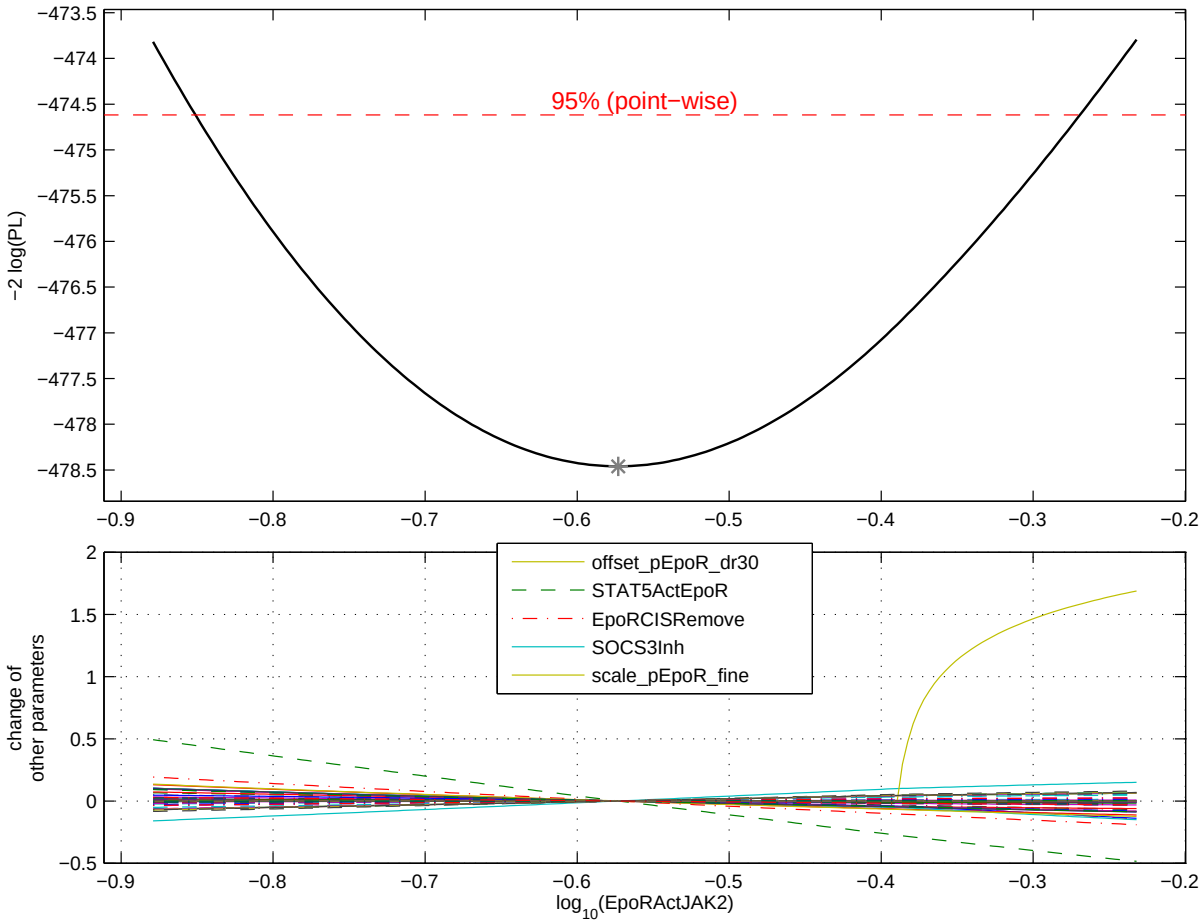

Figure S31: Profile likelihood of parameter EpoRActJAK2
Upper panel: The solide line indicates the profile likelihood. The broken line indicates the threshold to assess confidence intervals. The asterisk indicate the optimal parameter values. Lower panel: The functional relations to the other parameters along the profile likelihood of EpoRActJAK2 are displayed. In the legend the top five parameters showing the strongest variations are given. The calculation time was 00:05:29.96.

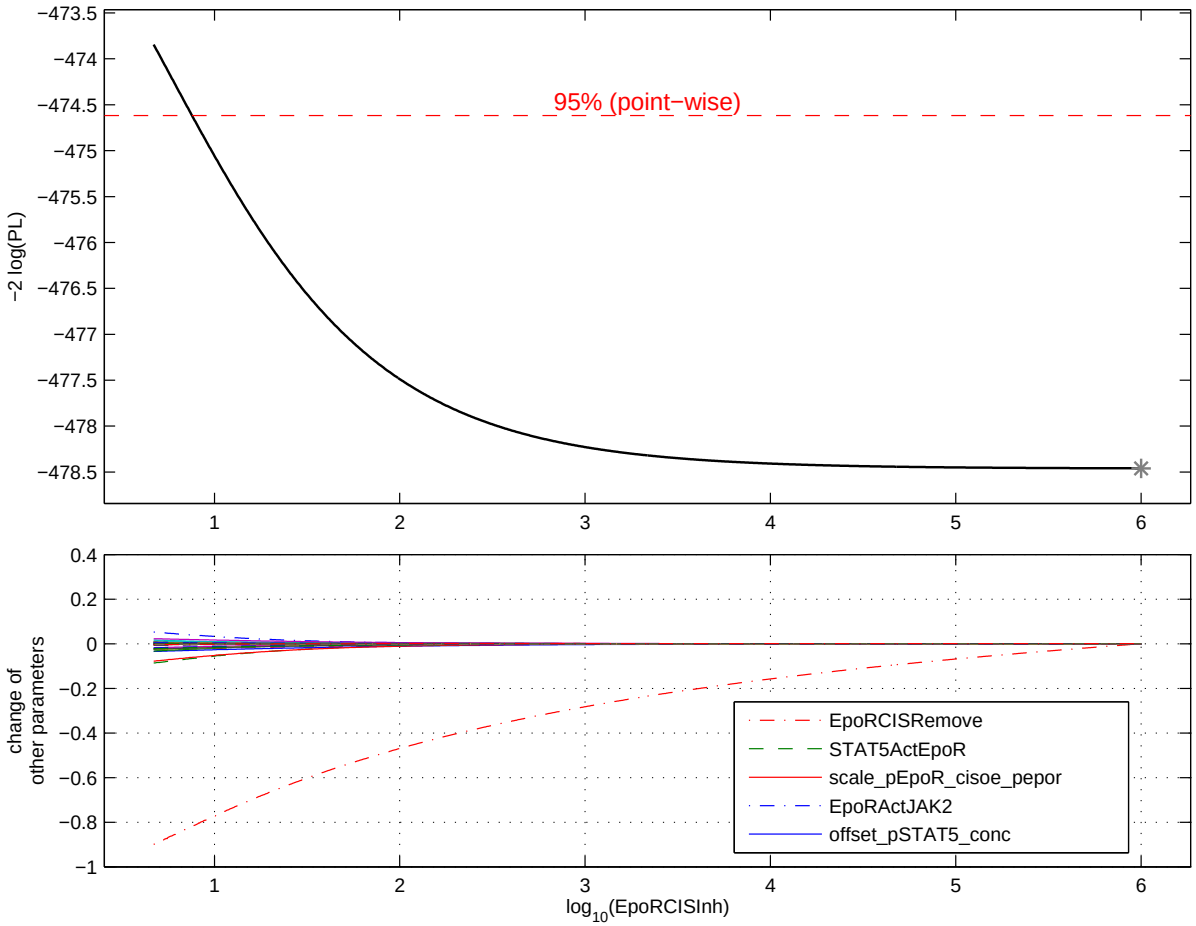

Figure S32: Profile likelihood of parameter EpoRCISInh
Upper panel: The solide line indicates the profile likelihood. The broken line indicates the threshold to assess confidence intervals. The asterisk indicate the optimal parameter values. Lower panel: The functional relations to the other parameters along the profile likelihood of EpoRCISInh are displayed. In the legend the top five parameters showing the strongest variations are given. The calculation time was 00:17:32.37.

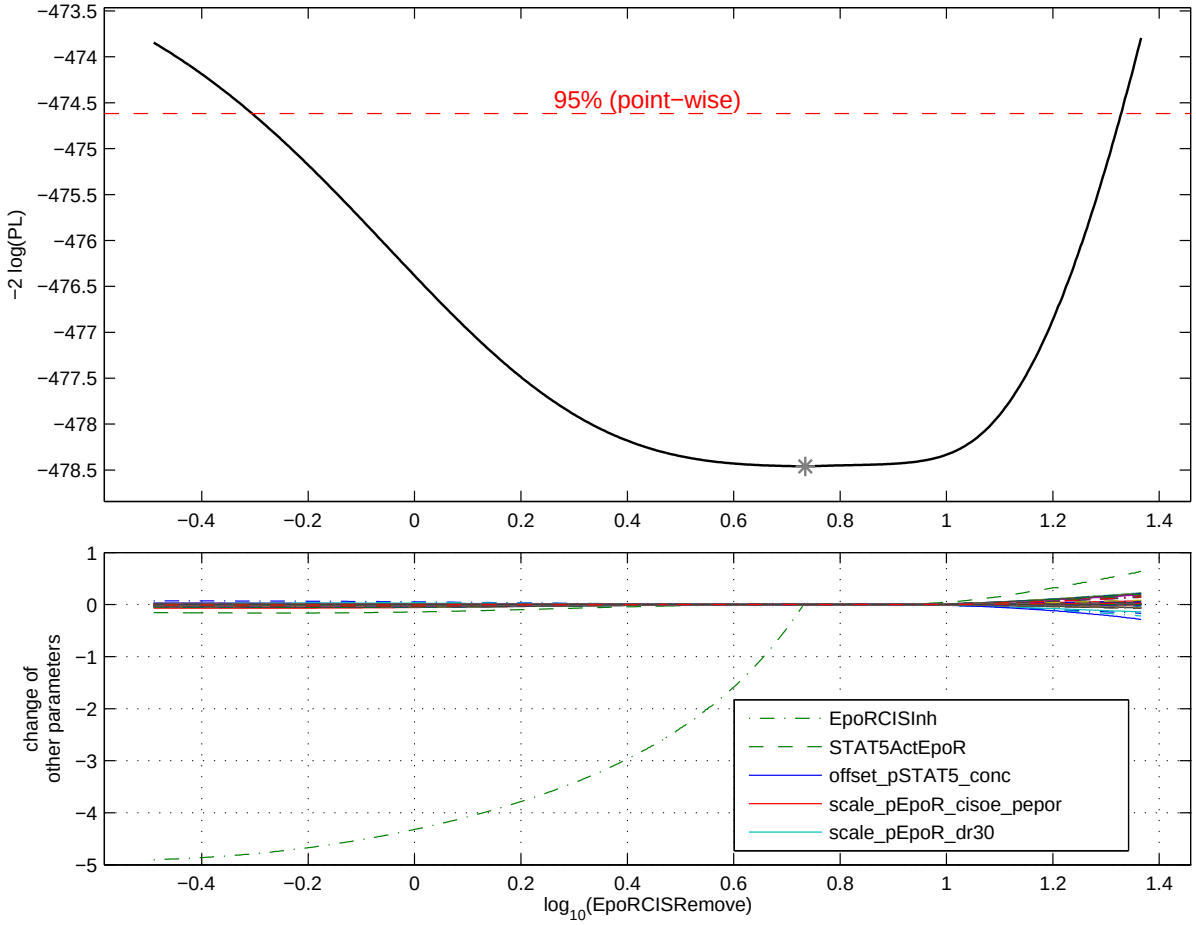

Figure S33: Profile likelihood of parameter EpoRCISRemove
Upper panel: The solide line indicates the profile likelihood. The broken line indicates the threshold to assess confidence intervals. The asterisk indicate the optimal parameter values. Lower panel: The functional relations to the other parameters along the profile likelihood of EpoRCISRemove are displayed. In the legend the top five parameters showing the strongest variations are given. The calculation time was 00:09:23.39.

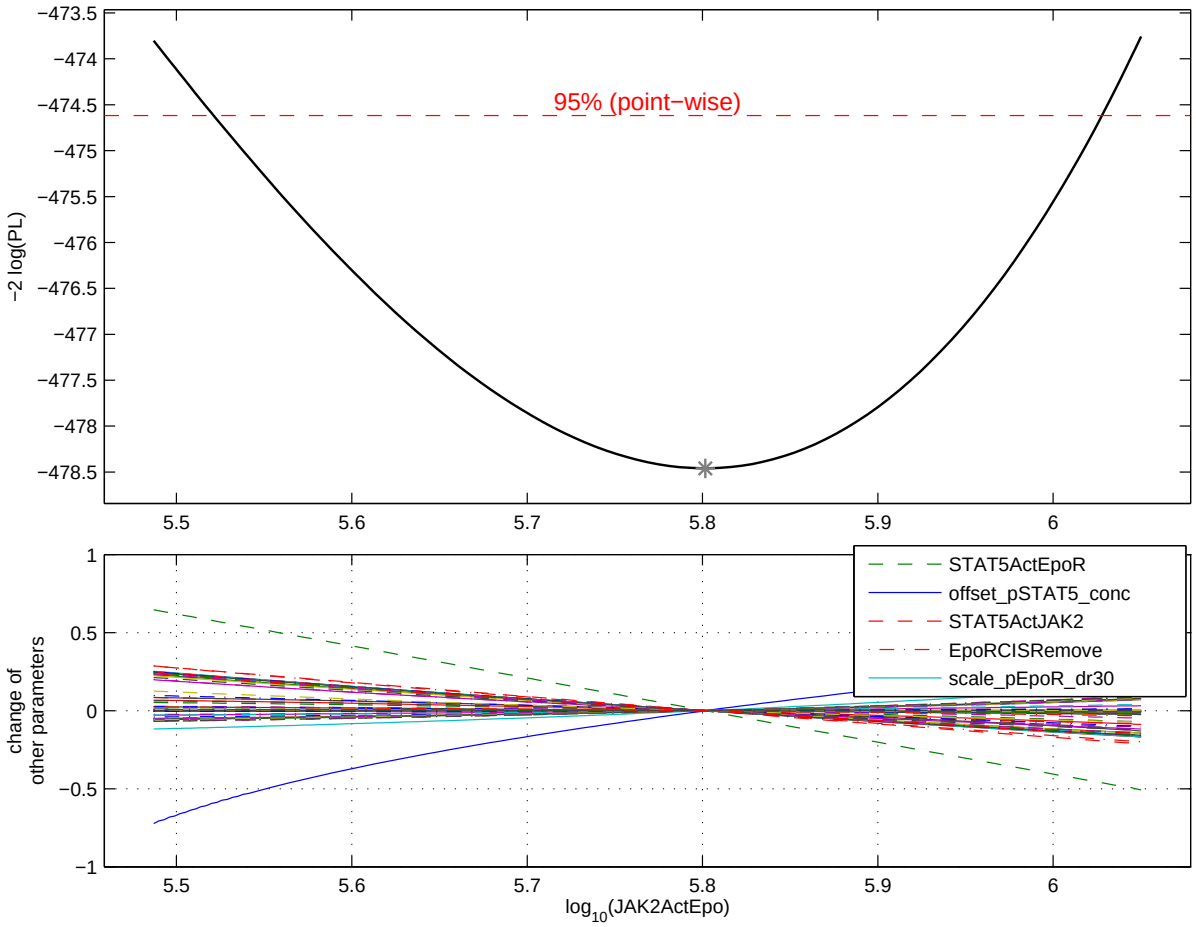

Figure S34: Profile likelihood of parameter JAK2ActEpo
Upper panel: The solide line indicates the profile likelihood. The broken line indicates the threshold to assess confidence intervals. The asterisk indicate the optimal parameter values. Lower panel: The functional relations to the other parameters along the profile likelihood of JAK2ActEpo are displayed. In the legend the top five parameters showing the strongest variations are given. The calculation time was 00:04:34.26.

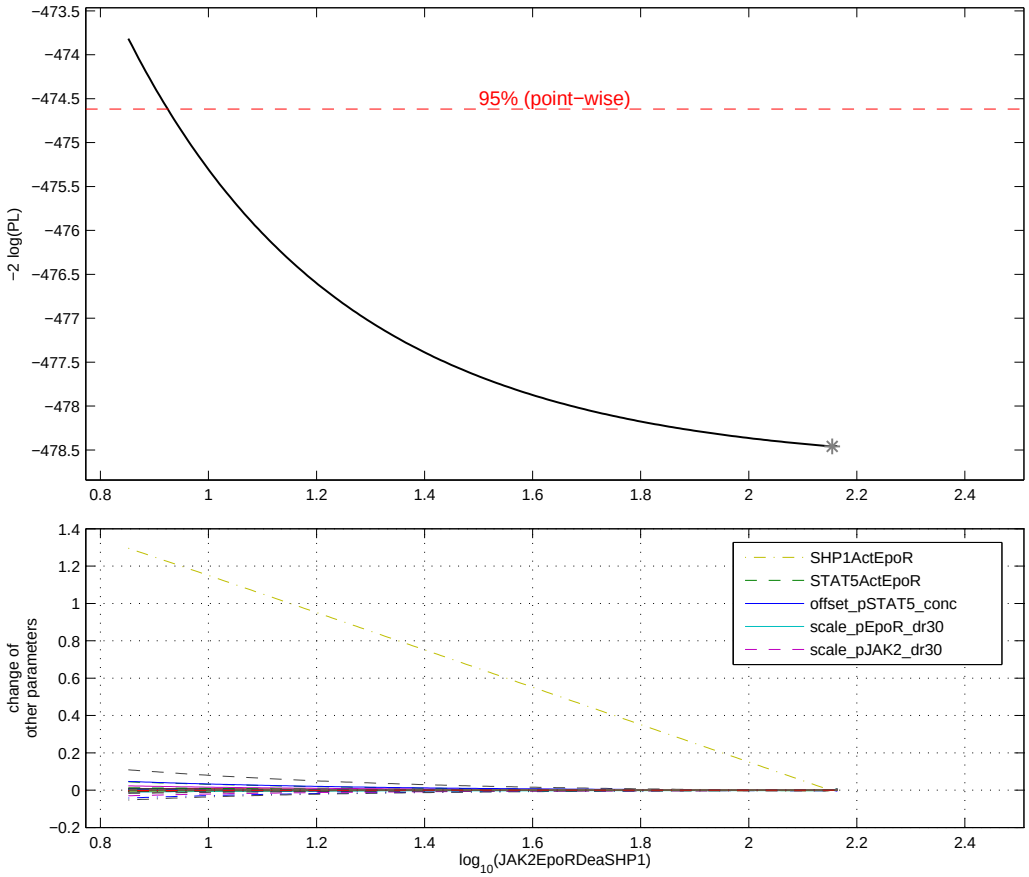

Figure S35: Profile likelihood of parameter JAK2EpoRDeaSHP1
Upper panel: The solide line indicates the profile likelihood. The broken line indicates the threshold to assess confidence intervals. The asterisk indicate the optimal parameter values. Lower panel: The functional relations to the other parameters along the profile likelihood of JAK2EpoRDeaSHP1 are displayed. In the legend the top five parameters showing the strongest variations are given. The calculation time was 00:07:00.61.

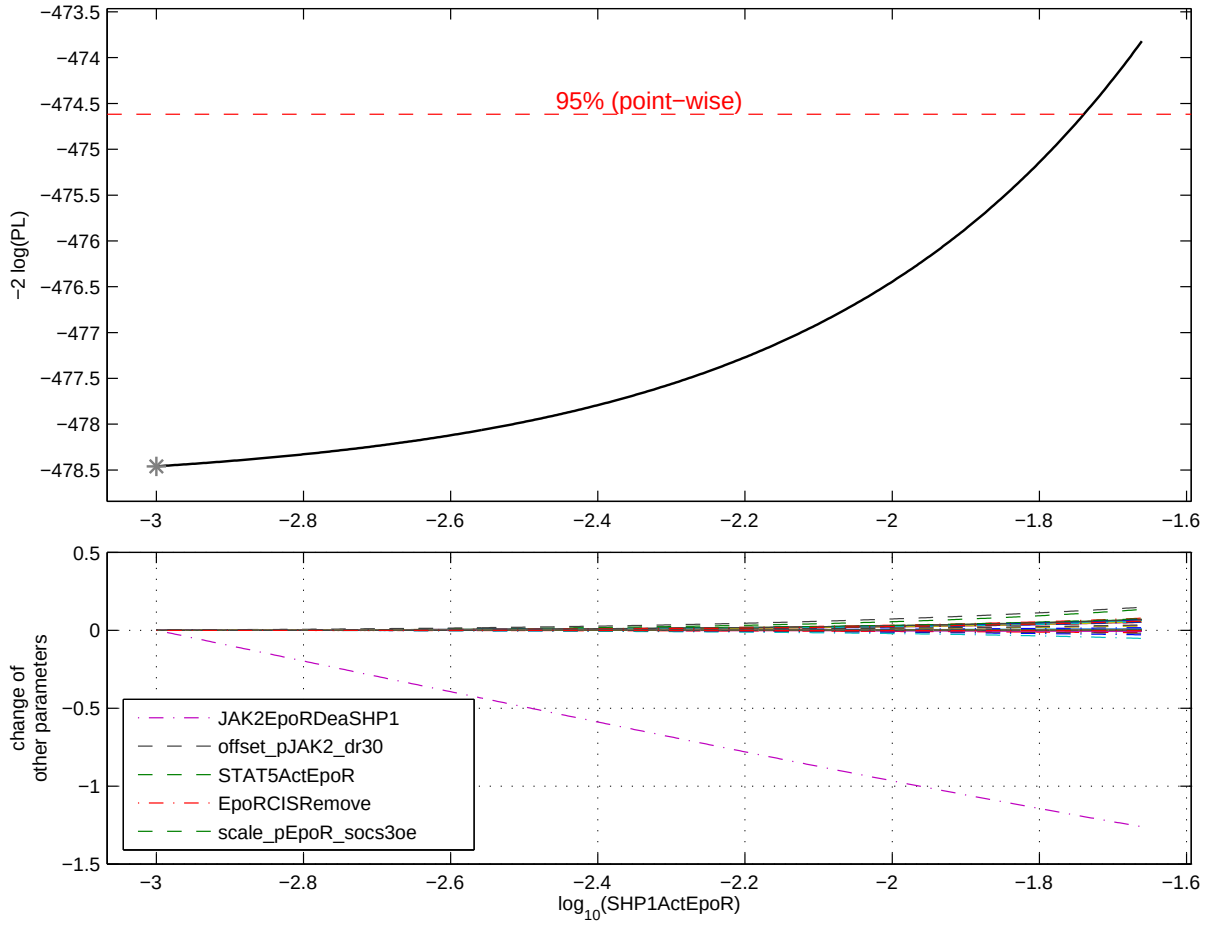

Figure S36: Profile likelihood of parameter SHP1ActEpoR
Upper panel: The solide line indicates the profile likelihood. The broken line indicates the threshold to assess confidence intervals. The asterisk indicate the optimal parameter values. Lower panel: The functional relations to the other parameters along the profile likelihood of SHP1ActEpoR are displayed. In the legend the top five parameters showing the strongest variations are given. The calculation time was 00:15:15.65.

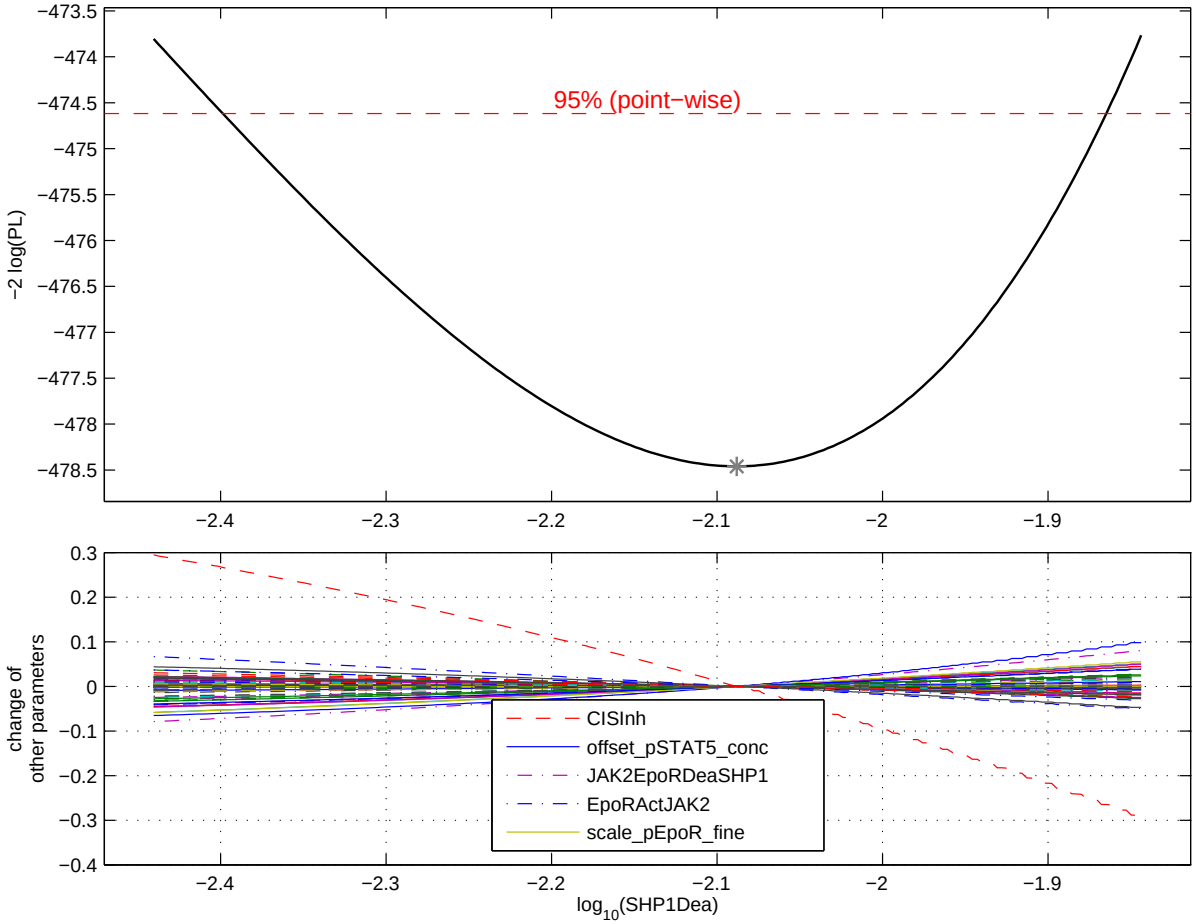

Figure S37: Profile likelihood of parameter SHP1Dea
Upper panel: The solide line indicates the profile likelihood. The broken line indicates the threshold to assess confidence intervals. The asterisk indicate the optimal parameter values. Lower panel: The functional relations to the other parameters along the profile likelihood of SHP1Dea are displayed. In the legend the top five parameters showing the strongest variations are given. The calculation time was 00:03:53.24.

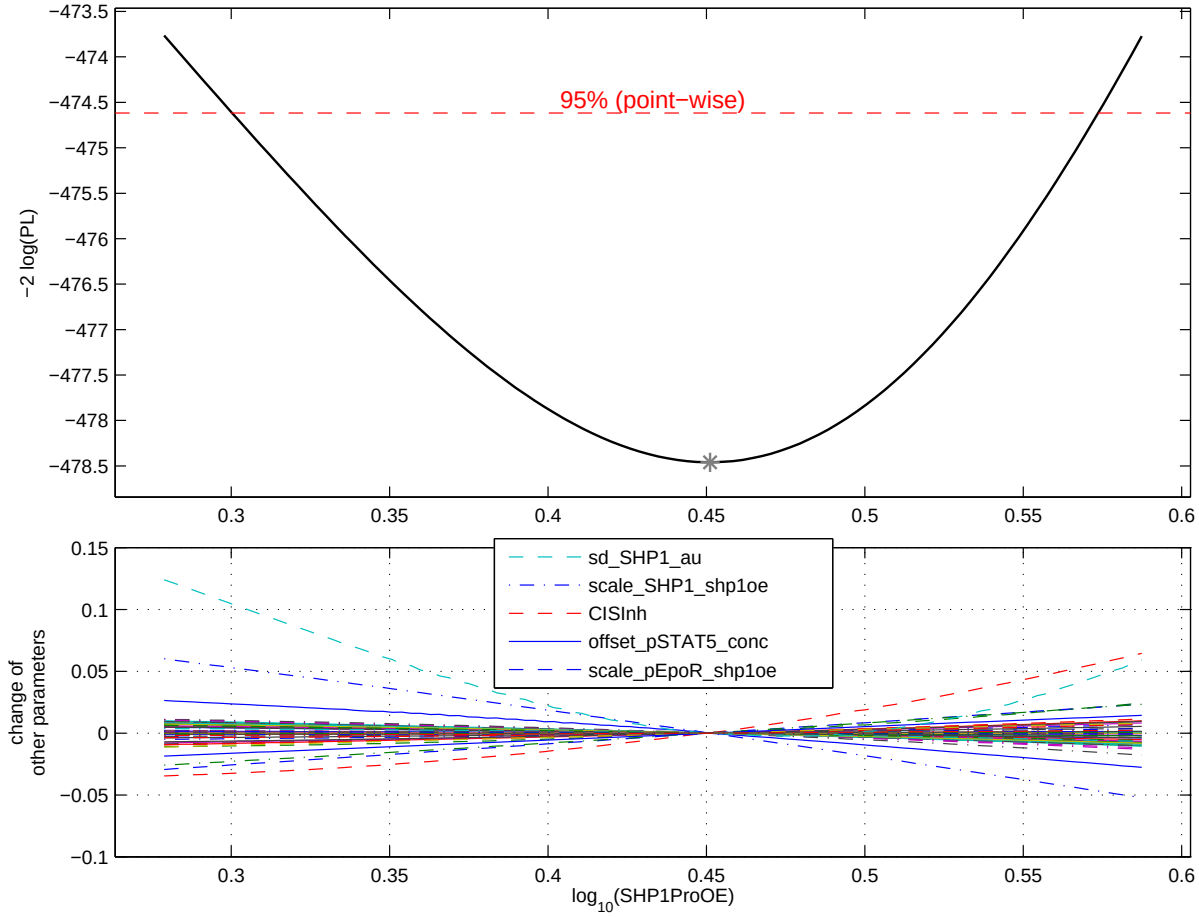

Figure S38: Profile likelihood of parameter SHP1ProOE
Upper panel: The solide line indicates the profile likelihood. The broken line indicates the threshold to assess confidence intervals. The asterisk indicate the optimal parameter values. Lower panel: The functional relations to the other parameters along the profile likelihood of SHP1ProOE are displayed. In the legend the top five parameters showing the strongest variations are given. The calculation time was 00:02:10.94.

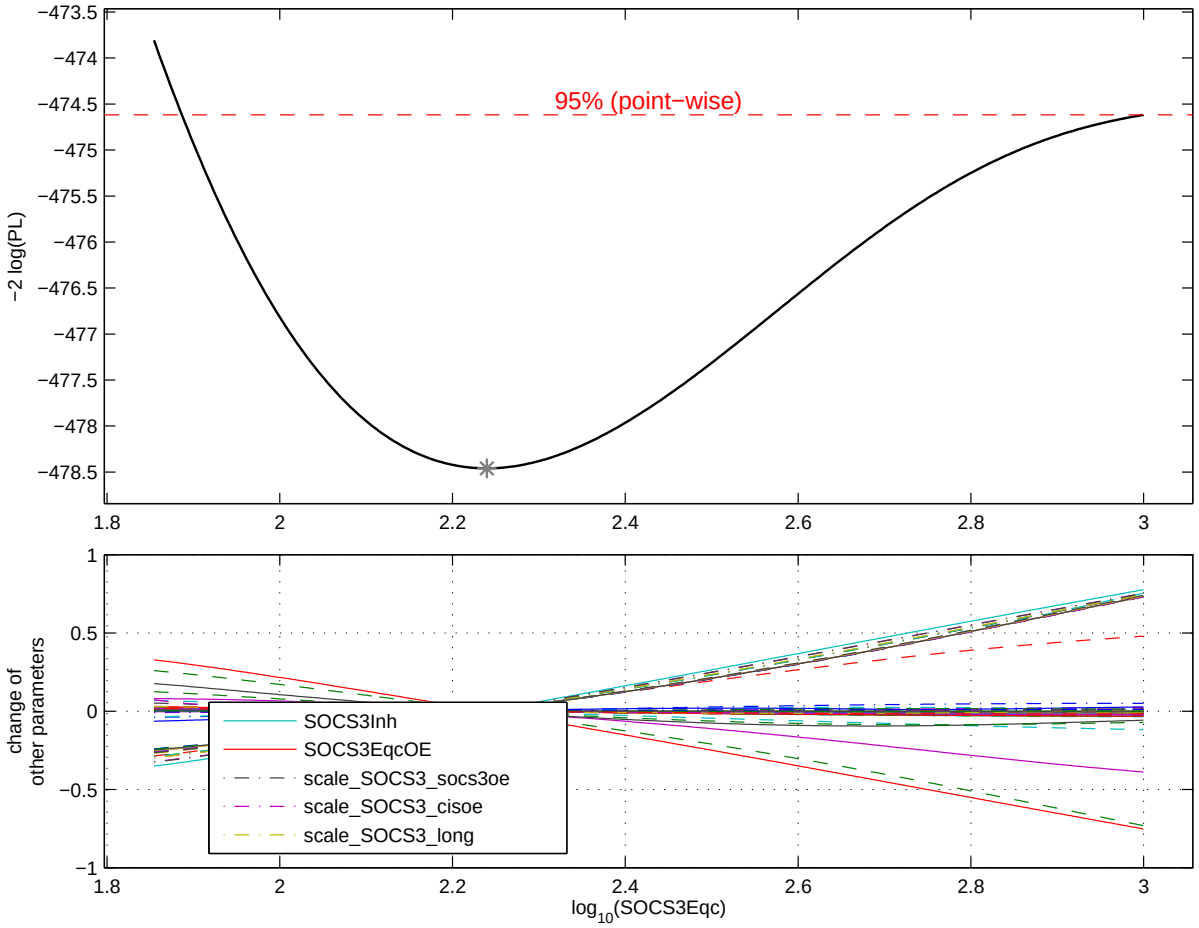

Figure S39: Profile likelihood of parameter SOCS3Eqc
Upper panel: The solide line indicates the profile likelihood. The broken line indicates the threshold to assess confidence intervals. The asterisk indicate the optimal parameter values. Lower panel: The functional relations to the other parameters along the profile likelihood of SOCS3Eqc are displayed. In the legend the top five parameters showing the strongest variations are given. The calculation time was 00:07:16.20.

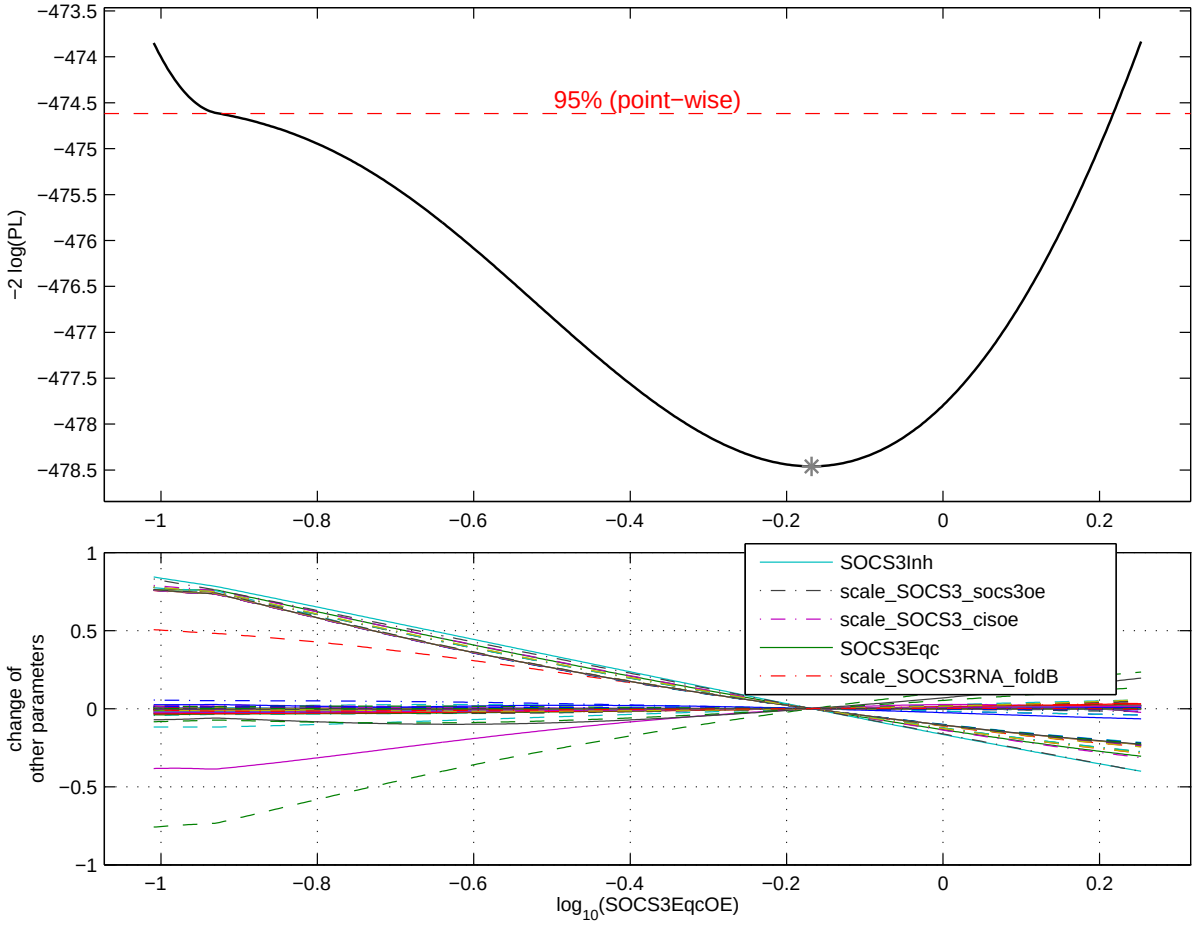

Figure S40: Profile likelihood of parameter SOCS3EqcOE
Upper panel: The solide line indicates the profile likelihood. The broken line indicates the threshold to assess confidence intervals. The asterisk indicate the optimal parameter values. Lower panel: The functional relations to the other parameters along the profile likelihood of SOCS3EqcOE are displayed. In the legend the top five parameters showing the strongest variations are given. The calculation time was 00:07:52.27.

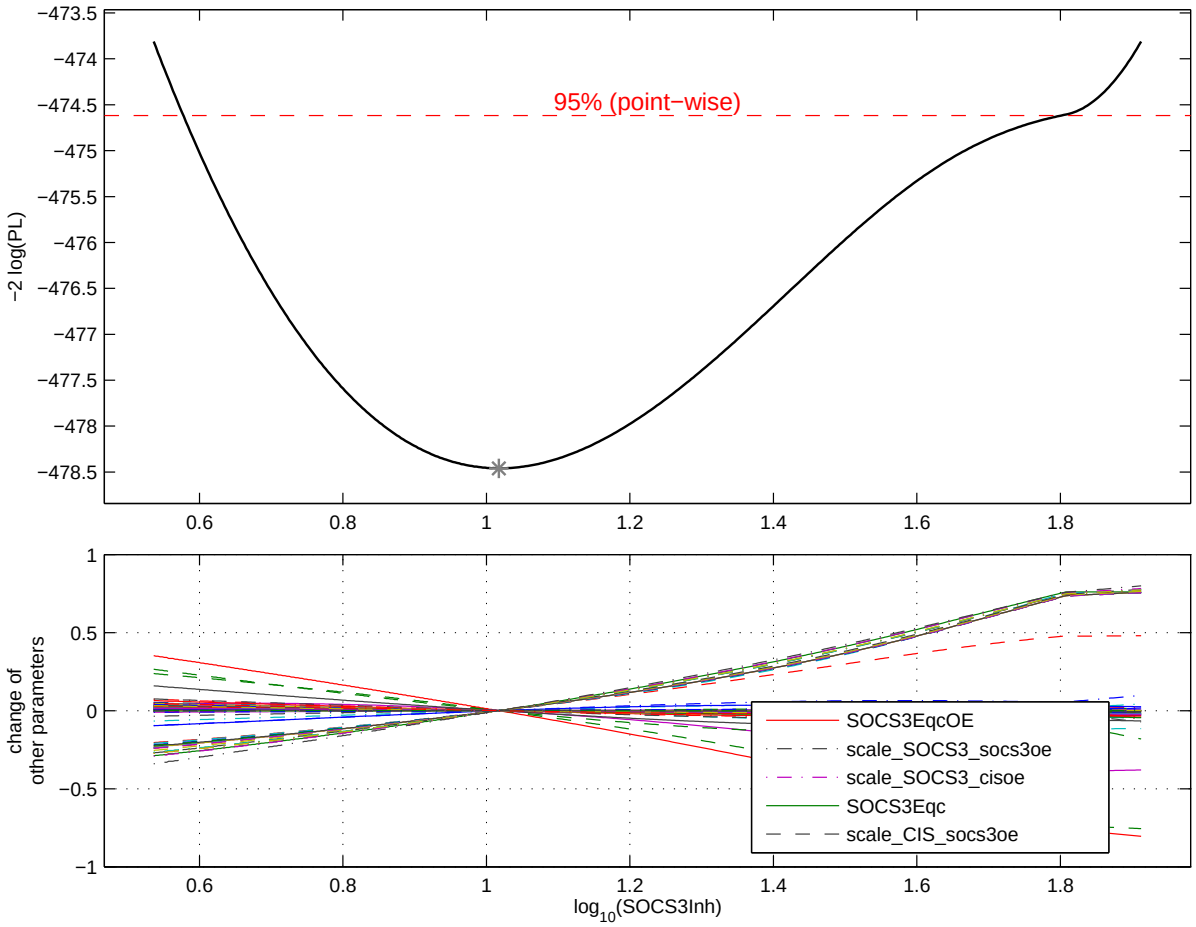

Figure S41: Profile likelihood of parameter SOCS3Inh
Upper panel: The solide line indicates the profile likelihood. The broken line indicates the threshold to assess confidence intervals. The asterisk indicate the optimal parameter values. Lower panel: The functional relations to the other parameters along the profile likelihood of SOCS3Inh are displayed. In the legend the top five parameters showing the strongest variations are given. The calculation time was 00:08:35.29.

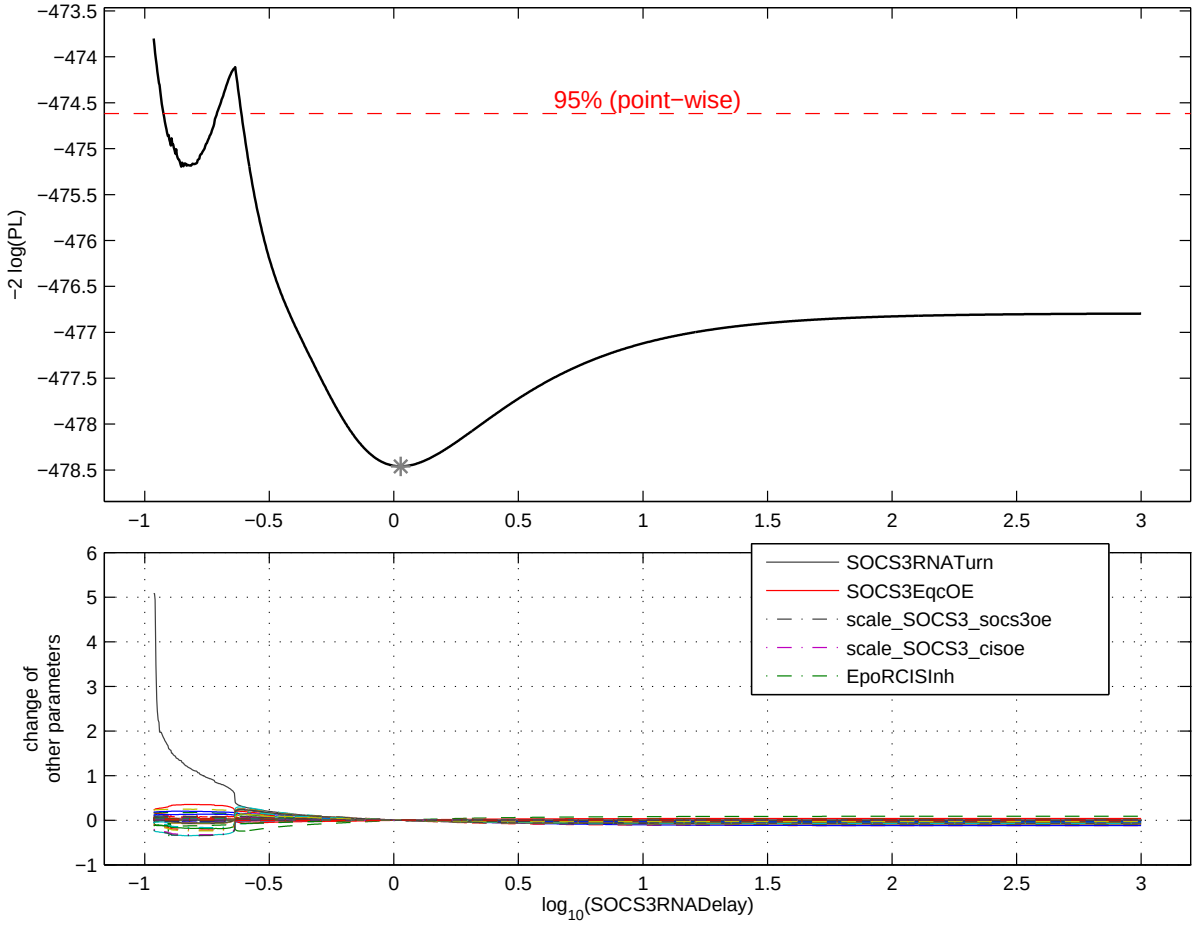

Figure S42: Profile likelihood of parameter SOCS3RNADelay
Upper panel: The solide line indicates the profile likelihood. The broken line indicates the threshold to assess confidence intervals. The asterisk indicate the optimal parameter values. Lower panel: The functional relations to the other parameters along the profile likelihood of SOCS3RNADelay are displayed. In the legend the top five parameters showing the strongest variations are given. The calculation time was 00:19:56.76.

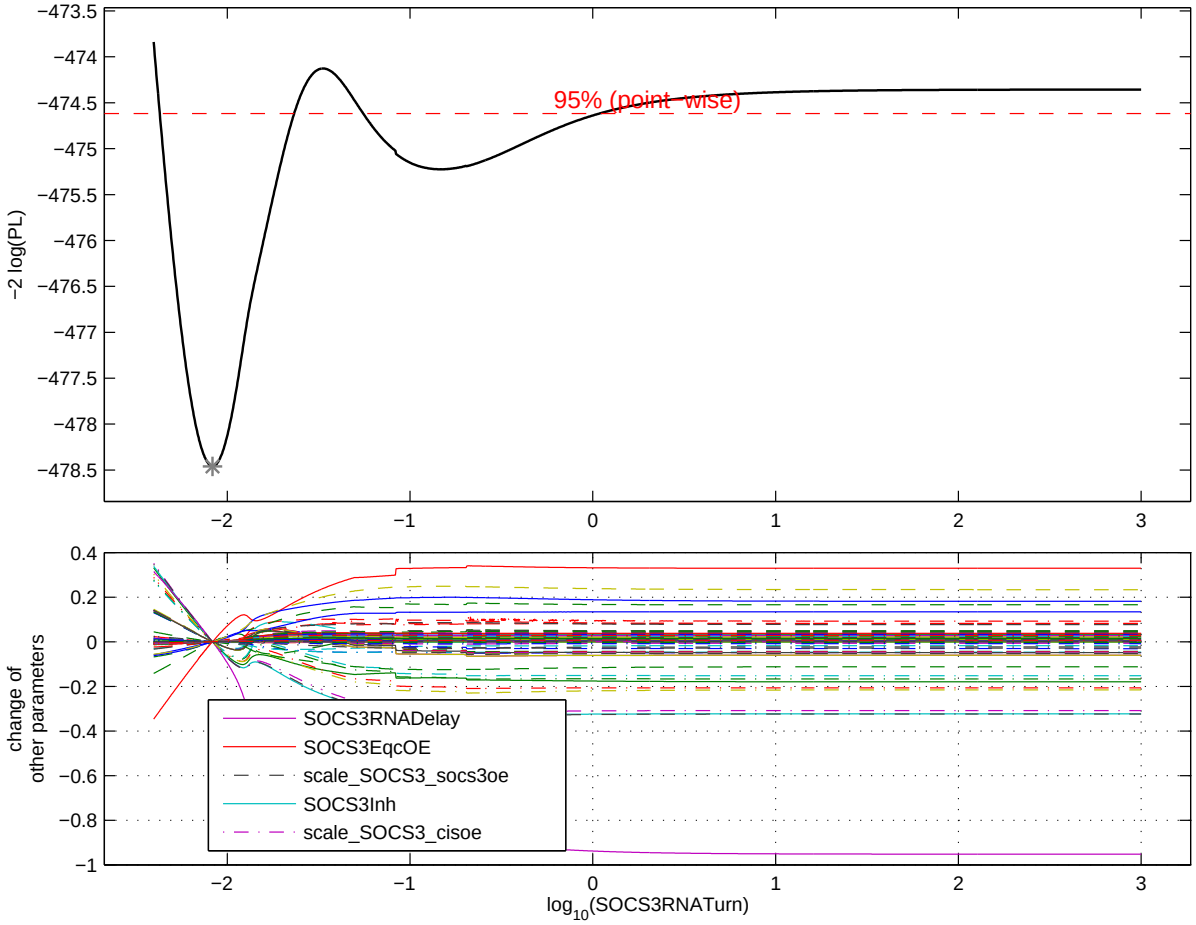

Figure S43: Profile likelihood of parameter SOCS3RNATurn
Upper panel: The solide line indicates the profile likelihood. The broken line indicates the threshold to assess confidence intervals. The asterisk indicate the optimal parameter values. Lower panel: The functional relations to the other parameters along the profile likelihood of SOCS3RNATurn are displayed. In the legend the top five parameters showing the strongest variations are given. The calculation time was 00:28:01.92.

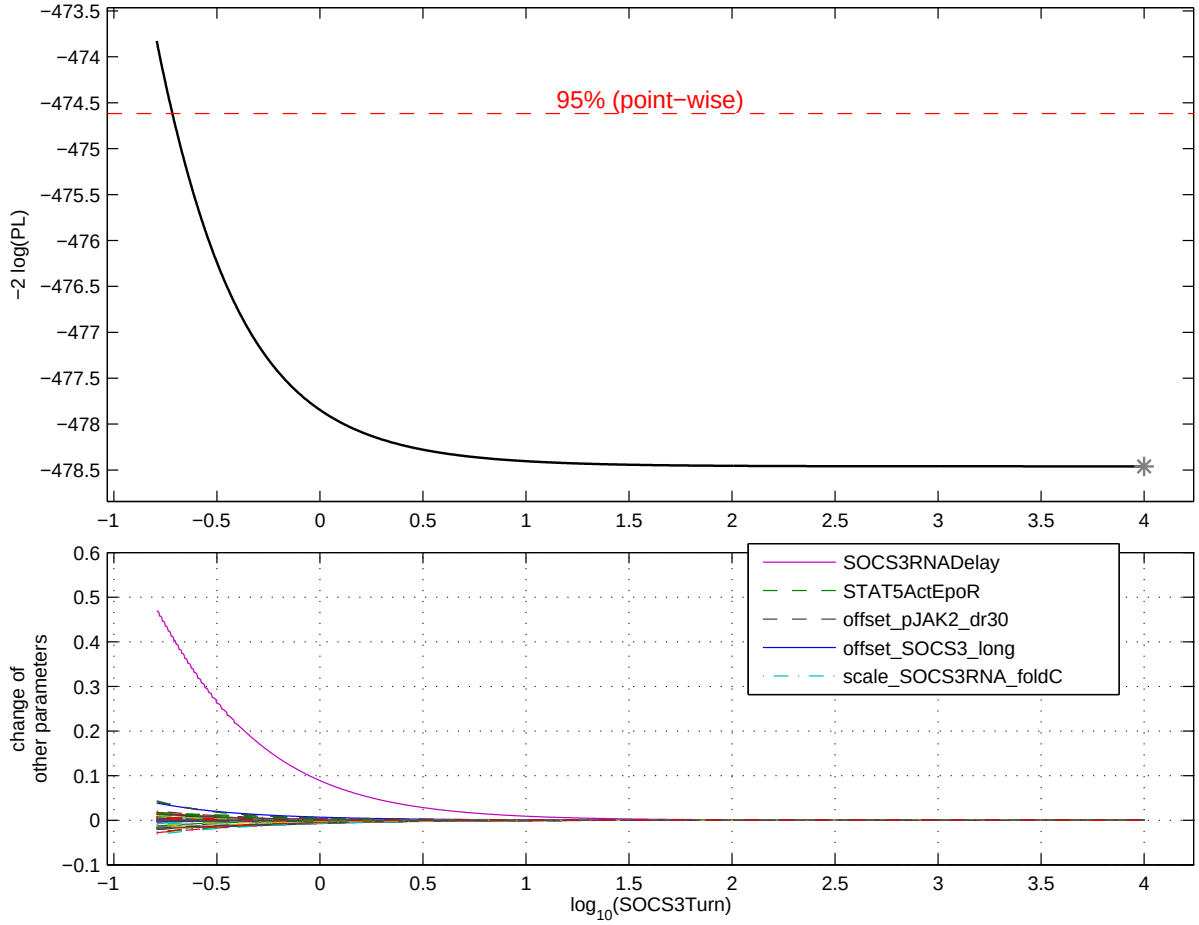

Figure S44: Profile likelihood of parameter SOCS3Turn
Upper panel: The solide line indicates the profile likelihood. The broken line indicates the threshold to assess confidence intervals. The asterisk indicate the optimal parameter values. Lower panel: The functional relations to the other parameters along the profile likelihood of SOCS3Turn are displayed. In the legend the top five parameters showing the strongest variations are given. The calculation time was 00:19:43.90.

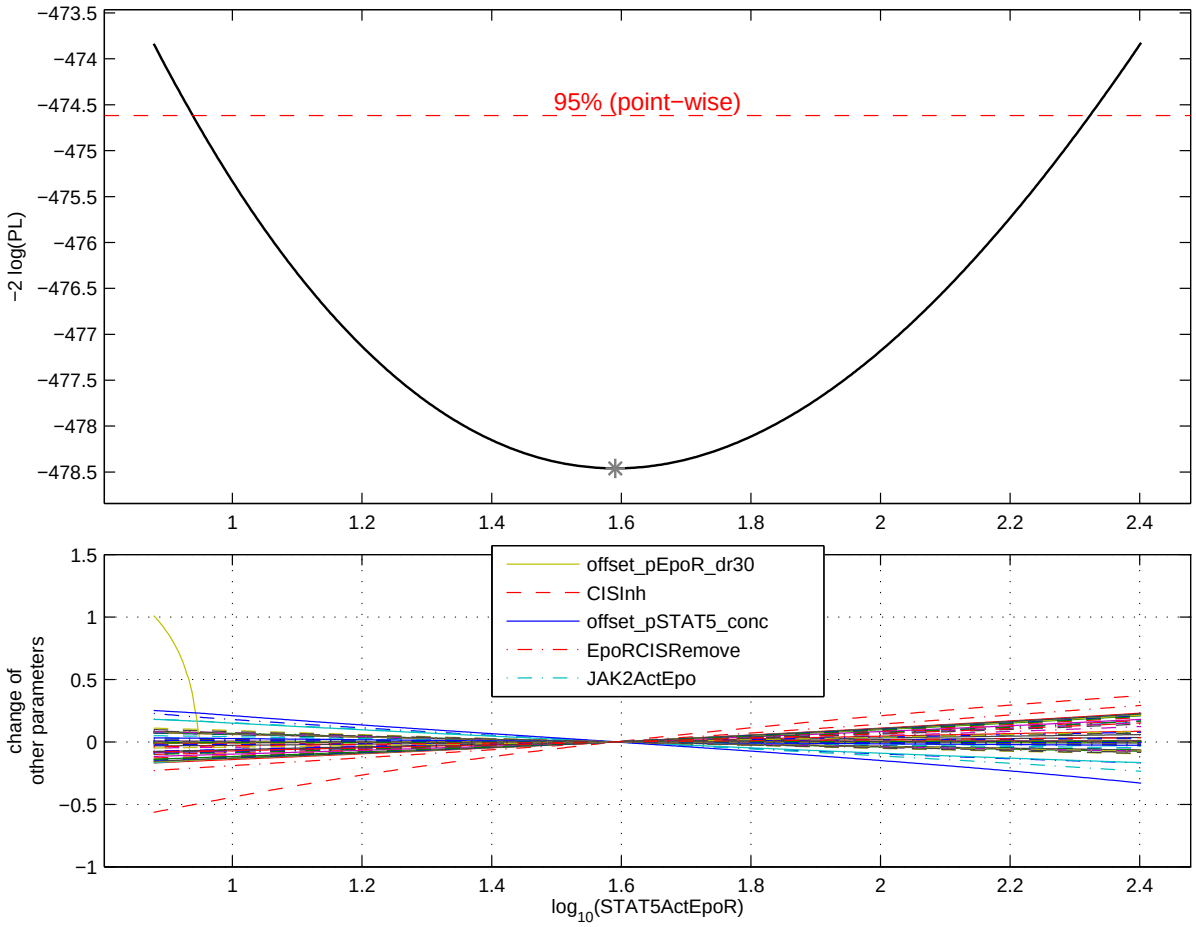

Figure S45: Profile likelihood of parameter STAT5ActEpoR
Upper panel: The solide line indicates the profile likelihood. The broken line indicates the threshold to assess confidence intervals. The asterisk indicate the optimal parameter values. Lower panel: The functional relations to the other parameters along the profile likelihood of STAT5ActEpoR are displayed. In the legend the top five parameters showing the strongest variations are given. The calculation time was 00:10:50.77.

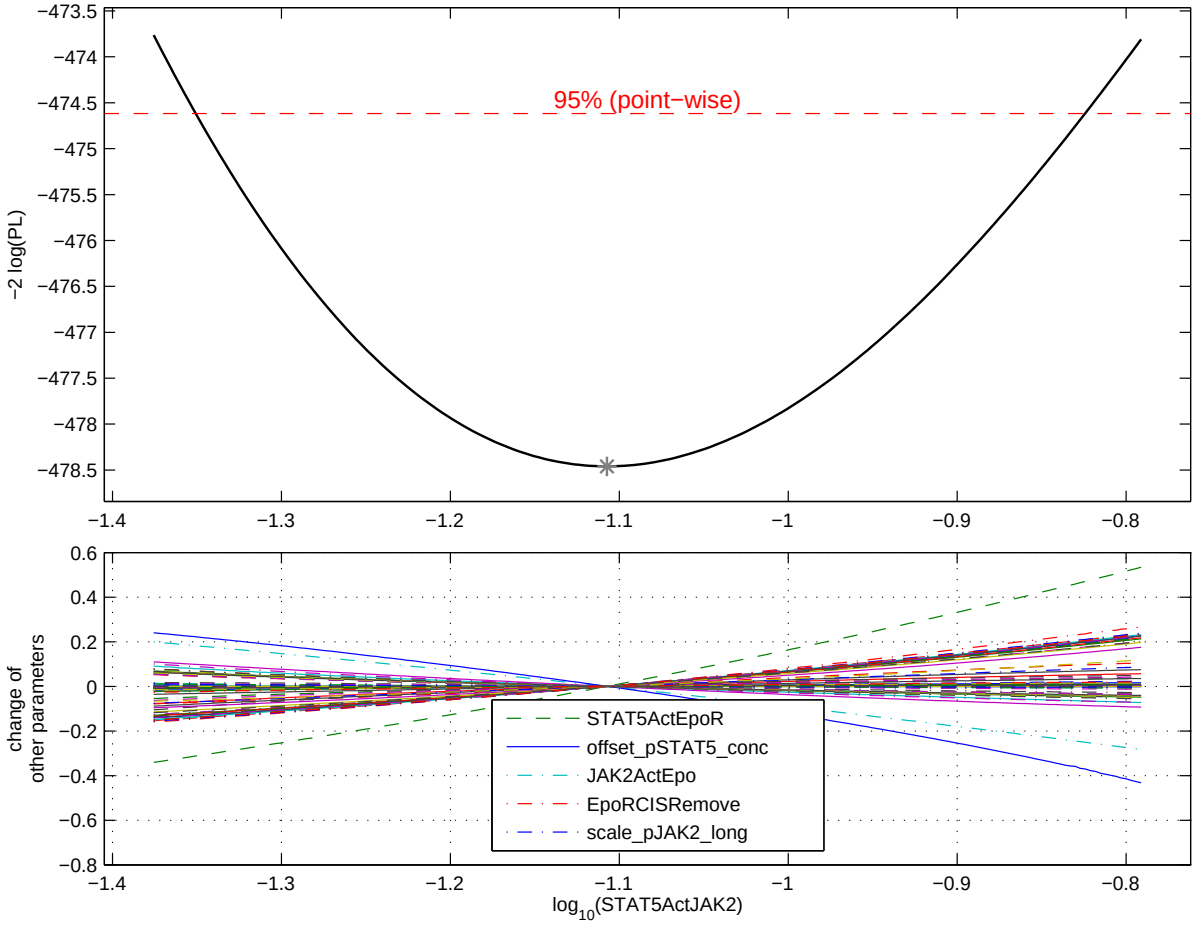

Figure S46: Profile likelihood of parameter STAT5ActJAK2
Upper panel: The solide line indicates the profile likelihood. The broken line indicates the threshold to assess confidence intervals. The asterisk indicate the optimal parameter values. Lower panel: The functional relations to the other parameters along the profile likelihood of STAT5ActJAK2 are displayed. In the legend the top five parameters showing the strongest variations are given. The calculation time was 00:04:01.25.

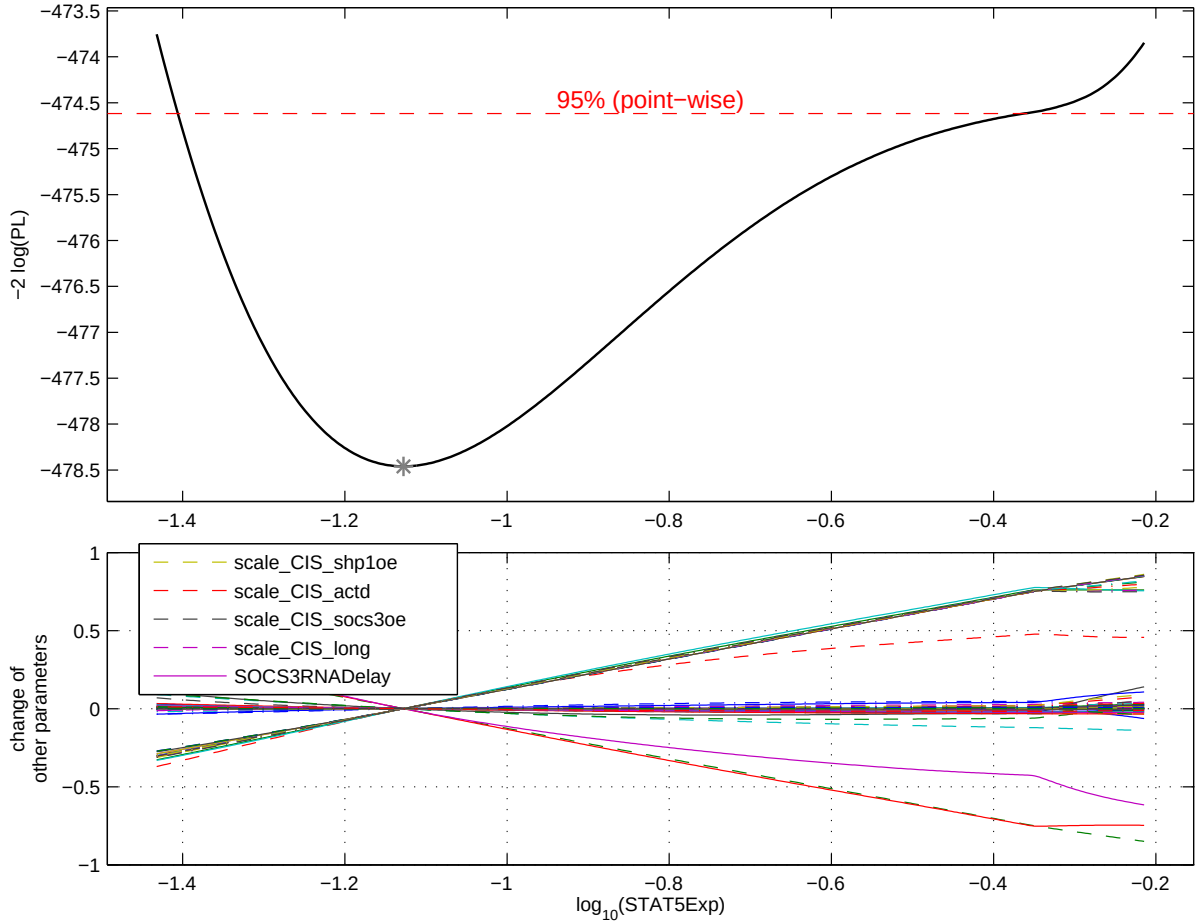

Figure S47: Profile likelihood of parameter STAT5Exp
Upper panel: The solide line indicates the profile likelihood. The broken line indicates the threshold to assess confidence intervals. The asterisk indicate the optimal parameter values. Lower panel: The functional relations to the other parameters along the profile likelihood of STAT5Exp are displayed. In the legend the top five parameters showing the strongest variations are given. The calculation time was 00:09:36.78.

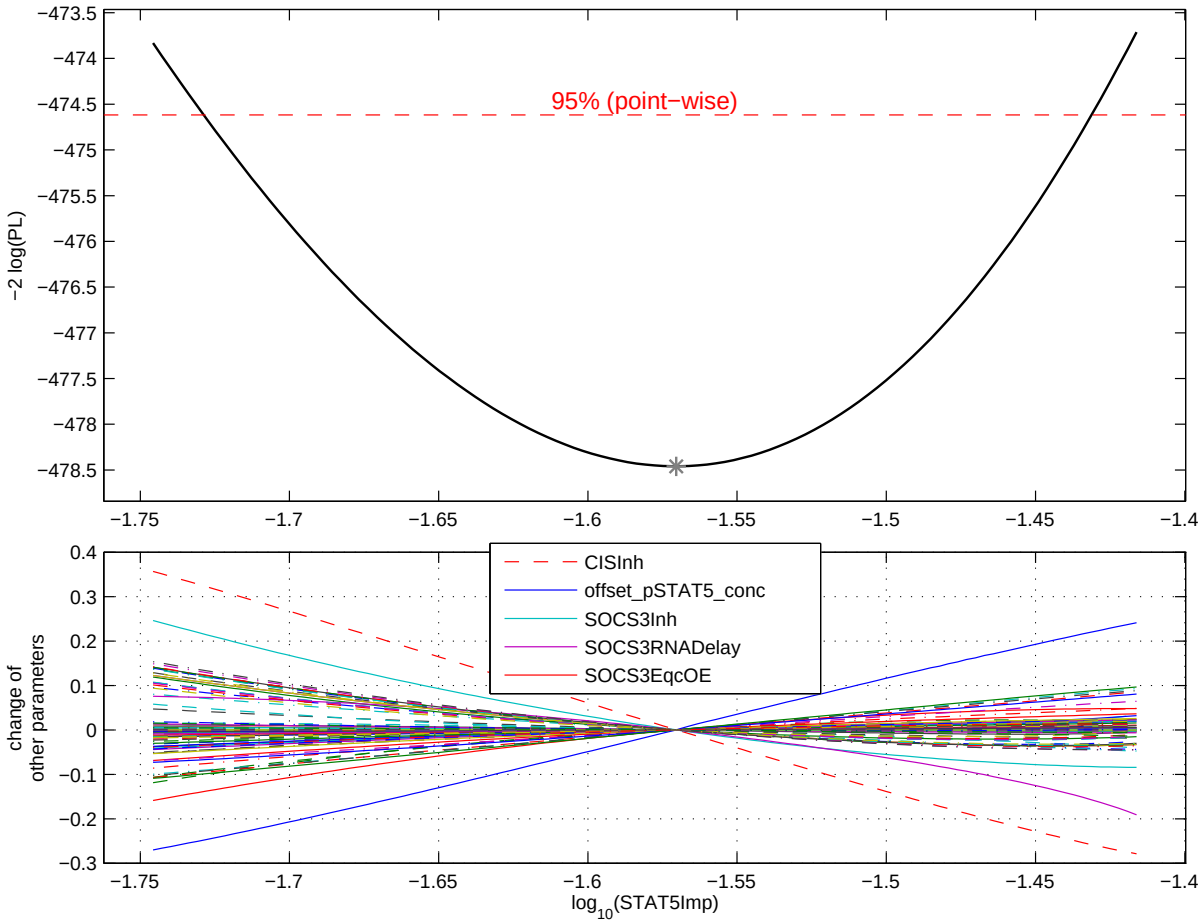

Figure S48: Profile likelihood of parameter STAT5Imp
Upper panel: The solide line indicates the profile likelihood. The broken line indicates the threshold to assess confidence intervals. The asterisk indicate the optimal parameter values. Lower panel: The functional relations to the other parameters along the profile likelihood of STAT5Imp are displayed. In the legend the top five parameters showing the strongest variations are given. The calculation time was 00:02:31.67.

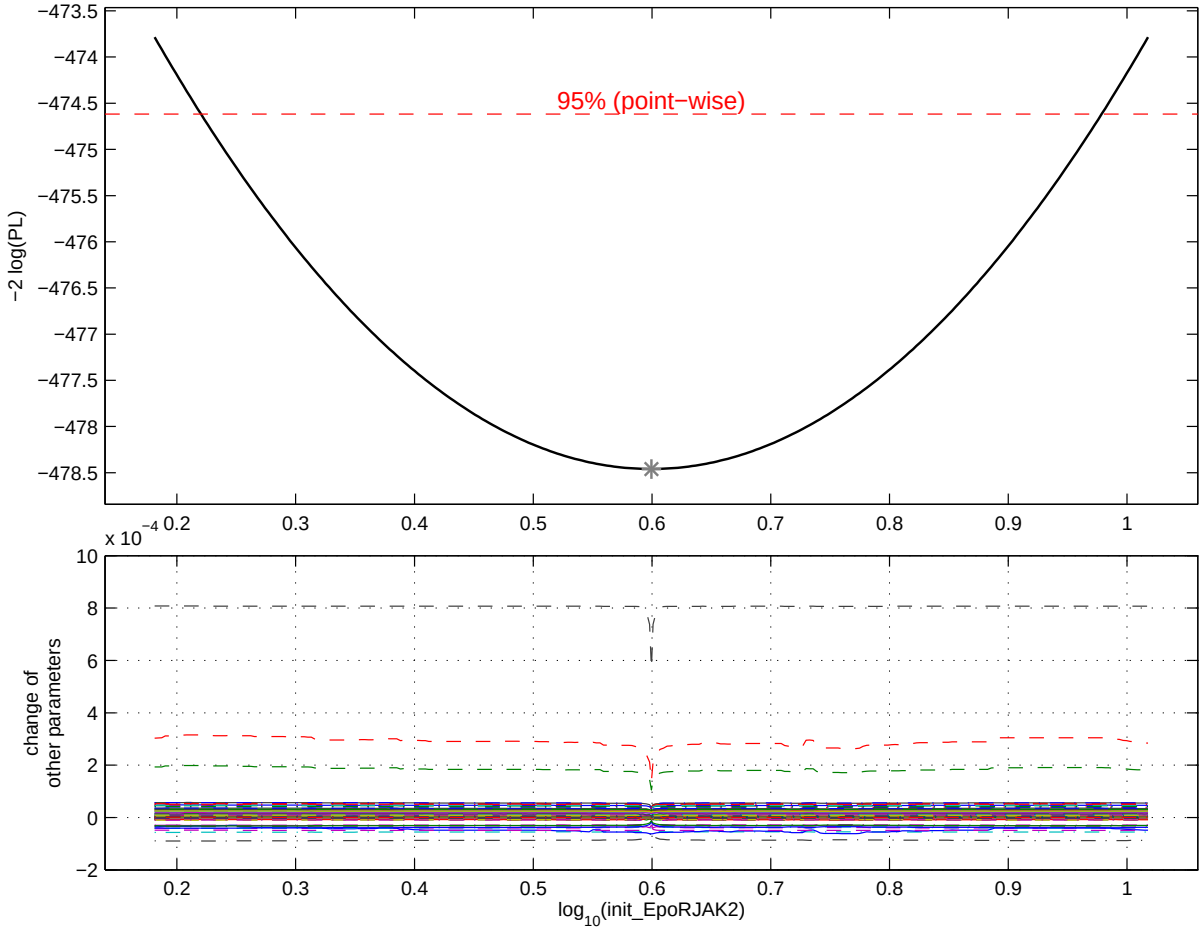

Figure S49: Profile likelihood of parameter init_EpoRJAK2
Upper panel: The solide line indicates the profile likelihood. The broken line indicates the threshold to assess confidence intervals. The asterisk indicate the optimal parameter values. Lower panel: The functional relations to the other parameters along the profile likelihood of init_EpoRJAK2 are displayed. The calculation time was 00:05:10.13.

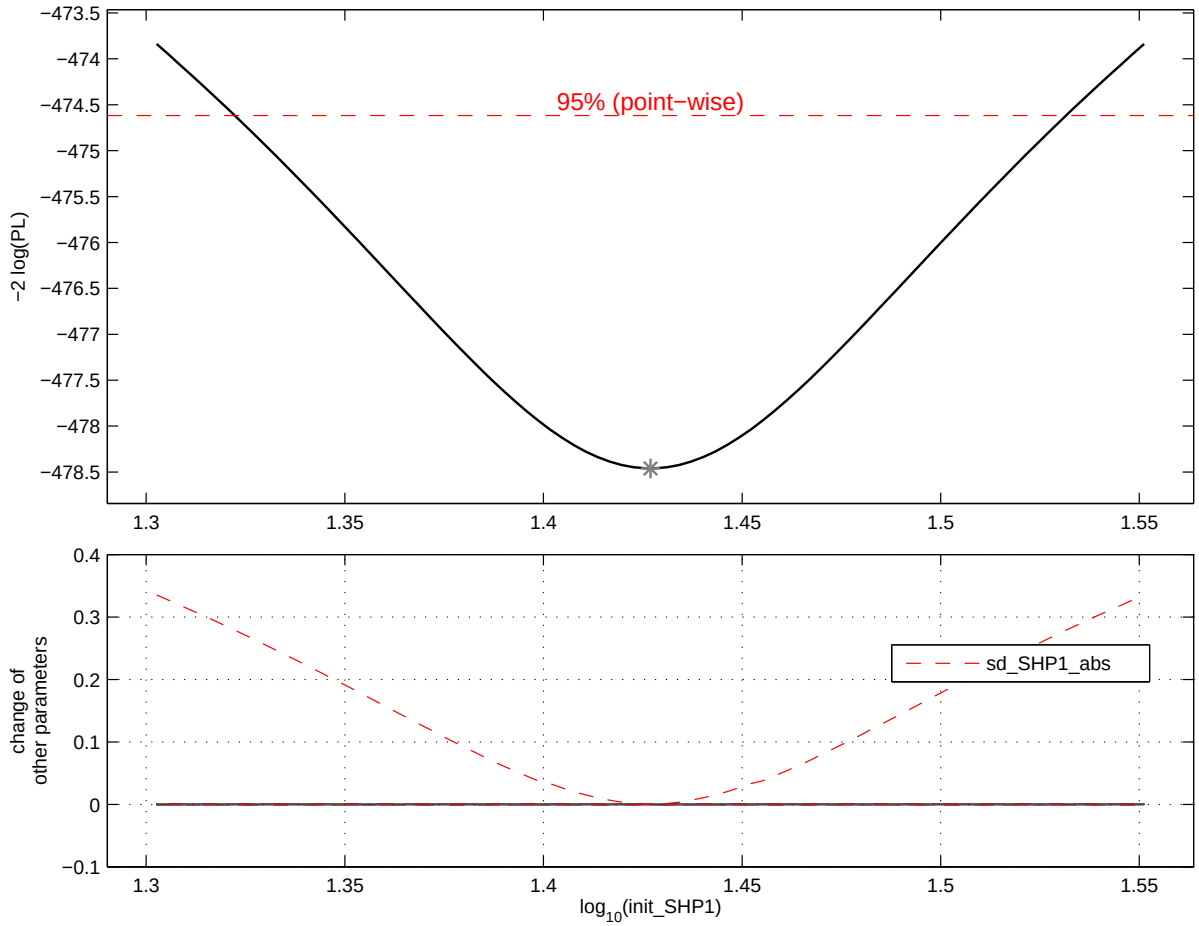

Figure S50: Profile likelihood of parameter init_SHP1
Upper panel: The solide line indicates the profile likelihood. The broken line indicates the threshold to assess confidence intervals. The asterisk indicate the optimal parameter values. Lower panel: The functional relations to the other parameters along the profile likelihood of init_SHP1 are displayed. In the legend the parameter showing the strongest variation is given. The calculation time was 00:01:59.08.

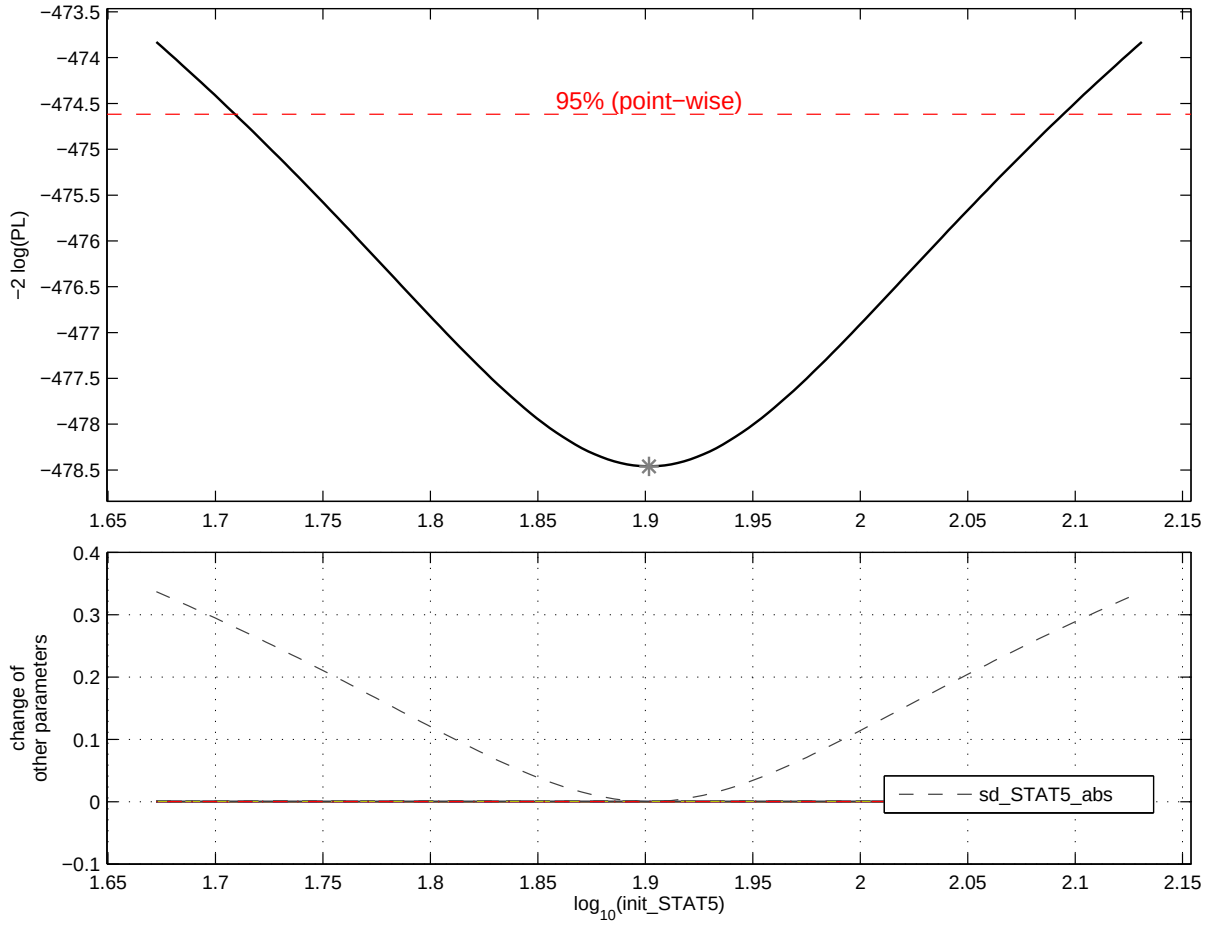

Figure S51: Profile likelihood of parameter init_STAT5
Upper panel: The solide line indicates the profile likelihood. The broken line indicates the threshold to assess confidence intervals. The asterisk indicate the optimal parameter values. Lower panel: The functional relations to the other parameters along the profile likelihood of init_STAT5 are displayed. In the legend the parameter showing the strongest variation is given. The calculation time was 00:02:05.24.

	name	$\hat{\theta}$	σ^-	σ^+
1	CISEqc	+2.636	+2.289	+3.382
2	CISEqcOE	-0.276	-1.034	+0.319
3	CISInh	+8.895	+7.955	+10.699
4	CISRNADelay	-0.839	-0.969	-0.717
6	CISRNATurn	+3.000	-1.501	+Inf
7	CISTurn	-2.076	-2.643	-1.771
8	EpoRActJAK2	-0.573	-0.851	-0.269
9	EpoRCISInh	+6.000	+0.879	+Inf
10	EpoRCISRemove	+0.735	-0.305	+1.328
11	JAK2ActEpo	+5.802	+5.521	+6.028
12	JAK2EpoRDeaSHP1	+2.154	+0.924	+Inf
13	SHP1ActEpoR	-3.000	-Inf	-1.740
14	SHP1Dea	-2.088	-2.399	-1.865
15	SHP1ProOE	+0.451	+0.300	+0.574
16	SOCS3Eqc	+2.240	+1.887	+Inf
17	SOCS3EqcOE	-0.168	-0.925	+0.218
18	SOCS3Inh	+1.017	+0.577	+1.801
19	SOCS3RNADelay	+0.027	-0.925	+Inf
21	SOCS3RNATurn	-2.080	-2.369	+0.035
22	SOCS3Turn	+4.000	-0.716	+Inf
23	STAT5ActEpoR	+1.591	+0.939	+2.323
24	STAT5ActJAK2	-1.107	-1.351	-0.824
25	STAT5Exp	-1.128	-1.406	-0.363
26	STAT5Imp	-1.570	-1.729	-1.431
27	init_EpoRJAK2	+0.599	+0.220	+0.979
28	init_SHP1	+1.427	+1.322	+1.532
29	init_STAT5	+1.902	+1.709	+2.094

Table S20: Confidence intervals for the estimated parameter values derived by the profile likelihood
$\hat{\theta}$ indicates the estimated optimal parameter value. σ^- and σ^+ indicate 95% point-wise confidence intervals.

2.6 Confidence intervals of the predicted model dynamics

The remaining uncertainties in the parameter estimates are translated to confidence intervals of the model trajectories, see in Raue *et al.* (2010) for details. Therefore, the trajectories corresponding to all acceptable parameter values according to the profile likelihood are evaluated. The resulting upper and lower time point-wise confidence bands for each experimental setting are displayed in Fig. S52 – S61 for a 95% confidence level.

The dynamics of active SHP1 shows large confidence bands indicating that the relative amount of active and inactive SHP1 can not be determined well. This is a result of the corresponding practically non-identifiable parameters JAK2EpoRDeaSHP1 and SHP1ActEpoR, see in Fig. S35 and Fig. S36. Similarly, the absolute concentration amounts of npSTAT5 and the RNA species of CIS and SOCS3 show large variations. This due to the lack of absolute concentration measurements in the nuclear compartment or of a measurement of the ratio of cytoplasmatic to nuclear STAT5. Please not that the model predictions shown in Fig. 5 and Fig. 6 of the main text display the relative changes of npSTAT5 between different conditions. The relative changes of npSTAT5 is less affected by uncertainty and therefore allows for a reasonable biological interpretation.

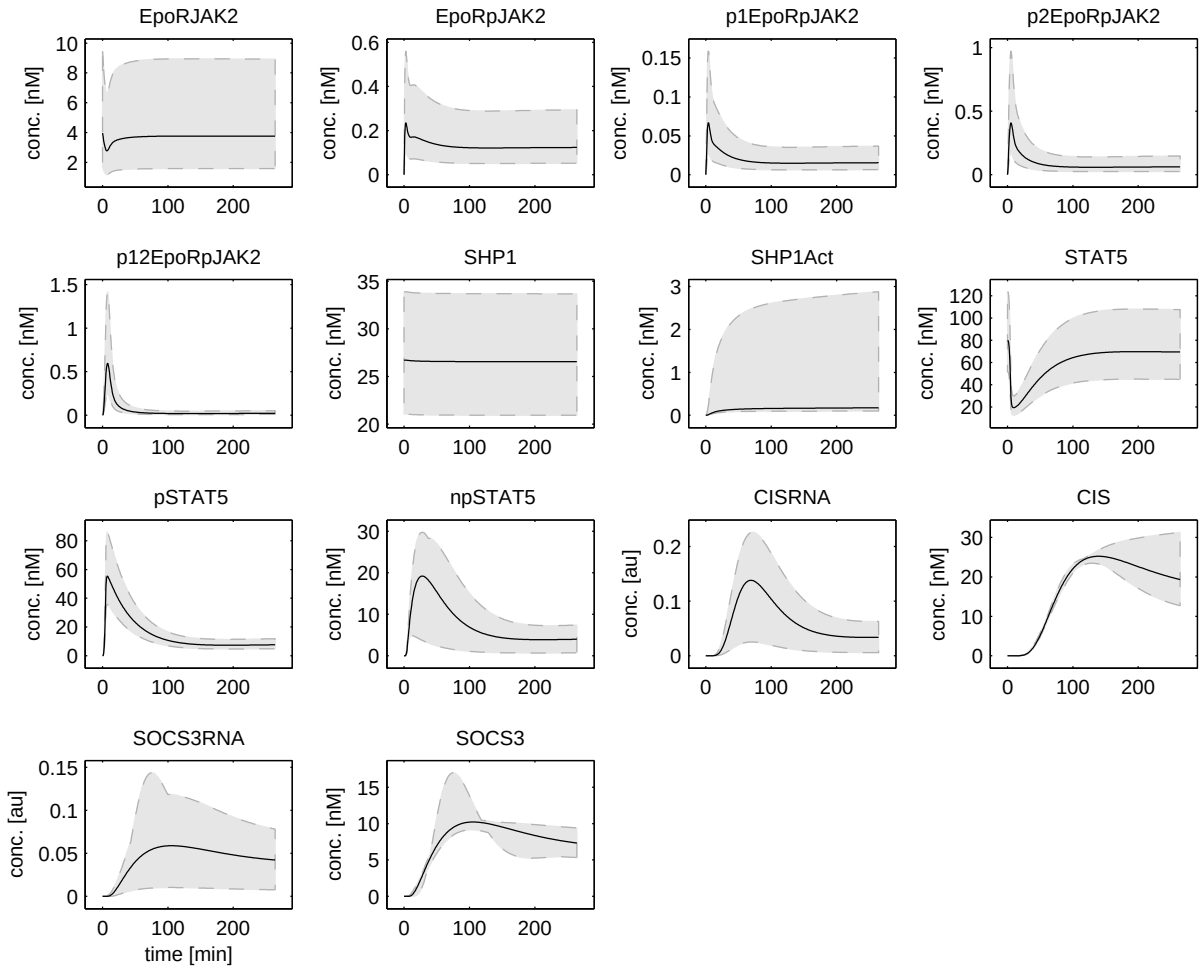

Figure S52: Trajectories of the dynamical variables and external inputs for the experiment CFU-E_Long The dynamical behaviour is determined by the ODE system, see Eq. 49 – 73.

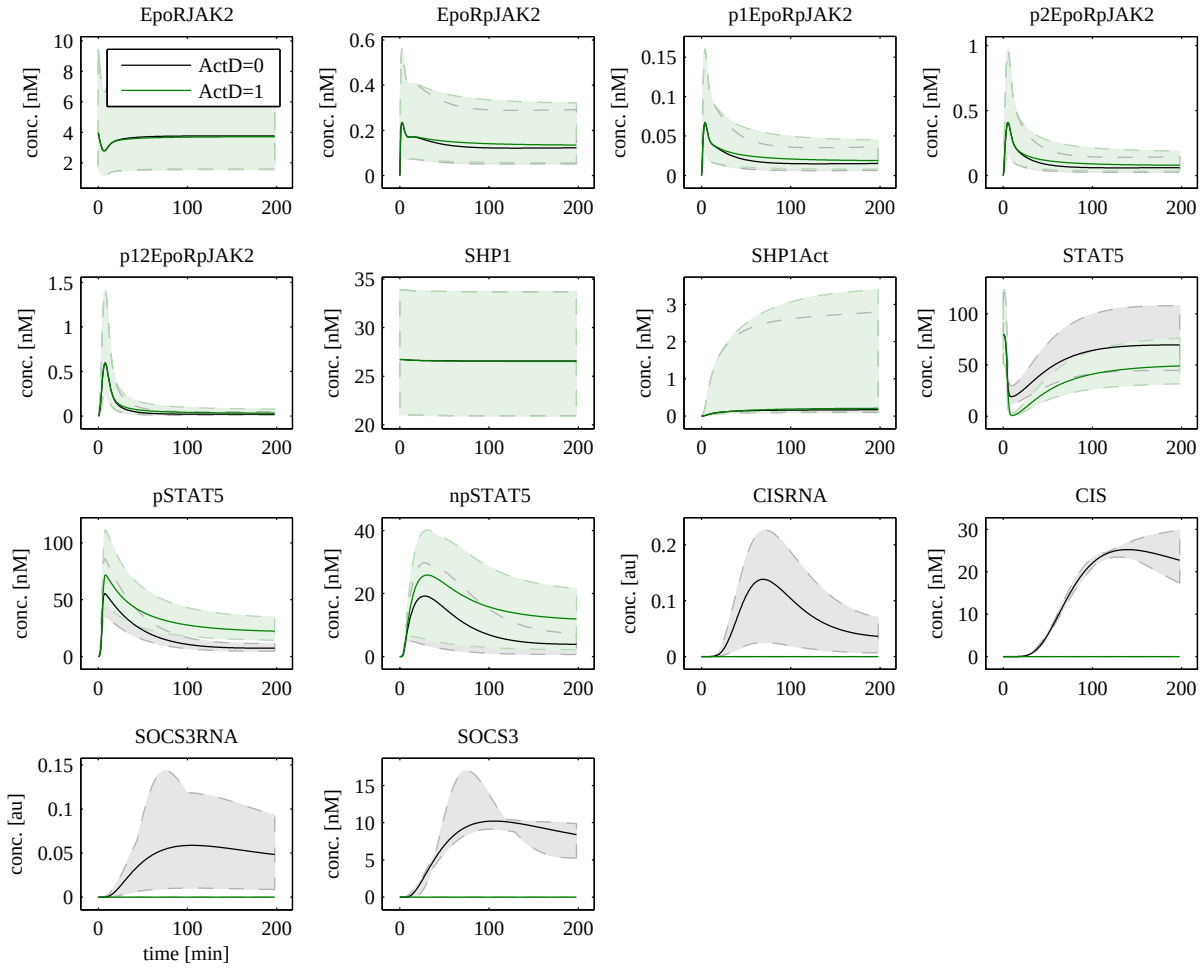

Figure S53: Trajectories of the dynamical variables and external inputs for the experiment CFU-E_ActD The dynamical behaviour is determined by the ODE system, see Eq. 49 – 73.

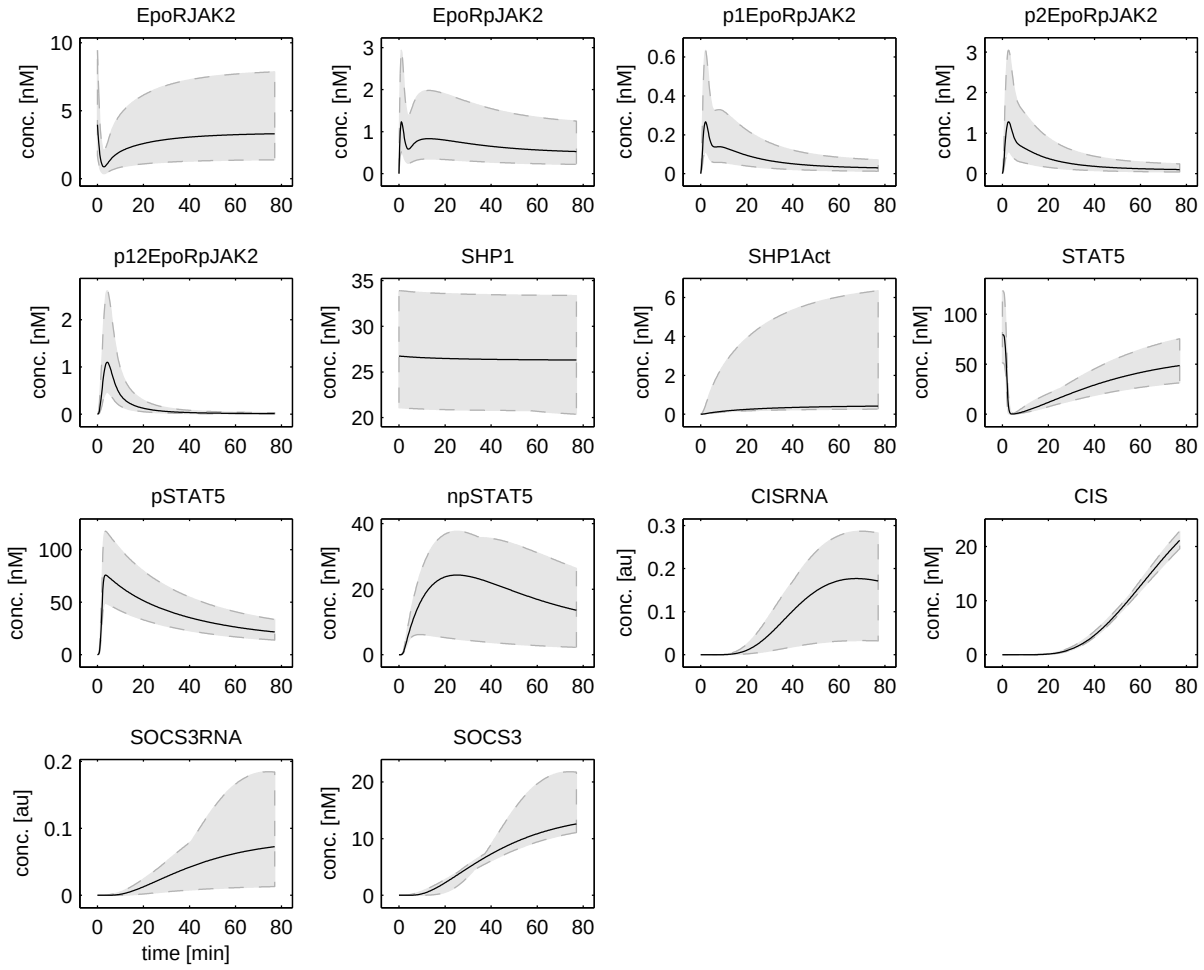

Figure S54: Trajectories of the dynamical variables and external inputs for the experiment CFU-E_Fine
The dynamical behaviour is determined by the ODE system, see Eq. 49 – 73.

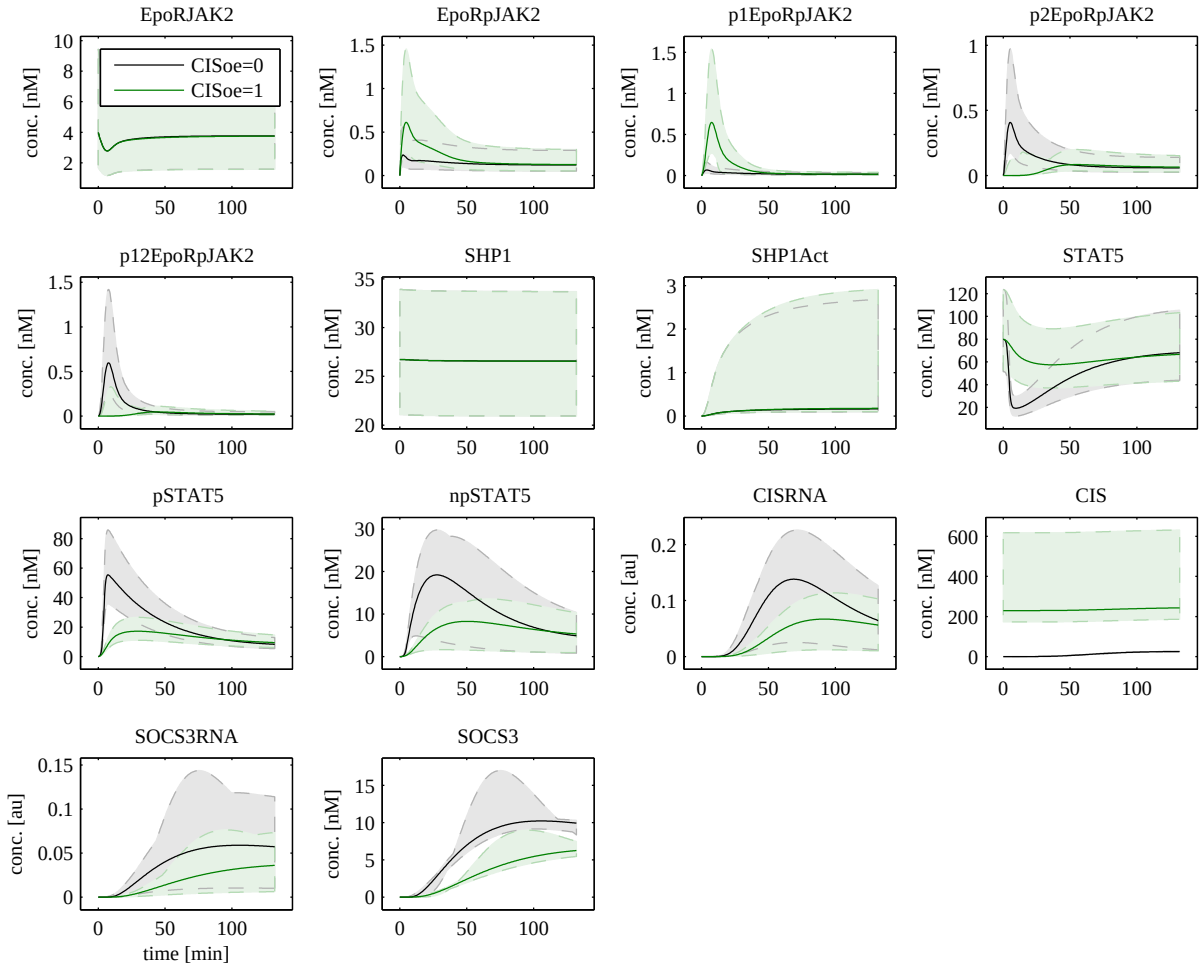

Figure S55: Trajectories of the dynamical variables and external inputs for the experiment CFU-E_CISoe The dynamical behaviour is determined by the ODE system, see Eq. 49 – 73.

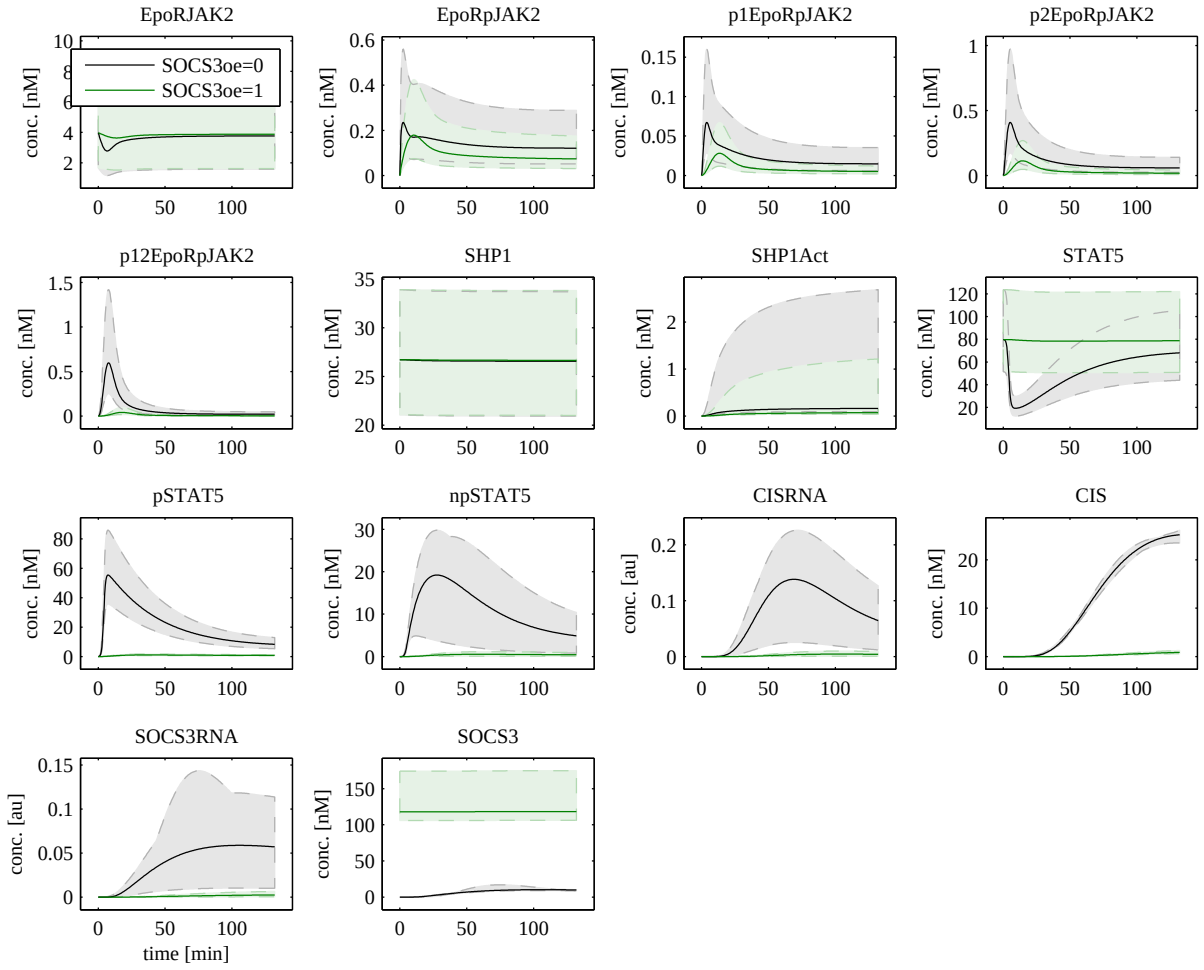

Figure S56: Trajectories of the dynamical variables and external inputs for the experiment CFU-E_SOCS3oe
The dynamical behaviour is determined by the ODE system, see Eq. 49 – 73.

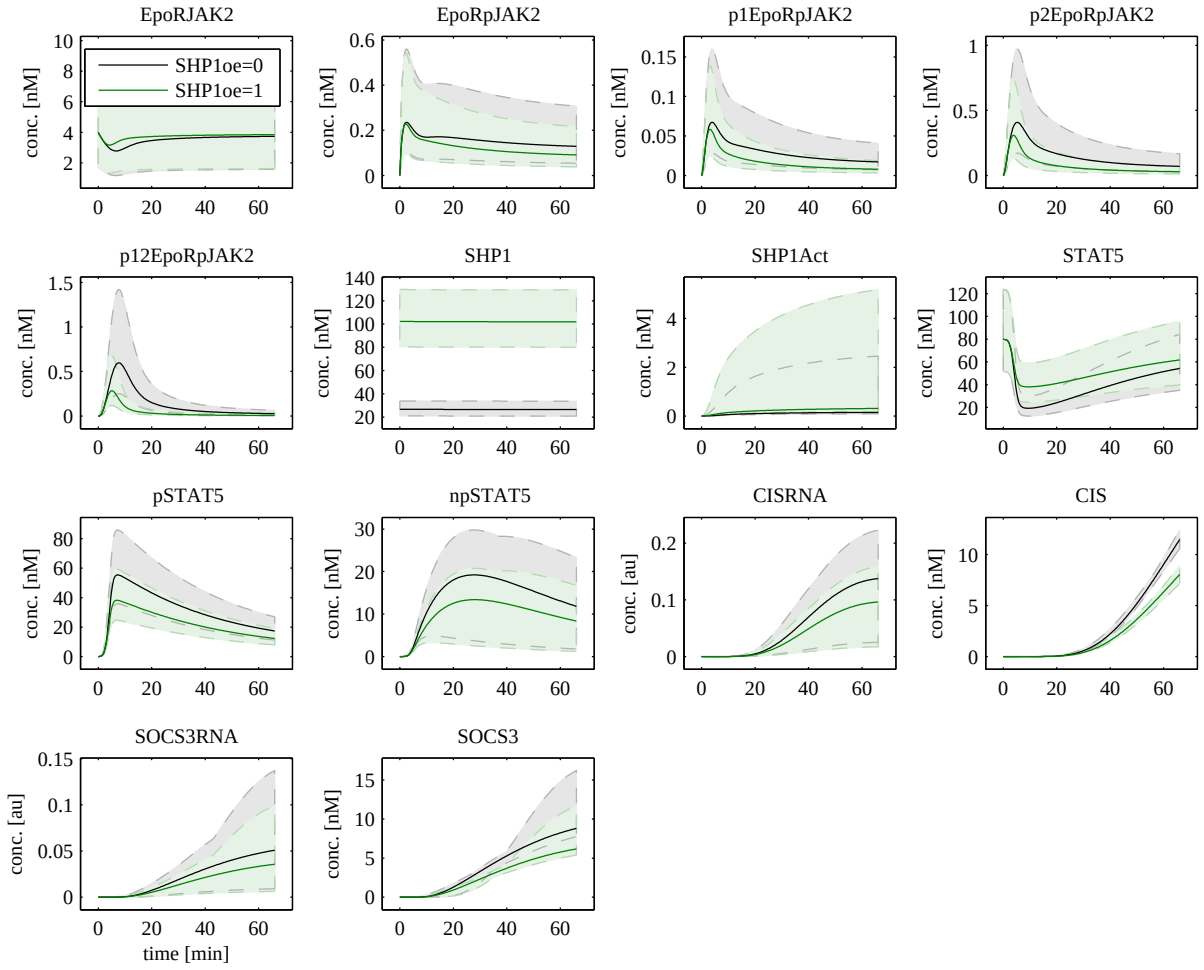

Figure S57: Trajectories of the dynamical variables and external inputs for the experiment CFU-E_SHP1oe
The dynamical behaviour is determined by the ODE system, see Eq. 49 – 73.

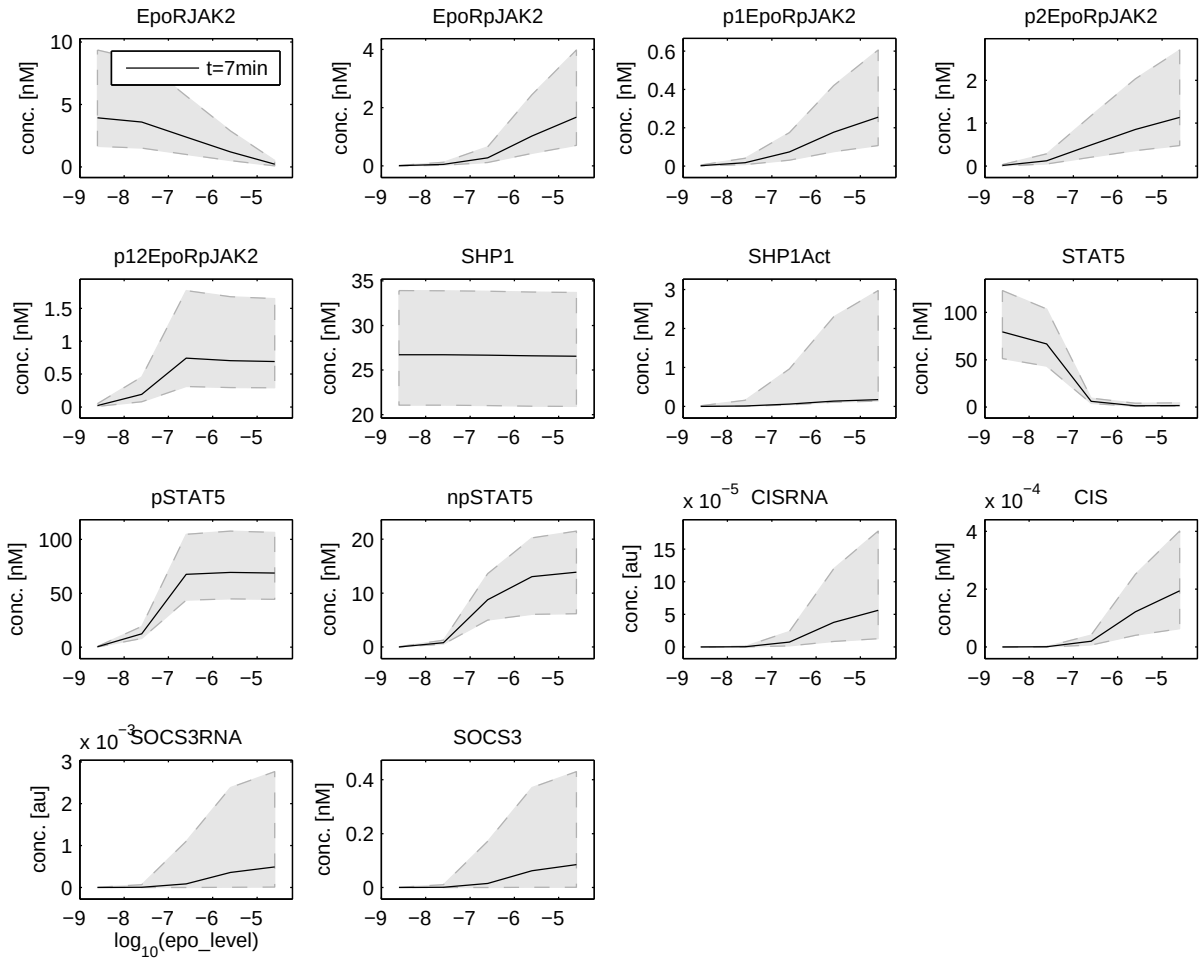

Figure S58: Trajectories of the dynamical variables and external inputs for the experiment CFU-E_DoseResp_7min
The dynamical behaviour is determined by the ODE system, see Eq. 49 – 73.

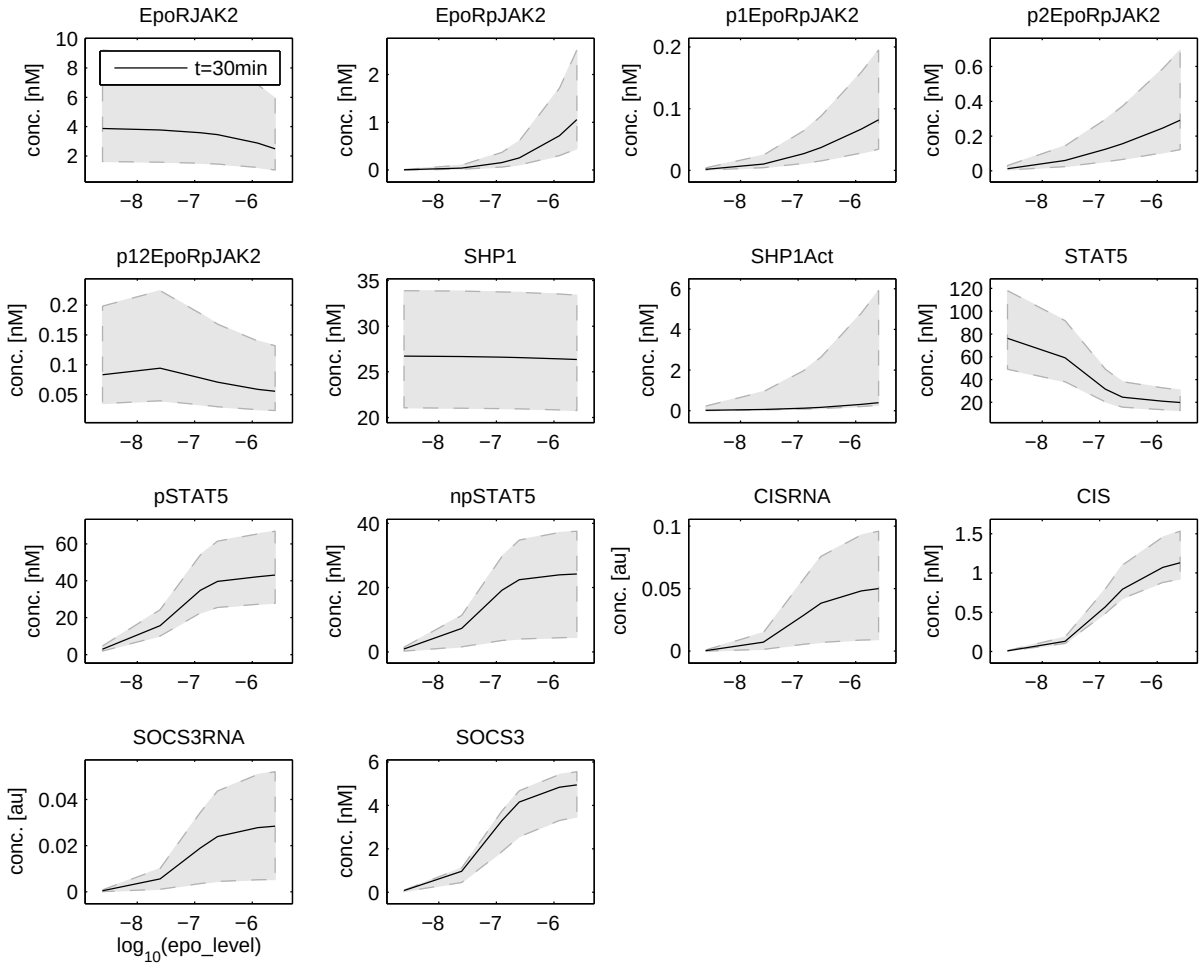

Figure S59: Trajectories of the dynamical variables and external inputs for the experiment CFU-E_DoseResp_30min
The dynamical behaviour is determined by the ODE system, see Eq. 49 – 73.

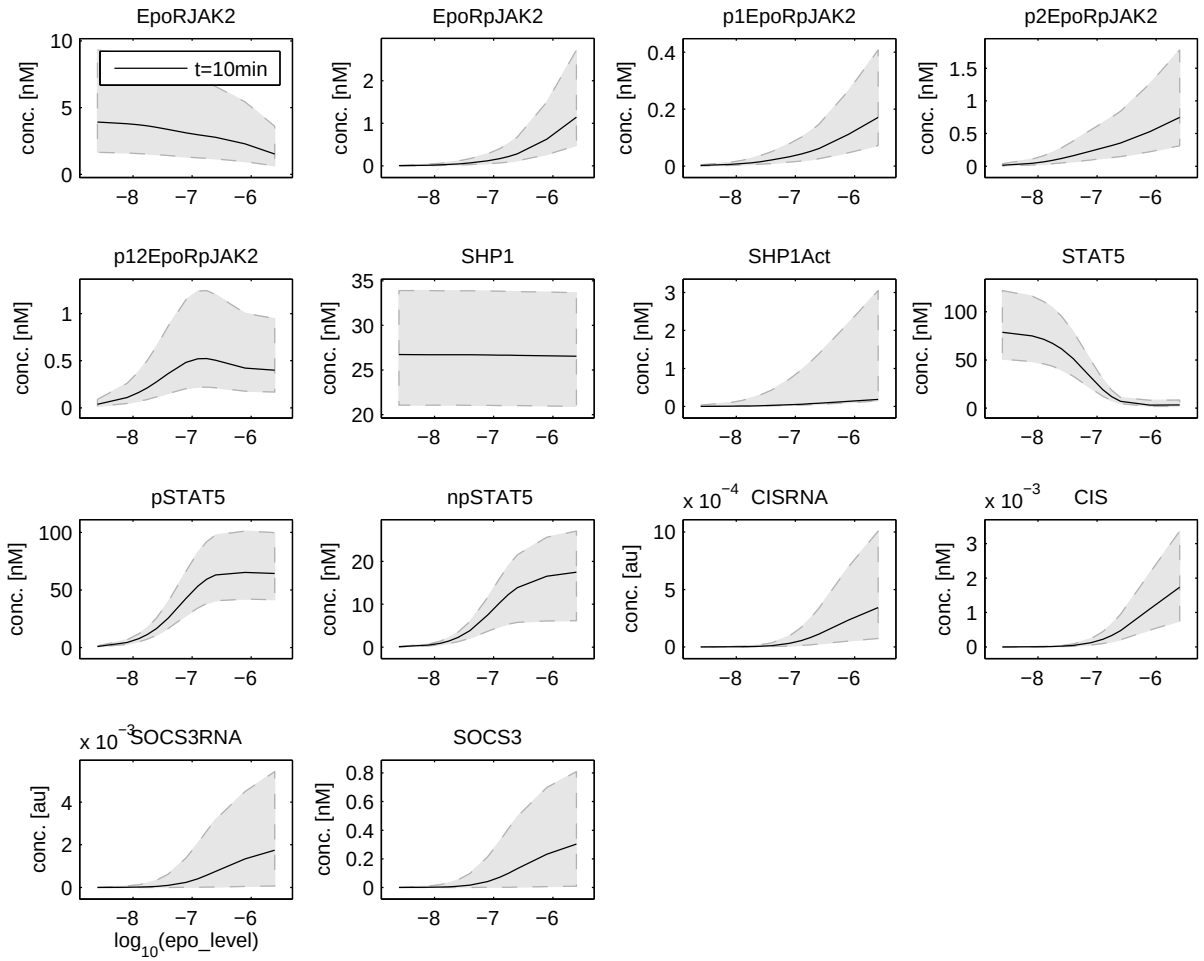

Figure S60: Trajectories of the dynamical variables and external inputs for the experiment CFU-E_DoseResp_pSTAT5_10min
The dynamical behaviour is determined by the ODE system, see Eq. 49 – 73.

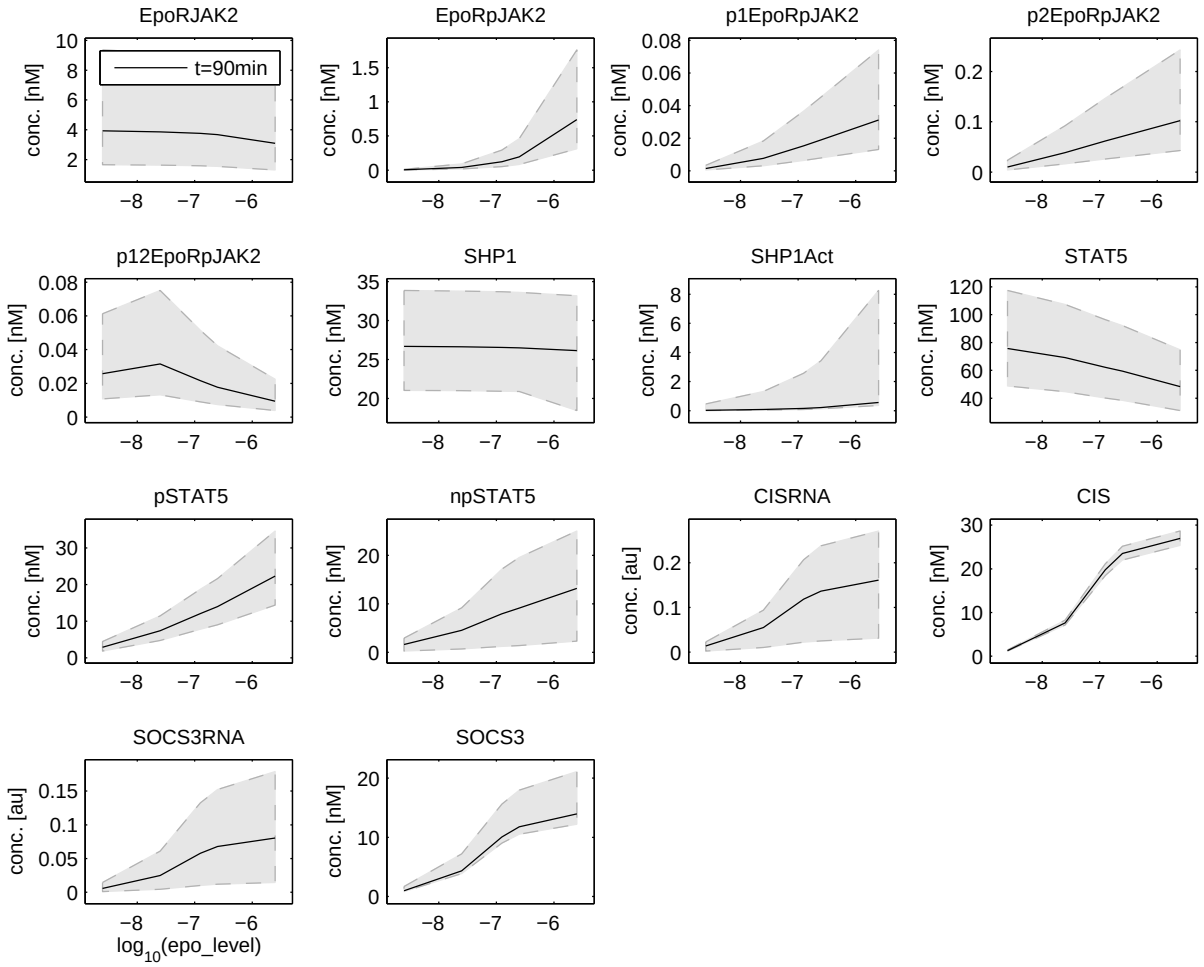

Figure S61: Trajectories of the dynamical variables and external inputs for the experiment CFU-E_DoseResp_CIS_90min
The dynamical behaviour is determined by the ODE system, see Eq. 49 – 73.

References

Alexander, W. and Hilton, D. (2004). The role of suppressors of cytokine signaling (socs) proteins in regulation of the immune response. *Annu. Rev. Immunol.*, **22**, 503–529.

Babon, J., McManus, E., Yao, S., DeSouza, D., Mielke, L., Sprigg, N., Willson, T., Hilton, D., Nicola, N., Baca, M., *et al.* (2006). The structure of SOCS3 reveals the basis of the extended SH2 domain function and identifies an unstructured insertion that regulates stability. *Molecular cell*, **22**(2), 205–216.

Backhaus, K., Erichson, B., Plinke, W., and Weiber, R. (1996). *Multivariate analysemethoden*. Springer.

Barber, D., Beattie, B., Mason, J., Nguyen, M., Yoakim, M., Neel, B., D'Andrea, A., and Frank, D. (2001). A common epitope is shared by activated signal transducer and activator of transcription-5 (stat5) and the phosphorylated erythropoietin receptor: implications for the docking model of stat activation. *Blood*, **97**(8), 2230.

Coleman, T. and Li, Y. (1996). An interior, trust region approach for nonlinear minimization subject to bounds. *SIAM Journal on Optimization*, **6**, 418–445.

Gillespie, D. (1977). Exact stochastic simulation of coupled chemical reactions. *The Journal of Physical Chemistry*, **81**(25), 2340–2361.

Gobert, S., Chretien, S., Gouilleux, F., Muller, O., Pallard, C., Dusanter-Fourt, I., Groner, B., Lacombe, C., Gisselbrecht, S., and Mayeux, P. (1996). Identification of tyrosine residues within the intracellular domain of the erythropoietin receptor crucial for stat5 activation. *The EMBO Journal*, **15**(10), 2434.

Heinrich, R. and Schuster, S. (1996). *The Regulation of Cellular Systems*. Chapman & Hall.

Hindmarsh, A., Brown, P., Grant, K., Lee, S., Serban, R., Shumaker, D., and Woodward, C. (2005). Sundials: Suite of nonlinear and differential/algebraic equation solvers. *ACM T Math Software*, **31**(3), 363–396.

Hörtner, M., Nielsch, U., Mayr, L., Heinrich, P., and Haan, S. (2002). A new high affinity binding site for suppressor of cytokine signaling-3 on the erythropoietin receptor. *European Journal of Biochemistry*, **269**(10), 2516–2526.

Huang, L. J., Constantinescu, S. N., and Lodish, H. F. (2001). The n-terminal domain of janus kinase 2 is required for golgi processing and cell surface expression of erythropoietin receptor. *Mol Cell*, **8**(6), 1327–1338.

Ketteler, R., Moghraby, C., Hsiao, J., Sandra, O., Lodish, H., and Klingmüller, U. (2003). The cytokine-inducible scr homology domain-containing protein negatively regulates signaling by promoting apoptosis in erythroid progenitor cells. *Journal of Biological Chemistry*, **278**(4), 2654.

Klingmüller, U., Lorenz, U., Cantley, L., Neel, B., and Lodish, H. (1995). Specific recruitment of the hematopoietic protein tyrosine phosphatase sh-ptp1 to the erythropoietin receptor causes inactivation of jak2 and termination of proliferative signals. *Cell*, **80**, 729–738.

Klingmüller, U., Bergelson, S., Hsiao, J., and Lodish, H. (1996). Multiple tyrosine residues in the cytosolic domain of the erythropoietin receptor promote activation of stat5. *Proceedings of the National Academy of Sciences of the United States of America*, **93**(16), 8324.

Kreutz, C., Rodriguez, M. M. B., Maiwald, T., Seidl, M., Blum, H. E., Mohr, L., and Timmer, J. (2007). An error model for protein quantification. *Bioinformatics*, **23**(20), 2747–2753.

Landschulz, K. T., Noyes, A. N., Rogers, O., and Boyer, S. H. (1989). Erythropoietin receptors on murine erythroid colony-forming units: natural history. *Blood*, (73), 1476–86.

Larsson, E., Sander, C., and Marks, D. (2010). mrna turnover rate limits sirna and microrna efficacy. *Molecular systems biology*, **6**(1).

MacDonald, N. (1976). Time delay in simple chemostat models. *Biotechnology and Bioengineering*, **18**(6), 805–812.

Menon, M., Karur, V., Bogacheva, O., Bogachev, O., Cuetara, B., and Wojchowski, D. (2006). Signals for stress erythropoiesis are integrated via an erythropoietin receptor-phosphotyrosine-343-stat5 axis. *Journal of Clinical Investigation*, **116**(3), 683.

Pei, D., Wang, J., and Walsh, C. (1996). Differential functions of the two src homology 2 domains in protein tyrosine phosphatase sh-ptp1. *Proceedings of the National Academy of Sciences of the United States of America*, **93**(3), 1141.

Pfeifer, A., Kaschek, D., Bachmann, J., Klingmüller, U., and Timmer, J. (2010). Model-based extension of high-throughput to high-content data. *BMC Systems Biology*, **4**(1), 106.

Raue, A., Kreutz, C., Maiwald, T., Bachmann, J., Schilling, M., Klingmüller, U., and Timmer, J. (2009). Structural and practical identifiability analysis of partially observed dynamical models by exploiting the profile likelihood. *Bioinformatics*, **25**(15), 1923–1929.

Raue, A., Becker, V., Klingmüller, U., and Timmer, J. (2010). Identifiability and observability analysis for experimental design in non-linear dynamical models. *Chaos*, **20**(4), 045105.

Sasaki, A., Yasukawa, H., Suzuki, A., Kamizono, S., Syoda, T., Kinjyo, I., Sasaki, M., Johnston, J., and Yoshimura, A. (1999). Cytokine-inducible sh2 protein-3 (cis3/socs3) inhibits janus tyrosine kinase by binding through the n-terminal kinase inhibitory region as well as sh2 domain. *Genes to Cells*, **4**(6), 339–351.

Sasaki, A., Yasukawa, H., Shouda, T., Kitamura, T., Dikic, I., and Yoshimura, A. (2000). Cis3/socs-3 suppresses erythropoietin (epo) signaling by binding the epo receptor and jak2. *J Biol Chem*, **275**(38), 29338–29347.

Sathyanarayana, P., Dev, A., Fang, J., Houde, E., Bogacheva, O., Bogachev, O., Menon, M., Browne, S., Pradeep, A., Emerson, C., *et al.* (2008). Epo receptor circuits for primary erythroblast survival. *Blood*, **111**(11), 5390.

Schilling, M., Maiwald, T., Bohl, S., Kollmann, M., Kreutz, C., Timmer, J., and Klingmüller, U. (2005). Computational processing and error reduction strategies for standardized quantitative data in biological networks. *FEBS Journal*, **272**(24), 6400–6411.

Schilling, M., Maiwald, T., Hengl, S., Winter, D., Kreutz, C., Kolch, W., Lehmann, W., Timmer, J., and Klingmüller, U. (2009). Theoretical and experimental analysis links isoform-specific erk signalling to cell fate decisions. *Molecular systems biology*, **5**(1).

Seber, G. and Wild, C. (2003). *Nonlinear Regression*. Wiley.

Silva, M., Benito, A., Sanz, C., Prosper, F., Ekhterae, D., Nuñez, G., and Fernandez-Luna, J. (1999). Erythropoietin can induce the expression of bcl-xlthrough stat5 in erythropoietin-dependent progenitor cell lines. *Journal of Biological Chemistry*, **274**(32), 22165.

Socolovsky, M., Fallon, A., Wang, S., Brugnara, C., and Lodish, H. (1999). Fetal anemia and apoptosis of red cell progenitors in stat5a-/-5b-/-mice:: A direct role for stat5 in bcl-xl induction. *Cell*, **98**(2), 181–191.

Spencer, S., Gaudet, S., Albeck, J., Burke, J., and Sorger, P. (2009). Non-genetic origins of cell-to-cell variability in trail-induced apoptosis. *Nature*, **459**(7245), 428–432.

Swameye, I., Müller, T., Timmer, J., Sandra, O., and Klingmüller, U. (2003). Identification of nucleocytoplasmic cycling as a remote sensor in cellular signaling by databased modeling. *Proceedings of the National Academy of Sciences*, **100**(3), 1028–1033.

Taniguchi, Y., Choi, P., Li, G., Chen, H., Babu, M., Hearn, J., Emili, A., and Xie, X. (2010). Quantifying e. coli proteome and transcriptome with single-molecule sensitivity in single cells. *Science*, **329**(5991), 533.

Wolkenhauer, O. (2008). *Systems Biology*. Portland Press.

Yoshimura, A., Ohkubo, T., Kiguchi, T., Jenkins, N., Gilbert, D., Copeland, N., Hara, T., and Miyajima, A. (1995). A novel cytokine-inducible gene CIS encodes an SH2-containing protein that binds to tyrosine-phosphorylated interleukin 3 and erythropoietin receptors. *The EMBO Journal*, **14**(12), 2816.

Yu, C., Mahdi, R., Ebong, S., Vistica, B., Gery, I., and Egwuagu, C. (2003). Suppressor of cytokine signaling 3 regulates proliferation and activation of t-helper cells. *Journal of Biological Chemistry*, **278**(32), 29752.